Role of interferon-α and interferon-β in glomerular injury and repair

Dissertation

zum Erwerb des Doktorgrades der Humanbiologie

an der Medizinischen Fakultät der

Ludwig-Maximilians-Universität München

vorgelegt von

Adriana Migliorini

aus Caserta, Italien

2014

Mit Genehmigung der Medizinischen Fakultät

der Ludwig-Maximilians-Universität München

1. Berichterstatter   : Prof. Dr. med. Hans-Joachim Anders

   Mitberichterstatter   : Prof. Dr. Martin Storr

   Mitberichterstatter   :Prof. Dr. Peter Bartenstein

   Dekan   : Prof. Dr. med. Dr. h.c. M. Reiser, FACR, FRCR

Tag der mündlichen Prüfung   : 13.03.2014

Dedicated to
MY FAMILY

Declaration

I hereby declare that all of the present work embodied in this thesis was carried out by me from 01/2010 until 04/2013 under the supervision of Prof. Dr. Hans Joachim Anders, Nephrologisches Zentrum, Medizinische Klinik und Poliklinik IV, Innenstadt Klinikum der Universität München. This work has not been submitted in part or full to any other university or institute for any degree or diploma.

Part of the work has been performed at the University of Florence, in the laboratory of Prof Paola Romagnani, as mentioned below:

- In-vitro experiment using human renal progenitors
- In-vivo studies using SCID mice

Part of the work has been submitted and accepted for publication in the *American Journal of Pathology* (March 2013).

Date: ……………............ Signature………………….

Place: Munich, Germany

Contents

1. Introduction

1.1 Chronic Kidney Disease

According to recent statistics by the Center for Disease Control and Prevention (CDC), chronic kidney disease (CKD) has been placed 9th on the list of leading causes of death in the USA in 2007 [1]. CKD is defined as an irreversible and progressive decline of kidney function leading to kidney failure, known as end stage renal disease (ESRD). It has been estimated that 14-15% of the adult population in the USA is affected by CKD and its prevalence has been estimated to increase by 50 % over the next two decades [2]. Hypertension, diabetes, infections, glomerulonephritis, glomerulosclerosis and renal disease associated with genetic disorders are risk factors for developing CKD. In 2002, the National Kidney Foundation Kidney Disease Quality Outcome Initiative (NKF-K/DOQI) published the first guidelines to define and classify CKD. First in 2005 and later in 2013, the Kidney Disease Improving Global Outcomes (KDIGO) provided, in accordance with the document from K/DOQI, a revised definition of CKD[3-6]. In the latest document, CKD is defined by structural or functional abnormality of the kidney (albuminuria > 3 mg/mmol; glomerular filtration rate (GFR) < 60 ml/min/1.73 m^2 present for 3 months, with implications for health. This document provides an updated and revised guide for the management and classification of CKD based on five GFR and three albuminuria categories.

Table 1. Criteria for CKD (taken and adapted from *New KDIGO CKD 2013 [6])*

Markers of Kidney damage (one or more)	Albuminuria (AER >30 mg/24 h; ACR >30 mg/g [>3 mg/mmol]) Urine sediment abnormalities Electrolyte and other abnormalities due to tubular disorders Abnormalities detected by histology Structural abnormalities detected by imaging History of kidney transplantation
Decreased glomerular filtration rate (GFR)	GFR < 60 ml/min/1.73 m^2 (GFR categories G3a–G5)

Table 2. GFR categories in CKD (taken and adapted from *New KDIGO CKD 2013 [6]*)

GFR category	GFR (ml/min/1.73m^2)	Terms
G1	≥ 90	Normal or high
G2	60-89	Mildly decreased*
G3a	45-59	Mildly to moderately decreased
G3b	30-44	Moderately to severely decreased
G4	15-29	Severely decreased
G5	<15	Kidney failure

*Relative to young adult level

Table 3. Albuminuria categories in CKD (taken and adapted from *New KDIGO CKD 2013 [6]*)

Category	AER(mg/24h)	ACR(mg/g)	Terms
A1	<30	<30	Normal to mildly increased
A2	3-300	3-300	Mildly increased*
A3	≥ 300	≥ 300	Severely increased**

*Relative to young adult level.

**Including nephrotic syndrome (albumin excretion usually >2200 mg/24 h [ACR >2220 mg/g; >220 mg/mmol]).

1.1.1 Pathogenesis of glomerulosclerosis

Sclerosis of the glomerulus occurs as a response to injury. The parenchyma is then replaced by scarring tissue, leading to progressive and irreversible loss of function. The glomerular structure consists of an endocapillary compartment containing mesangial cells and capillaries, and an extracapillary compartment containing podocytes and the parietal epithelial cells (PECs) lying on the Bowman´s capsule [7, 8]. The harmony and the functionality of this architecture are maintained by podocytes. Podocytes, also known as glomerular visceral epithelial cells, are terminally differentiated epithelial cells that are specialized to their architecture, and are responsible for the maintenance of the glomerular filtration barrier (GFB). A recent study was able to show that all forms of glomerulosclerosis start with either a lesion or a dysfunction of podocytes [9]. This is a common feature of many clinical pathologic

syndromes including hereditary glomerular disease and kidney disease with late onset like diabetic disease [10, 11], focal segmental glomerulosclerosis (FSGS), membranous glomerulopathy or amyloid nephropathy [12, 13]. As a consequence of their high degree of differentiation and complexity, podocytes have a limited capacity for cell cycle re-entry and thus for replacing podocyte loss [14]. Remaining podocytes may compensate this loss by one of the following mechanism:

- Activating stem cell recruitment [15-17]

- Cell hypertrophy taking over the increased workload [18]

Independent of the mechanism involved, podocyte hypertrophy or replacement occurs slowly. Insufficient repair can lead to podocytopenia and subsequently threaten glomerular integrity [19]. The classical concept of development and progression of glomerulosclerosis has been accurately described in several animal models [20, 21]

The major culprit in the progression of glomerulosclerosis is the podocyte. Upon insult, podocyte loss and the failure of neighboring podocytes to cover the defect will result in a formation of naked glomerular basement membrane (GBM) area. Loss of separation between the capillary tuft and the Bowman´s capsule allow PECs of the Bowman´s capsule to access the GBM leading to a parietal "beach head" on the tuft. PECs attach to the capillary tuft giving rise to a gap and displacing podocytes to the GBM, establishing a synechia, which represents the first step in the development of segmental glomerulosclerosis [22]. This adhesion might develop either into a proteinaceous crescent based on the misdirected filtration towards the cortical interstitium, characteristic of the degenerative kidney disease, or into a cellular mixed crescent generally found in inflammatory kidney disease [9]. In the early stage of crescent formation, the cellular compositions of crescents appear to change over time with a predominance of proliferating PECs [23-25].
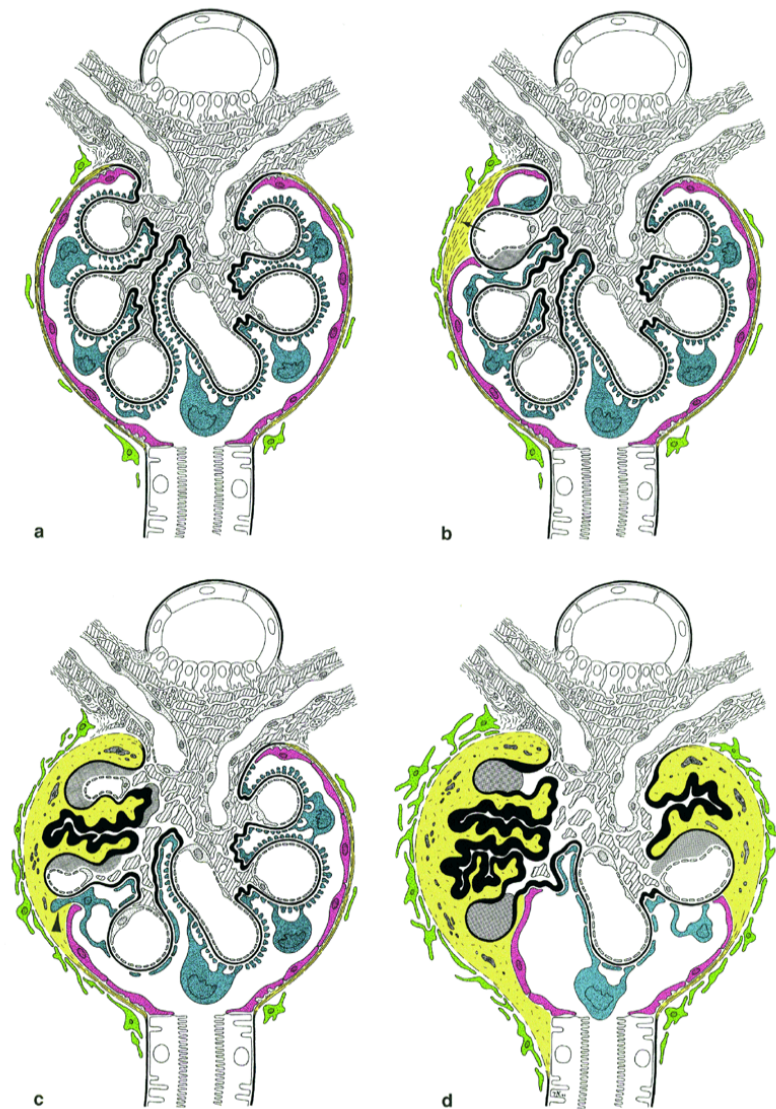
Figure 1. Schematic to show the progression of segmental to global glomerulosclerosis. (a) Normal glomerulus with vascular and urinary poles. Smooth muscle cells, extra glomerular mesangial cells, and mesangial cells are hatched; podocytes are shown in blue-green, parietal epithelial cells in red. The GBM is shown in black, the parietal basement membrane in yellow, tubular epithelia are shown in white (b) .A denuded capillary is attached to Bowman's capsule. Parietal cells attach to the naked GBM. (c) The adhesion has spread to neighboring capillaries resulting in either the collapse or in hyalinosis (shown in a dark grey pattern). The parietal epithelium may either appose the degenerated podocytes (arrowhead) or attach directly to the GBM at the flanks of the adhesion. Fluid leakage from perfused capillaries inside the adhesion has created a paraglomerular space (shown in yellow) that contains the sclerotic tuft remnants (that is, collapsed or hyalinized GBM formations). Towards the cortical interstitium this paraglomerular space has become separated by a layer of sheet-like fibroblast processes (shown in green). (d) The sclerotic process jumps, via the vascular pole, to a neighbouring lobule. Even in late stages of injury perfused capillaries are regularly found within the sclerotic regions. In later stages, In the sclerotic area invaded by cortical fibroblats, fibrosis will appear. (Taken from Kriz et al., 1998 [21])

In the latter stage, the capillary tuft inside the adhesion either collapses or is occluded by hyalinosis, and the podocyte located next to the synechia will degenerate by a variety of mechanisms. Abnormal fluid leakage from perfused capillaries onto/into the outer surface of the glomerulus creates a para-glomerular space. Here, an infiltration of macrophages, lymphocytes and myofibroblasts can be observed, accompanied by a sustained deregulation of PEC proliferation [24, 26]. Later, fibroblast will establish a dense sheet-like fibrous organization to enclose the focus of misdirected filtration, forming a fibrous crescent. PECs play an active role in the progression from cellular to fibrous crescents, producing monocyte chemo-attractants (MIP-1a and MIP-1b) and IL-8, a chemokine involved in the transmigration of neutrophils into the peri-glomerular and intra-glomerular space [27-29]. Furthermore, PECs contribute to the scaring of crescents by producing extracellular matrix molecules and pro-fibrotic growth factors [30-33]. Crescent formation may stop after an entire lobule has been engulfed presenting a segmental synechia. Yet, this process compromises the other lobules leading to global sclerosis [22] (Figure 1).

Podocyte loss and aberrant proliferation of PECs are crucial events for initiating the scar formation and glomerular remodeling process. There are several studies with transgenic animal models that have shown a correlation between the severity and progression of sclerotic lesions and the degree of podocyte loss [19, 34, 35] (Figure 2). When mild podocyte loss is accruing (20% or less) the effects on the glomerular architecture are subtle, that is to say little capsular adhesion formation with transient mild proteinuria and no measurable change in renal function [36]. It can be hypothesized that the remaining podocytes have the capacity to rapidly cover the denudated GBM, due in part to the recruitment of progenitor stem cells from the Bowman's capsule [37, 38]. Podocyte loss of 40% is associated with synechiae formation, FSGS and low-level proteinuria in absence of change in renal function [36]. Probably, the remaining podocytes cannot compensate for the GBM area exposed within the critical time and the scar formation can be seen as result of an inefficacious repair mechanism [36, 38]. When podocyte depletion exceeds 40% an increased proportion of glomeruli with adhesion to the Bowman's capsule, a high level of proteinuria and decreased renal function is observed. Similarly, this has been described in human biopsy material [39, 40].
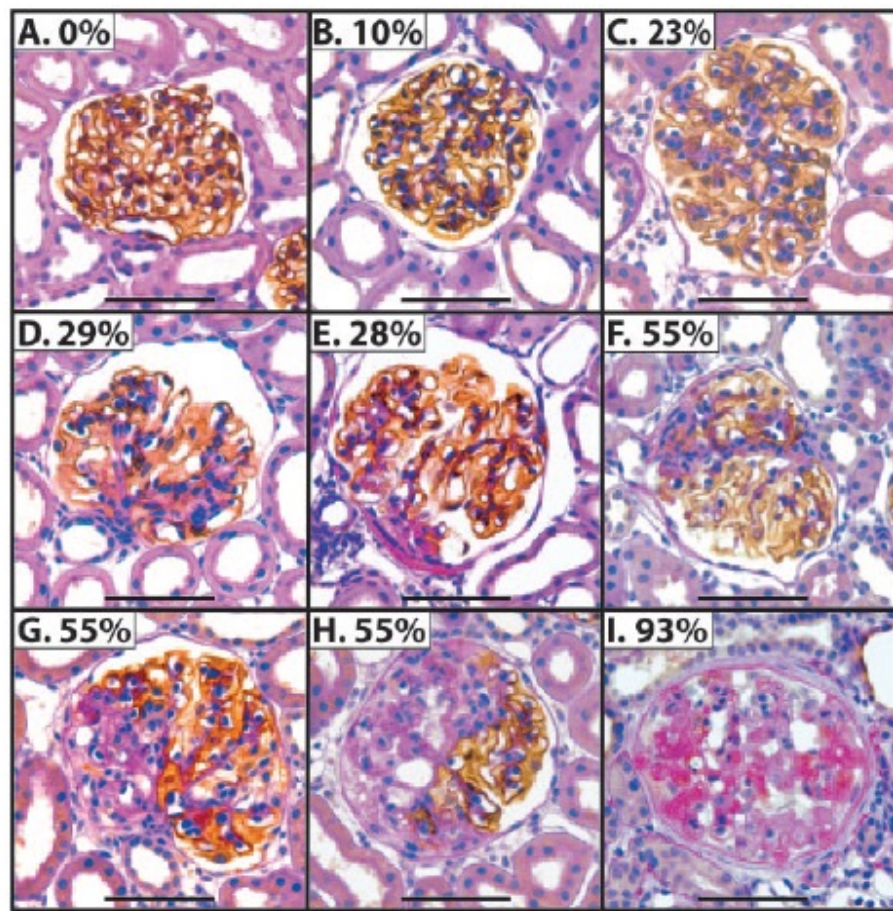
Figure 2. Photomicrographs of glomeruli from rats with increasing podocyte depletion at 28 d. Sections are stained for podocytes by immunoperoxidase anti-GLEPP1 (brown) and counterstained by PAS (pink) and hematoxylin (blue). In the box at the top left of each photomicrograph, the average proportion of podocytes depleted for that animal as counted by WT-1 nuclear staining is shown. The normal small amount of pink-stained mesangial space is shown (A). As podocyte number is depleted by up to 23%, the amount of PAS-positive (pink) space increases (B and C). At 28% podocyte depletion, adhesions between the glomerular tuft and Bowman's capsule can be seen (E). With further podocyte depletion, increasingly larger segments of glomeruli are sclerotic and devoid of podocytes (F through H). With _90% podocytes depleted, some glomeruli contain no detectable podocytes and a collapsing sclerotic appearance (I). We conclude that there was a proportionate change in histologic features in relation to theproportion of podocytes lost in the model. Bars _ 50 _m. (Taken from Wharram et al., 2007 [36])

1.1.2 Focal segmental glomerulosclerosis

Focal segmental glomerulosclerosis is not a single disease but rather a group of clinical-pathologic syndromes sharing a common glomerular lesion and mediated by different types of insult within podocytes [41]. FSGS is characterized by the presence of focal and segmental lesions with mesangial sclerosis, obliteration of glomerular capillaries with hyalinosis and foam cells, adhesion with the glomerular tuft and

Bowman´s capsule, and podocyte hypertrophy [27]. Even though the pathogenesis of FSGS has been the subject of many studies, 80% of FSGS cases are classified as idiopathic (primary), where the cause is unknown, or it is believed that they are related to circulating permeability factors. Recently elevated serum levels of soluble urokinase receptor have been reported in up to 2/3 of patients with primary FSGS. Both, the mechanisms involving this receptor and course of podocyte foot process effacement have been demonstrated [42]. Genetic mutation affecting podocytes proteins have been identified in up to two thirds of the familial and sporadic types of FSGS already present within the first year of life [43]. Most of these mutations, correlate with the nephrotic syndrome and have been found in genes coding for podocyte proteins located in the slit diaphragm (nephrin, podocin and CD2-associated protein) [44-46], cell membrane (β4 integrin, CD151, TRPC6 and lamininbeta2) [47-49], cytosol (PLCE) [50], cytoskeleton (INF2, nonmuscle myosin IIA,ACTN4 and MYo1E) [51-54], nucleus (WT-1) [55, 56] and mitochondria (COQ6) [57]. Other forms of secondary FSGS have been attributed to viral infections (human immunodeficiency virus type 1, parvovirus B19, simian virus 40 and Epstein-Barr virus) [58-61] or to drug abuse (Heroin; IFN-α/β and IFN-γ: lithium; parmidronate; sirolimus; calcineurin-inibitor nephrotoxicity; anabolic steroids)[62-64]. Sclerotic lesions observed in FSGS differ anatomically in their location and quality with respect to glomerular hypercellularity and capillary collapse [41]. The light microscopic morphology and the location of sclerotic lesions are used to define the histological variants of FSGS: cellular variant (hypercellularity of the capillary space), tip variant (lesion involving the tubular pole), perihilar variant (involving sclerosis of the vascular pole), collapsing variant and   not-otherwise-specified (NOS) variant (Figure 3).
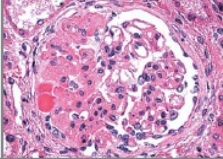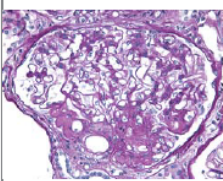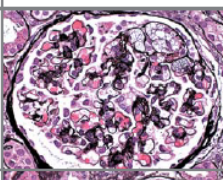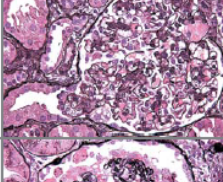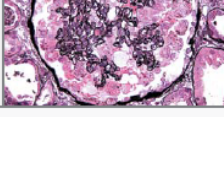
Histologic Subtype	Glomerular Lesion	Defining Features	Associations	Clinical Features
NOS		The usual generic form of FSGS. FSGS(NOS) does not meet defining criteria for any other variant. Foot-process effacement is variable.	Primary or secondary (including genetic forms and other diverse secondary causes). Cross-sectional studies suggest this is the most common subtype. Other variants can evolve into FSGS (NOS) over time.	May present with the nephrotic syndrome or subnephrotic proteinuria.
Perihilar		Perihilar hyalinosis and sclerosis involving the majority of glomeruli with segmental lesions. Perihilar lesions are located at the glomerular vascular pole. In adaptive FSGS, there is usually glomerular hypertrophy (glomerulomegaly). Foot-process effacement is relatively mild and focal, which probably reflects the heterogeneous adaptive responses of glomeruli.	Common in adaptive FSGS associated with obesity, elevated lean body mass, reflux nephropathy, hypertensive nephrosclerosis, sickle cell anemia, and renal agenesis. Predisposition for vascular pole is probably due to normally increased filtration pressures at the proximal afferent end of glomerular capillary bed, which are heightened under conditions of compensatory demand and vasodilatation of the afferent arteriole.	In adaptive FSGS, patients are more likely to present with subnephrotic proteinuria and normal serum albumin levels.
Cellular		Expansile segmental lesion with endocapillary hypercellularity, often including foam cells and infiltrating leukocytes, with variable glomerular epithelial-cell hyperplasia. There is usually severe foot-process effacement.	Usually primary, but also seen in a variety of secondary forms. This is the least common variant. It is thought to represent an early stage in the evolution of sclerotic lesions.	Usually presents with the nephrotic syndrome.
Tip		Segmental lesion involving the tubular pole, with either adhesion to tubular outlet or confluence of podocytes and tubular epithelial cells. Compared with other variants, it has the least tubular atrophy and interstitial fibrosis. There is usually severe foot-process effacement.	Usually primary. Probably mediated by physical stresses on the paratubular segment owing to the convergence of protein-rich filtrate on the tubular pole, causing shear stress and possible prolapse.	Usually presents with abrupt onset of the nephrotic syndrome. More common in white race. Best prognosis, with highest rate of responsivity to glucocorticoids and lowest risk of progression.
Collapse		Implosive glomerular-tuft collapse with hypertrophy and hyperplasia of the overlying visceral epithelial cells. Hyperplastic glomerular epithelial cells may fill the urinary space, resembling crescents. Severe tubular injury and tubular microcysts are common. There is usually severe foot-process effacement.	Primary or secondary to Viruses: HIV-1, parvovirus B19, SV40, EBV, CMV, hemophagocytic syndrome Drugs: pamidronate and interferon Vaso-occlusive disease: atheroemboli, calcineurin inhibitor nephrotoxicity, and chronic allograft nephropathy	Most aggressive variant of primary FSGS with black racial predominance and severe nephrotic syndrome. Worst prognosis, with poor responsivity to glucocorticoids and rapid course to renal failure.

Figure 3. Histological variants of Focal Segmental Glomerulosclerosis. Cytomegalovirus. (CMV), Epstein-Barr virus type 1 (EBV) and Simian virus 40 (SV40). (Taken from D'Agati et al., 2011 [41])

1.1.3 Adriamycin-induced focal segmental glomerulosclerosis

Adriamycin nephropathy is a highly reproducible and robust model of chronic proteinuric renal disease, resulting from selective podocyte injury [65]. In rodents, a single injection of adriamycin, induces kidney damage that mirrors human focal segmental glomerulosclerosis. Adriamycin (doxorubicin) is an anthracycline antibiotic with pleiotropic cytotoxic effects, used for treatment of a wide spectrum of human cancers. It is a DNA intercalating agent, which inhibits the enzyme topoisomerase II and thereby generates free radicals, which induce DNA damage and subsequent cell death [66]. Detailed pharmacokinetic studies showed that adriamycin is not significantly metabolized, however it is rapidly cleared from the plasma, deposited in tissue (mainly in the kidney) and slowly excreted into urine and bile. There is a well-known variability

in the susceptibility across strains due to a single gene defect with recessive inheritance located on the chromosome 16. The susceptibility alleles at this locus are associated with blunted expression of protein arginine methyltransferase7 (Prmt7), a protein implicated in cellular sensitivity to chemotherapeutic agents [67, 68]. BALB/c and derived inbred strains (e.g severe combined immunodeficient mice, SCID) show high susceptibility to adriamycin injection compared to C57BL/c mice who are highly resistant.

1-2 weeks after adriamycin administration, altered renal function and induced thinning of the glomerular endothelium together with specific damage at the filtration barrier, are observed. Increased free radical production [69] in the kidney and changes associated with key proteins of the slit diaphragm (nephrin, podocin and NEPH1) are the main mechanisms of adriamycin functionality [70]. Histological assessments of kidneys from animals injected with adriamycin show severe tubule interstitial inflammation with marked infiltration by immune cells (T and B lymphocytes and macrophages)[65]. However, studies in SCID mice have demonstrated that the structural and functional injury induced by adriamycin does not necessary require immune cell activation [71].

1.1.4 Podocytes

The renal corpuscle is a tuft of capillary loops supported by mesangial cells and surrounded by a basement membrane and podocytes [72, 73]. During nephrogenesis, four different stages of glomerular development are defined: vesicle stage, S-shaped body stage, developing capillary loop stage, and maturing stages (Figure 4). During the vesicle stage, precursor cells of the glomerular and tubular epithelium are joined by occluding junctions at their apices [74]. During the S-shape body stage epithelial precursor cells with apically located tight junction form the immature podocyte precursor population. At this stage, podocyte specific protein expression commences [73]. This includes the expression of podocalyxin and the tight junction protein zonula occludens-1 (ZO-1) and the transcription factors Williams tumor protein-1 (WT-1) and Pod-1 [75-78]. When podocyte precursor like cells enter the capillary loop stage, they lose their mitotic activity and branch into specialized cell architecture which involves a neuron-like complex differentiation process including the formation of foot processes

and slit membrane [73] [79]. The phonotypical conversion occurring during the S-shape body stage is accompanied by the expression of synaptodin [80] and by the reappearance of vimentin [81]. Mature podocytes are polarized cells with three well-defined and separated domains: a cell body, primary process and foot process. The foot processes have three separate membrane platforms: the apical membrane domain, the slit diaphragm and the basal membrane domain. Each domain has a unique function for facing different environments that are both physically and functionally linked to the actin cytoskeleton of the foot processes. The variety of proteins located on the podocyte membrane is indicative for this specialization [82]. There is a multitude of signaling events, including integrin activation and calcium influx, coming from these foot processes which modulate active reorganization of actin filaments and allow podocytes to change their morphology and regulate the permeability of the filtration barrier [83]. Interference with any of the components of the actin cytoskeleton results in foot process effacement and loss of the normal interdigitating patterns, leading to proteinuria.
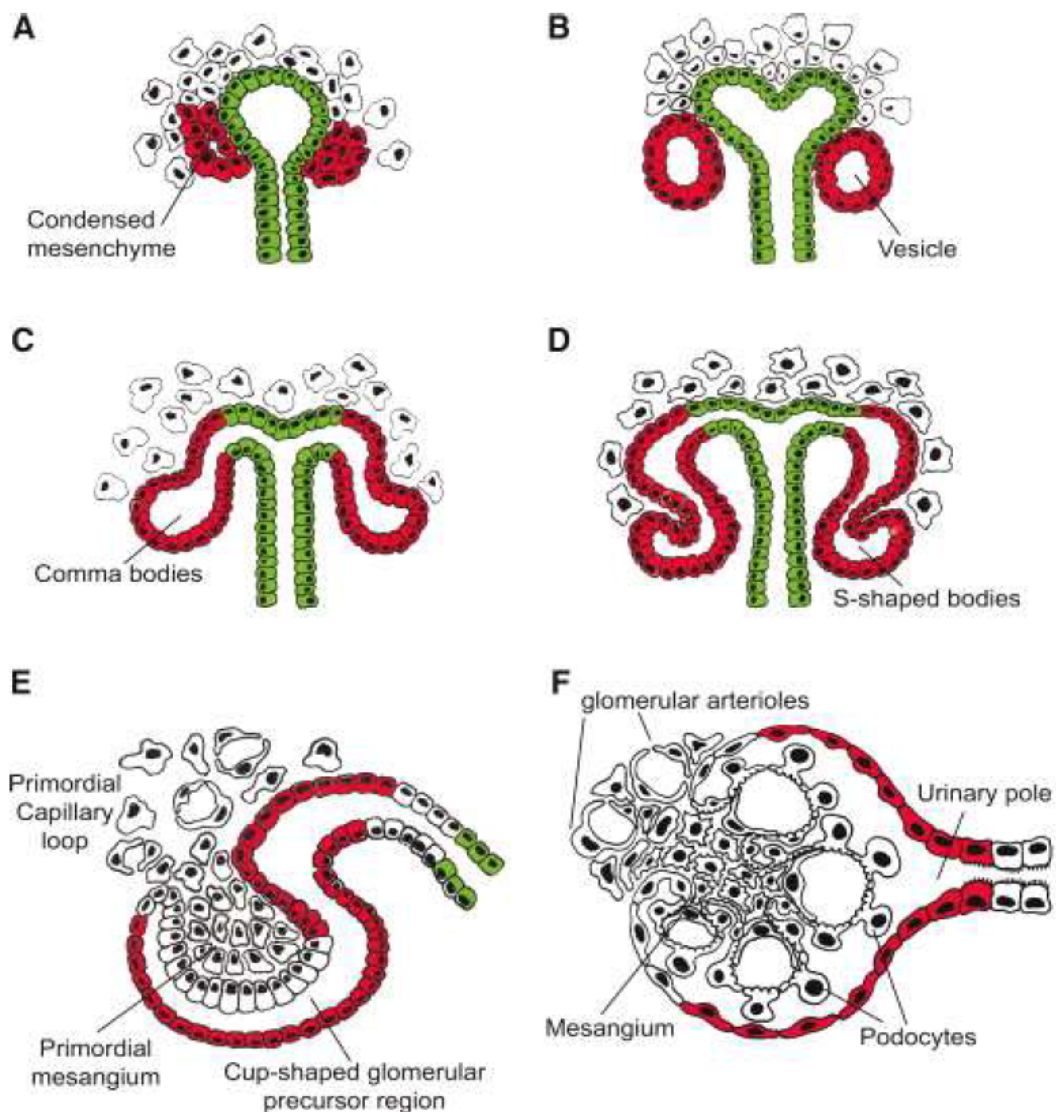
Figure 4. **Development of the nephron.** During the induction of the metanephric mesenchyme, cells condense around the tips of the branching ureteric bud, and convert to an epithelial cell type (MET, mesenchymal-to-epithelial transition). These early epithelial cells form a spherical cyst called the renal vesicle (B), the renal vesicle aggregates to the comma-shaped (C), and then the S-shaped bodies (D). At this stage, the proximal end of the S-shaped body becomes invaded by blood vessel, differentiates into podocytes and parietal epithelial cells, and then generates the glomerular tuft (E, F). Simultaneously, the middle and the distal segments of the S-shaped body that had remained in contact with the ureteric bud epithelium fuse to form a single, continuous epithelial tube and begin to express proteins that are characteristic of tubular epithelia (taken from Romagnani, 2009 [84])

1.1.5 Podocytes and the glomerular filtration barrier

The glomerular filtration barrier is a highly specialized blood filtration interface that displays permeability to small- and midsized solutes in plasma, but restricts the flow of larger plasma proteins into the urinary space (Figure 5). The GFB is a three-

layered structure consisting of endothelial cells, GBM and podocytes [85, 86]. Podocytes, located outside of the glomerular capillary loop, play a crucial role in the formation and maintenance of the glomerular filtration barrier. They have a complex cellular organization consisting of a large cell body leaning out of the urinary space and long cellular extensions (foot processes) that interdigitate with those of neighboring podocytes to cover the outer part of the GBM [85]. Podocyte foot processes are anchored to the GBM through α3βintegrins and β-dystroglycans [87]. These characteristics, interdigitating patterns between foot processes of neighboring podocytes are bridged by a 40nm wide zipper-like slit diaphragm [88]. Podocyte foot processes and the interposed slit diaphragm cover the outer part of the GBM and play a major role in establishing the selective permeability of the glomerular filtration barrier [73]. The GFB is highly permeable to water and small solutes, but the small pore size (5-15nm) of the slit diaphragm limits the passage of larger proteins, for example albumin [89].
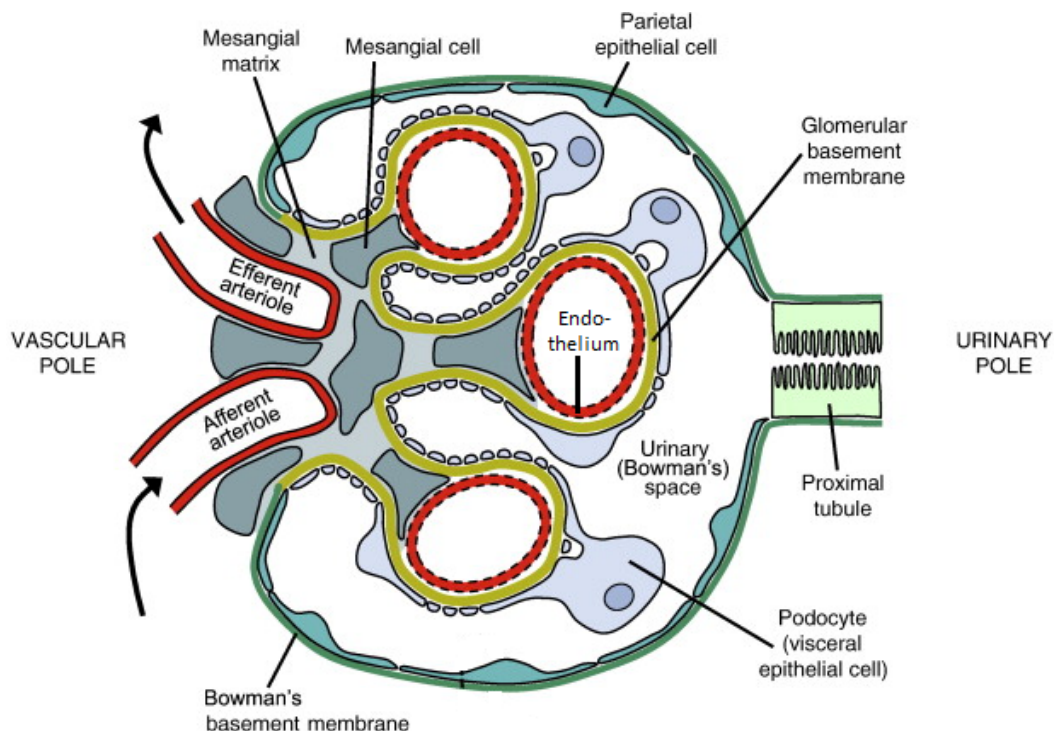
Figure 5 Schematic representations of glomerulus and glomerular filtration barrier. The GFB comprised of fenestrated glomerular endothelial cells, glomerular basement membrane and podocytes. The parietal epithelial cells are present along the Bowman´s basement membrane. (The image was adapted from Leeuwis J.W. *et. al. [90])*

1.1.6 Podocytes and the cell cycle control

During glomerulogenesis podocyte precursors proliferate during the S-shape body stage, but this capacity, within the transition to the capillary stage and the fully differentiated phenotypic switch, is lost. Studies showed that during glomerulogenesis a transient expression of p21 occurs, and the transition from a proliferating immature podocyte to a mature quiescent phenotype coincides with the de novo expression of the CKD inhibitors p27 and p57 [14, 91]. These CKD inhibitors are constitutively expressed in the mature podocyte and they contribute to maintaining a non-proliferating podocyte phenotype [14, 91, 92]. Certain glomerular diseases, like the cellular variant of FSGS, idiopathic CG, and HIVAN have been apparently reported to be associated with abnormal podocyte proliferation. In these diseases a uniformly decreased expression of p27 and p57, accompanied by the de novo expression of p21 in podocytes has been reported [93]. This form of non-reparative proliferation mechanism by podocytes, leading to a disruption of the glomerular architecture, is likely controlled by an aberrant reduction of CDK inhibitor expression, rather than a normal biological function of podocytes [92]. The tight regulation of cell cycle quiescence in podocytes, is needed to guaranty their highly specialized structure and function [94].

1.1.7 Podocytes response to injury: apoptosis or mitotic catastrophe?

Despite strong evidence that podocyte damage and loss is a prerequisite for glomerular sclerosis, the mechanisms through which podocytes respond to injury are still controversial. Based on the literature, it can be hypothesized that, independent of the type of insult, the podocyte responds to injury first by retracting their foot processes and later by detaching from the GBM and/or die [95]. How does podocyte death take place? Although evidence for terminal deoxynucleotidyl transferase mediated dUTP Nick End Labeling (TUNEL)-positive apoptotic podocytes has been reported, these accounts pertain only to particular environmental conditions and to a very low apoptotic rate [96]. Apoptosis of glomerular podocytes has been reported more often in-vitro than in-vivo [97]. Only a few studies, using animal models of progressive glomerular sclerosis, like diabetic mouse models, TGF-β transgenic mouse models and alport mouse models, have demonstrated podocyte apoptosis, detected by TUNEL staining

[98-100]. For example in alport model, characterized by an increased intrarenal expression of TNF-α, it has been observed that treatment with entanercept (TNF-α inhibitor) substantially ameliorates renal function and reduces apoptosis in podocytes (quantified by TUNEL staining). This highlighting the role of TNF-α in mediating apoptosis as a putative pathway of podocyte death [100]. So far, however, there is little scientific evidence supporting apoptosis as a general pathway of podocyte death in-vivo, suggesting an alternative way for podocyte death. Podocytes are terminally differentiated post-mitotic cells, regulating tightly their quiescent cell cycle. This is a prerequisite to guaranty their highly specialized structure and function. The development of an altered proliferative podocyte phenotype, bypassing the cell cycle check points, can be observed in certain glomerular diseases. This might represent a general mechanism of podocyte response to injury, ultimately leading to death [101-104]. A recent study reported that forced entry in mitosis is a trigger for *mitotic catastrophe* in podocytes, because these cells, even if they can initiate DNA synthesis and chromosome segregation, cannot complete cytokinesis due to poor expression of Aurora Kinase B, which is essential for this process [95, 105, 106] (Figure 6). Abnormal mitotic podocytes expressing histone H3 were observed in adriamycin-induced FSGS models and podocyte death through catastrophic mitosis was prevented by treatment with Notch inhibitors. This Notch activation mediated down regulation of cell cycle inhibitors that force podocytes to progress toward mitosis [105]. Forced cell cycle re-entry of podocytes has been described as a consequence of conditional over expression of telomerase reverse transcriptase enzyme. Subsequent regulation of Wnt signaling resulted in collapsing glomerulopathy [107].
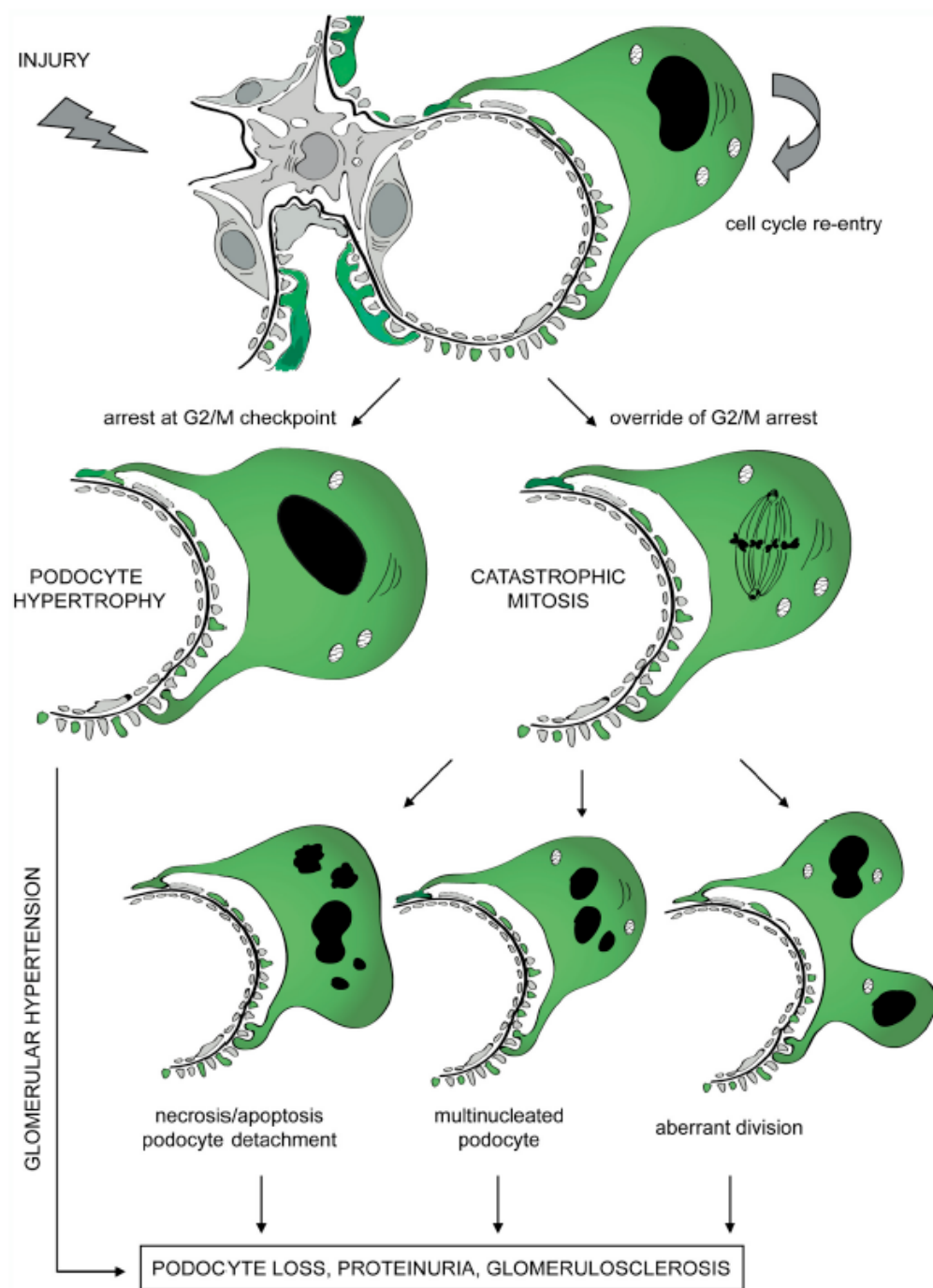
Figure 6. Pathological activation of podocyte cell cycle induces re-entry into G1 and S-phases and initiation of DNA replication. Podocytes complete the DNA synthesis but cannot proceed through the M phase owing to the activation of mitotic catastrophe. Cells arrested in mitosis can have different fates: a) increase their size thus becoming hypertrophic; b) when division cannot be complete and cytokinesis fails, cells with gross nuclear alterations (multinucleation) are generated which quickly undergo "mitotic death" program; c) cells can exit mitosis containing a variable number of nuclei or micronuclei; these cells are viable because lethal pathway is not executed until cells reach interphase of the next cell cycle, but are unstable and detach from the GBM; in this case, cell death can occur in a delayed fashion even after years; d) when the aberrant division is productive aneuploidy cells form; most of these are unviable, owing to chromosomal rearrangements that result in progressive detachment to eliminate genomically unstable cells. (Taken from Lasagni et.al 2013)[104]

1.1.8 Podocytes and parietal epithelial cells

Besides visceral epithelial cells and their major role in maintaining the glomerular filtration barrier, little attention has been given to the other glomerular epithelial cells: PECs of the Bowman' s capsule. Sir William Bowman first described these cells in 1842, as "flattened, inconspicuous cells pressed against the Bowman's capsule. PECs derive from the metanephric mesenchyme and their phenotype diverges from that of podocytes at the latter stages of kidney development [74, 108]. During the S- shaped body stage the Bowman's space begins to form, limited outside by a narrow band of PECs, and inside by a crown of visceral epithelial cells, the future podocytes [84, 109, 110]. During nephrogenesis both glomerular epithelial progenitors express common transcription factors like Pax-2, WT-1 and the keratin-containing intermediate filament, cytokeratin. Together with the acquisition of a differentiated phenotype, podocyte lose Pax-2 expression, but continue to express WT-1 and begin to express vimentin instead of cytokeratin. [111, 112] By contrast, during maturation, PECs lose WT-1 expression, but continue to express Pax-2 and cytokeratin proteins [27]. In the past, the close resemblance between PECs and podocytes has restricted researchers to distinguish these two cell types only on the basis of anatomical criteria. Recently discovered specific markers and the advent of genetic tagging has improved the characterization of their distinct role in renal physiology and pathology [25, 110]. Mature PECs express cadherins, a variety of tight junction proteins (like claudins), occludins and the Pax-2 and Pax-8 [113]. PECs form a monolayer lining on the Bowman's basement membrane, which resembles squamous epithelial cells, with a small cell body size ranging in thickness from 0.1 to 0.3 μm, increasing to 2.0–3.5 μm at the nucleus [114]. In-vivo and in-vitro studies have reported that the PECs monolayer might function as a final permeability barrier to the urinary filtrate [115] Scanning electron microscopy studies showed that PECs possess microvilli and primary cilia which are constantly exposed to flow from the glomerular filtrate, giving to PECs a mecchano-sensing function through its cilia [114, 116]. In humans the PEC population has been isolated and characterized as a stem cell population, which shows the ability to produce new podocytes, both in-vivo and in-vitro, opening prospective of new regenerative therapies. [117].

1.1.9 Podocytes regeneration from glomerular progenitors

Unlike other organs, such as liver or skin, the kidney, particularly the glomerulus, has been classically considered as an organ with minimal cellular turnover and low capacity for regeneration. Mesangial and endothelial cells have been reported to have the capacity to proliferate and replace the loss of neighboring cells upon insult, but this does not apply to visceral epithelial cells. Podocytes are terminally differentiated cells and are unable to proliferate, which might explain how the loss of such specialized cells is a common cause of kidney failure [38]. Data from experimental models have demonstrated that a regression of glomerulosclerosis can occur by increasing the number of podocytes, yet the underlying mechanisms are still poorly understood. Since podocytes cannot undergo mitosis, new podocytes might derive from a regeneration process rather than from podocyte proliferation [38, 118, 119]. However, the presence and biological role of kidney stem cells has been in debate.[120-122]. Recently, it has been proved that adult human glomeruli contain resident stem cell populations and committed progenitor cells localized at the urinary pole of the Bowman's capsule. This population is identified by the presence of CD24 and CD133 [84, 123, 124] and exhibits self-renewal properties. Further, they have the potential to either differentiate into podocytes or into tubular cells, in-vitro and in-vivo [38, 125]. Other studies using parietal epithelial tagging in mouse models confirm the findings reported on humans [120]. They were able to demonstrate that such cells proliferate and differentiate along the urinary space and move to the vascular stalk, generating neo-podocytes. However, in glomerular disorders, characterized by acute or severe podocyte loss, the regenerative capacity of epithelial glomerular stem cells is inadequate because of an imbalance between the proliferative response and the degree of damage [16, 126]. Glomerular epithelial stem cells display different regenerative potentials throughout distinct stages of their life and are modulated by the surrounding environment [127, 128]. In addition, crescentic glomerulonephritis or collapsing glomerulopathy show aberrant migration and excessive proliferative response by glomerular epithelial stem cells. This reflects the inability to restore lost podocytes, contributing to crescent formation and glomerulosclerosis [25, 33, 37].

1.2 Viral infection and Glomerulonephritis

Viral infections can cause a large spectrum of nephropathies. Several mechanisms are involved in the pathogenesis of virus-related nephropathy:

- direct cytopathogenic effects due to the tropism of the virus in the kidney
- induction of abnormal circulating immune complexes involving viral antigens or endogenous antigens modified by viral infection and host autoantibodies
- expression of viral proteins in tissues, inducing cell death and release of proinflammatory cytokines and chemokines.

Different viral infections can cause different nephropathies. In acute glomerulonephritis, direct viral infections of the glomerulus can induce proliferative changes, following the release of inflammatory cytokines [129]. Hepatitis A virus infections can cause an acute post infection glomerulonephritis with a pathology resembling IgA nephropathy [130]; Epstein-Barr virus and Parvovirus B19 (PVB19) infections have been associated with acute glomerulonephritis [131, 132].

PVB19 infections are also associated with chronic forms of glomerulonephritis, along with human immunodeficiency virus (HIV), Hepatitis B (HBV) and Hepatitis C (HCV) infections. Persistent virus infections provide continuous antigenic stimulation, resulting in antibody production and formation of immune complexes outside the kidney or in situ [133, 134]. A direct effect of viral proteins has been proved to increase inflammatory mediator production locally, resulting in glomerular sclerosis [129, 135]. Membranoproliferative glomerulonephritis (MPGN) is the most common HCV-related nephropathy, usually in the context of cryoglobulinemia [136, 137] whereas chronic HBV infection can cause IgA nephropathy. [138, 139]. Besides the classical HIV-associated nephropathy (HIVAN), HIV infection can give rise to a wide spectrum of glomerular lesion. In the course of HIV infection, has been reported a diffuse proliferative-mesangiocapillary glomerulonephritis, with predominantly mesangial immune-complex deposition, resembling lupus nephropathy [140]. Additionally, renal biopsy data from HIV patients with renal disease show that podocytes are infected with the virus [141], even in absence of the classical HIV receptors CD4, CXCR4 and CCR5, indicating that the viral infection is the cause of podocyte dysfunction [142]. PVB19 is also associated with chronic glomerulonephritis, particularly with collapsing glomerulonephritis. Here, viral DNA has been detected in glomerular podocytes and PECs [58].

1.2.1 Virus-induced focal segmental glomerulosclerosis: HIV-associated nephropathy

HIV-associated nephropathy is the most common cause of chronic kidney failure and end stage renal disease seen in patients with acquired immunodeficiency syndrome (AIDS)[143]. The collapsing variant of focal segmental glomerulosclerosis, together with tubular interstitial damage and focal prominent interstitial inflammatory cellular infiltrates are the most characteristic pathological changes in HIVAN. In most cases, all the glomeruli are affected by extensive collapse of the glomerular capillary lumen and a prominent hyperplasia of podocytes [61, 144].

Nearly 90% of the patients affected with HIVAN are African Americans; the prevalence of HIVAN among the African Americans has been correlated with strong genetic predisposition linked to African descent. Genetic studies have identified two genetic loci associated with susceptibility to HIVAN; polymorphisms in the MYH9 gene, expressed in visceral epithelial cells, which encodes nonmuscle myosin heavy chain IIA and in the neighboring gene APOL1, which encodes apolipoprotein L1 [145-147]. However, these studies did not elucidate any biological mechanism for the increased risk of FSGS associated with these genetic variants.

A direct role for HIV infections in the pathogenesis of HIVAN has been demonstrated in animal models (Tg26 HIV-transgenic mouse) and subsequently in human kidney tissue [141, 148]. Animal models and in-vitro studies have elucidated the importance of the viral gene *nef* in the development of glomerular lesions correlated with podocyte changes [149, 150]. Further studies suggest that renal epithelial cells, which do not express CD4 or the traditional co receptors for HIV, might be able to support low level viral replication, although there is no evidence of productive infection in these *in-vitro* system [151, 152].

1.2.2 Interferons type I-induced focal segmental glomerulosclerosis

Interferons (IFNs) are potent inflammatory cytokines with distinct functions and targets. The IFNs family is dived into two main groups, type I and type II IFNs. IFN-α and IFN-β, belongs to type I IFNs and virally infected cells usually produce them. The type I IFNs response is crucial for the control of viral infections. They induce cellular changes in neighboring cells that prevent viral replication and protein synthesis and they activate the adaptive immune system [63, 153]. Endogenous production is

strictly regulated by the innate immunity pattern recognition receptors, and aberrant IFNs type I production is associated with autoimmune disease like Systemic lupus erythematosus (SLE)[154]. Exogenous administration of IFN-α is used as a therapeutic agent for the treatment of HBV and HCV infections, follicular lymphoma and AIDS related Kaposi sarcoma. IFN-β , is indicated and approved for the treatment of multiple sclerosis (MS). Type I IFNs treatment is associated with renal adverse effects, like minimal change disease and FSGS [155-160]. However, reports on FSGS and collapsing FSGS have increased during the past years.

IFNs are known to play a central role in innate and adaptive immune responses through the activation of innate and adaptive immune cells [161]. Activation and recruitment of lymphocytes and macrophages are key processes in inflammatory kidney disease associated with the FSGS scenario, like in lupus nephritis [154, 162]. In addition, it has been shown that podocytes have the receptor for IFN-α and IFN-β, suggesting a primary cytotoxic effect of IFNs on podocytes [41].

Table 4. Published reports of FSGS after treatment with IFN type I (taken and adapted from Markowitz et.al 2010 [62]).

IFN type	Renal presentation	Renal biopsy findings
α	Nephrotic Syndrome, Acute renal failure	Focal segmental glomerulosclerosis
α –2a	Nephrotic Syndrome, Acute renal failure	Focal segmental glomerulosclerosis
α–2b	Nephrotic Syndrome, Acute renal failure	Focal segmental glomerulosclerosis
α	Nephrotic Syndrome, Acute renal failure	Focal segmental glomerulosclerosis
α	Nephrotic Syndrome, Acute renal failure	Focal segmental glomerulosclerosis
α	Nephrotic Syndrome, Acute renal failure	Focal segmental glomerulosclerosis
α	Nephrotic Syndrome, Acute renal failure	Focal segmental glomerulosclerosis
α	Nephrotic Syndrome,	Focal segmental glomerulosclerosis
α –2b	Nephrotic Syndrome	Focal segmental glomerulosclerosis
α	Nephrotic Syndrome, Acute renal failure	Collapsing Focal segmental glomerulosclerosis
α	Nephrotic Syndrome, Acute renal failure	Collapsing Focal segmental glomerulosclerosis
α	Acute renal failure	Collapsing Focal segmental glomerulosclerosis
β	Nephrotic Syndrome	Collapsing Focal segmental glomerulosclerosis

1.3 Innate immune recognition in the kidney

The innate immune system plays a crucial role in disease pathology being the first response to pathogens and to tissue injury. This first line of defense is performed via germline-encoded receptors, expressed by macrophages, lymphocytes, dendritic cells, monocytes, neutrophils and natural killer cells, among others [163, 164]. These receptors, designated as pattern recognition receptors (PRRs), recognize several

pathogen-associated molecular patterns (PAMPs) displayed by different bacteria, viruses, and parasites, as well as several putative hosts derived endogenous ligands (DAMPs) [165-167]. There are several distinct classes of PRRs, including transmembrane proteins such as toll-like receptors (TLRs), as well as cytoplasmic proteins such as retinoic acid-inducible gene (RIG)-I-like receptors (RLRs) and nucleotide-binding oligomerization domains containing (NOD)-like receptors (NLRs) [168-170] (Figure 7).

TLRs are transmembrane receptors characterized by an extracellular domain with leucine-rich repeats and a cytoplasmic signaling domain termed the toll-interleukine 1 receptor (TIR)[171]. According to their localization, these receptors are divided into two categories: those expressed on the cell surface (TLR-1, -2,-4,-5,-6,-10,-11,-12 and 13) mainly recognizing microbial components such as lipids, and those found exclusively in intracellular compartments (TLR-3,-7,-8 and -9) recognizing microbial nucleic acids [172]. When activated, TLRs trigger intracellular signaling pathways via MyD88 (Myeloid differentiation primary response gene 88) or via TRIF (TIR domain containing adapter inducing IFN-β), which culminate in the synthesis of a broad range of molecules through the NFkB (nuclear factor kappa-light-chain-enhancer of activated B cells) or AP-1 (activator protein 1) pathways [164, 173, 174]. Intrinsic renal cells do not express all TLRs. The intracellular receptor for TLR-3 has been reported to be expressed in mesangial cells and podocytes, triggering pro-inflammatory cytokine production [175, 176]. The LPS receptor TLR-4 is expressed in podocytes [177] as well as in tubular cells, which also express TLR-2. Systemic exposure to TLR-4 and TLR-2 ligands can aggravate kidney diseases, as displayed by the nephrotoxic serum nephritis model and by renal ischemia reperfusion injury, both of which primarily elicit intra renal cytokine release and glomerular autoantibody production [178, 179].

The retinoic acid-inducible gene (RIG)-I-like receptors, RIG-I and MDA5, are cytosolic receptors for viral RNA and DNA respectively. These receptors are associated with mitochondrial-associated adaptor proteins, which interact with the kinases TBK1 and IKKε. These in turn trigger the phosphorylation of IRFs and induce type I IFN production [180, 181]. Kidney biopsies from Lupus patients show co-localization of RIG I proteins into the mesangium. Cultured glomerular endothelial cells, mesangial cells and tubular epithelial cells express basal levels of RIG-I and MDA5 in culture, however the role of these nucleic acid receptors, in regards to intrarenal nucleic acid

recognition, is still unclear [182, 183]. Recently, RIG I has been reported to be also expressed in glomerular podocytes [175].

The cytosolic NLRs include NOD1 and NOD2 (nucleotide-binding oligomerization domain1 and 2) receptors that recognize intracellular molecules that originate from bacterial infection, like peptidoglycan [184]. When these receptors recognize their ligands, they oligomerise and activate NFKB with subsequent production of TNF-α and IL-6 [185]. Intrinsic renal expression of NOD receptors has been shown in tubular cells, playing a role in sustaining inflammation during IRI [186].
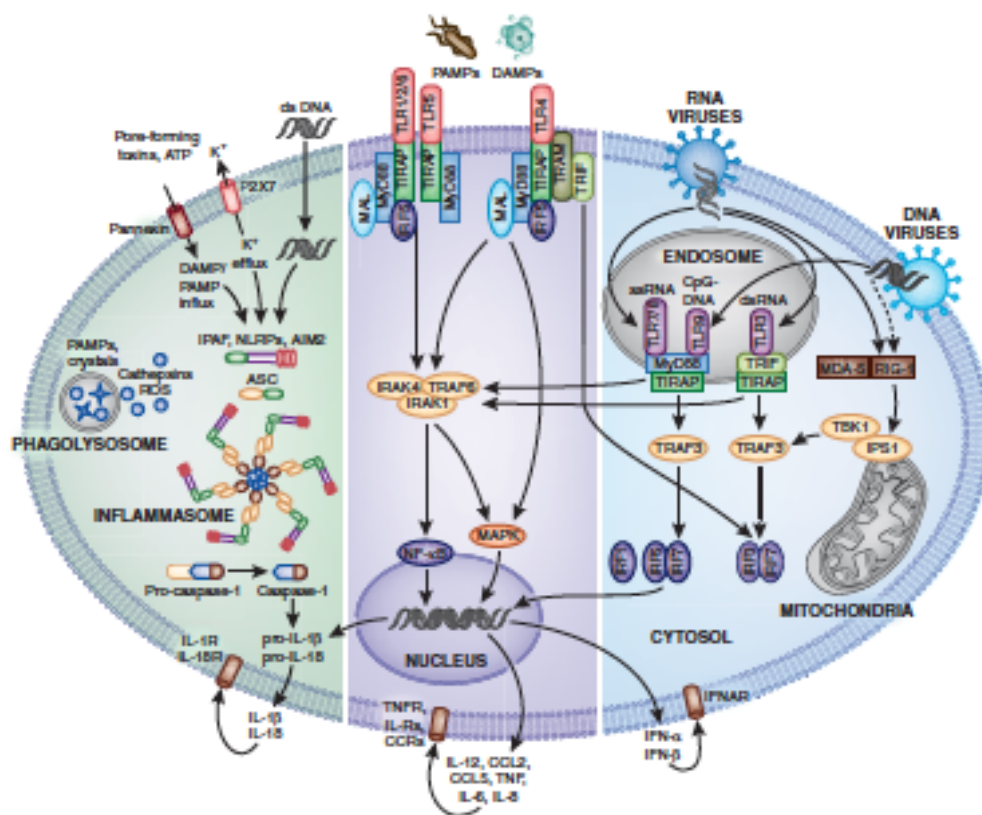
Figure 7 How pattern recognition receptors induce innate immunity. Several groups of extracellular or intracellular innate pattern recognition receptors exist. TLR-1/2/4/5/6 recognizes microbes at the cell surface. TLR3/7/8/9 recognize viral and bacterial nucleic acids in intracellular endosomes. All TLRs use the intracellular adaptor MyD88 for downstream signaling, except for TLR3, which uses TRIF. TLR4 uses MyD88 and TRIF. All TLRs can induce the expression of NF*k*B-dependent genes, including most proinflammatory cytokines and chemokines. TLRs also induce the pro cytokines IL-1 and IL-18 (signal 1). These cytokines need caspase-1 activation as a second step before they can be released. Caspase-1 activation is under the control of the inflammasomes. Type I IFNs represent a separate class of antiviral cytokines. Release of type I IFNs is strongest upon recognition of viral nucleic acids via TLR3/7/8/9 in endosomes or via cytosolic RNA and DNA receptors. The latter signal via the mitochondrial adaptor interferon promotor stimulator 1, but all pathways finally activate the transcription factors IRF3/7 for expression of the type I IFNs. (taken from Anders et al., 2011 [187])

1.3.1 Interferon type I

IFN-α and IFN-β central mediators of antiviral immunity and they belong to the type I interferon family. These cytokines are specialized in coordinating immunity against viruses and other intracellular infections. Type I IFNs are produced by infected cells and act in an autocrine and paracrine manner to signal the presence of a viral infection [161]. Both IFN-α and IFN-β share a common heterodimeric receptor (IFNAR1/2), however they have different properties [188]. Despite the fact that the type I IFN receptor is broadly expressed in every organ, type I IFN response has been reported to be stronger in liver, kidney and spleen compared to other organs [189]. By signaling through the type I IFN receptor, IFNs activate the inducible expression of hundreds of genes called ISGs that together establish the ''antiviral state'' on target cells [190-192]. The antiviral state leads to the transcription of various cellular antiviral genes coding for host defense proteins. In addition to cell-intrinsic effects that confer the antiviral state, IFNs type I regulate the elimination of virally infected cells. The IFNs type I system is linked to a variety of effector responses of innate and adaptive immunity [161]. Type I IFN activates and regulates natural killer and cytotoxic T cells and facilitates dendritic cell cross presentation of viral antigens to CD8+ lymphocytes [193]. The mechanisms whereby type I IFNs orchestrate the antiviral adaptive immune response are diverse and include the production of chemokines and cytokines that positively regulate cytotoxic cell numbers and activities [194, 195]. Plasmacytoid dendritic cells are the main type I IFNs producer, however many other cells have been reported to produce large amounts of IFNs during viral infection. In the kidney, both mesangial and endothelial cells are the major source of intrarenal IFNs production. Classically, only collapsing FSGS and lupus nephritis have been directly correlated to the type I IFN response, however, there are many other non-viral kidney diseases related to type I IFN [181]. Animal studies have documented the functional significance of type I IFN in murine models of both lupus nephritis and serum nephritis [196, 197]. Type I IFN receptor-deficient mice have been shown to display a marker suppression of disease activity in serum nephritis models and genetic mouse models eliciting lupus nephritis [198, 199]. Further studies report that augmenting IFN-α release amplifies antibody triggered nephritis, contributing to the disease pathology and promoting end-

organ disease [197]. In contrast, injection of IFN-β has been shown to ameliorate lupus nephritis in MRF-*Fas-lpr* mouse models and in nephritis rat models [200, 201]. However, IFN-β, but not IFN-α, has well documented immunosuppressive properties [202, 203]. This might explain contradictions in findings between data reported on nephritis induced in type I IFN receptor-deficient mice and human data of patients that developed FSGS because of IFN α/β therapy.

In summary, podocyte loss and PEC homeostasis are the major hallmark in the pathogenesis of FSGS. Thus, it is necessary to investigate the mechanisms, molecules and pathways that promote loss and deregulation of glomerular epithelial cells and their progenitors in the context of viral glomerular damage. IFN-α and IFN-β are potent antiviral cytokines, secreted in large amounts during viral infections, which target somatic and immune cells. Both of these cytokines have been found to be associated with the development of collapsing FSGS. Yet, so far their role in viral glomerulonephritis has not been studied in detail. Within the scope of this thesis, the role of IFN α/β in FSGS shall be analyzed and discussed.

2. Hypotheses

Based on the above literature, systemic viral infections are frequently associated with several kidney diseases. Some viruses cause glomerulopathies also by directly infecting glomerular epithelial cells. For example, human immunodeficiency virus (HIV) and parvoviruses can infect glomerular epithelial cells, i.e. podocytes and PECs. Beside the clinical relevance of viral glomerulonephritis, little is known about the impact of nucleic acid recognition and its consequence (type I IFNs) on glomerular epithelial cells.

Therefore we hypothesized that during glomerulonephritis, e.g HIVAN, viral replication inside podocytes and PECs would trigger IFN-dependent antiviral responses, the process that contributes to glomerular damage. To address this hypothesis we employed an in-vitro model of synthetic viral infection using nucleic acid complexes with lipofectamine to simulate viral infection in glomerular cells. Furthermore we studied the functional impact of nucleic acid on glomerular epithelial cells and their progenitors. Once viral nucleic acids reach the intracellular cytosol, they are recognized by distinct recognition receptors that induce massive secretion of interferon IFN-α and IFN-β. Generally, the induction of IFN-α and IFN-β is a central element of the host`s antiviral response. Even though IFN type I receptor deficiency has been reported to protect mice from glomerulonephritis [199, 204, 205], other studies have documented anti-proteinuric properties of IFN-β in different glomerular diseases model in immunocompetent rodents [201] [200].

Assuming that in course of viral glomerulopathies the podocytes and PECs are exposed to IFN-α and IFN-β, we seeked to elucidate the mechanisms of type I IFNs affecting podocyte and PEC homeostasis and decipher whether they exhibit protective or detrimental properties. We hypothesized that both IFN-α and IFN-β modulate podocytes and PECs homeostasis. To address this hypothesis we first established an in-vitro study to investigate the effect of both cytokines on podocytes permeability, using this parameter to evaluate glomerular filtration barrier. Furthermore we investigated the influence of both cytokines on podocyte survival. Next we studied the functional and structural impact of both type I IFNs on PECs homeostasis in-vitro, by proliferation, migration and differentiation assay.

Finally, to validate our in-vitro findings we evaluated the functional role of IFN-α and IFN-β in an adriamycin-inducing nephropathy model which mirrors FSGS. In

order to study the local effect of these cytokines we first established this model in non-immunocompetent mice (SCID) and later we confirmed our findings in immunocompetent mice.

.

3. Material and Methods

Instruments and Chemicals

Instruments

<u>Balance:</u>

Analytic Balance, BP 110 S	Sartorius, Göttingen, Germany
Mettler PJ 3000	Mettler-Toledo, Greifensee, Switzerland

<u>Cell Incubators:</u>

Type B5060 EC-CO_2	Heraeus Sepatech, München, Germany

<u>Centrifuges:</u>

Heraeus, Minifuge T	VWR International, Darmstadt, Germany
Heraeus, Biofuge primo	Kendro Laboratory Products GmbH, Hanau, Germany
Heraeus, Sepatech Biofuge A	Heraeus Sepatech, München, Germany

<u>ELISA-Reader:</u>

Tecan, GENios Plus	Tecan, Crailsheim, Germany

<u>Electric Cell-substrate Impedence Sensing</u>

ECIS	Applied BioPhisics, New York, USA

<u>Confocal microscopy</u>

LSM501 META laser	CarlZeiss, Jena, Germany

<u>TaqMan Sequence Detection System:</u>

ABI prism ™ 7700 sequence detector	PE Biosystems, Weiterstadt, Germany

Other Equipments:

Nanodrop	PEQLAB Biotechnology GMBH, Erlangen, Germany
Cryostat RM2155	Leica Microsystems, Bensheim, Germany
Cryostat CM 3000	Leica Microsystems, Bensheim, Germany
Homogenizer ULTRA-TURRAX T25	IKA GmbH, Staufen, Germany
Microtome HM 340E	Microm, Heidelberg, Germany
pH meter WTW	WTW GmbH, Weilheim, Germany
Thermomixer 5436	Eppendorf, Hamburg, Germany
Vortex Genie 2™	Bender & Hobein AG, Zürich, Switzerland
Water bath HI 1210	Leica Microsystems, Bensheim, Germany

3.1.2 Chemicals and reagents

RNeasy Mini Kit	Qiagen GmbH, Hilden, Germany
RT-PCR primers	PE Biosystems, Weiterstadt, Germany

Cell culture:

DMEM-F12 medium	Sigma, Munich, Germany
RPMI-1640 medium	GIBCO/Invitrogen, Paisley, Scotland, UK
FBS	Biochrom KG, Berlin, Germany
FBS Hyclone	ThermoScientific, UT, USA
EBM	Lonza, Cologne, Germany
EGM-MV	Lonza, Cologne, Germany
Dulbecco's PBS (1×)	PAA Laboratories GmbH, Cölbe, Germany
Trypsine/EDTA (1×)	PAA Laboratories GmbH, Cölbe, Germany
Penicillin/Streptomycin (100×)	PAA Laboratories GmbH, Cölbe, Germany
All-trans retinoic acid	Sigma, Munich, Germany
Vitamin 3D	Sigma, Munich, Germany

Antibodies:

p21	Santa Cruz Biotechnology, Santa Cruz, CA
CD68	Abcam, Cambridge, UK

Claudin-1	Invitrogen, Carlsbad, CA
Nephrin	Santa Cruz Biotechnologies, Santa Cruz, CA
WT-1	Santa Cruz Biotechnologies, Santa Cruz, CA
P-H3	Abcam, Cambrige, UK
Alexa Fluor 488 anti-rat IgG	Invitrogen, Darmstadt, Germany
Alexa Fluor 546 anti-rabbit IgG	Invitrogen, Darmstadt, Germany
Alexa flour 488 anti-goat	Invitrogen, Darmstadt, Germany
Alexa Fluor 488 anti-mouse IgG1	Invitrogen, Darmstadt, Germany
Alexa Fluor 546 anti-mouse IgG1	Invitrogen, Darmstadt, Germany
HRP linked Anti-Rabbit secondary	Cell signaling, Danvers, MA
HRP linked Anti-Mouse secondary	Cell signaling, Danvers, MA
HRP linked Anti-Goat secondary	Dianova, Hamburg, Germany
β-Actin	Cell signaling, Danvers, MA
CD3+	AbD Serotec, Düsseldorf, Germany

Elisa Kits:

Mouse Albumin	Bethyl Laboratories, TX, USA
Creatinine FS	DiaSys Diagnostic System, GmBH, Holzheim, Germany

Chemicals:

Acetone	Merck, Darmstadt, Germany
AEC Substrate Packing	Biogenex, San Ramon, USA
Bovines Serum Albumin	Roche Diagnostics, Mannheim, Germany
Skim milk powder	Merck, Darmstadt, Germany
DEPC	Fluka, Buchs, Switzerland
DMSO	Merck, Darmstadt, Germany
Diluent C for PKH26 dye	Sigma-Aldrich Chemicals, Germany
EDTA	Calbiochem, SanDiego, USA
30% Acrylamide	Carl Roth GmbH, Karlsruhe, Germany
TEMED	Santa Cruz Biotechnology, Santa Cruz, CA
Eosin	Sigma, Deisenhofen, Germany
Ethanol	Merck, Darmstadt, Germany

Formalin	Merck, Darmstadt, Germany
Hydroxyethyl cellulose	Sigma-Aldrich, Steinheim, Germany
HCl (5N)	Merck, Darmstadt, Germany
Isopropanol	Merck, Darmstadt, Germany
Calcium chloride	Merck, Darmstadt, Germany
Calcium dihydrogenphosphate	Merck, Darmstadt, Germany
Calcium hydroxide	Merck, Darmstadt, Germany
MACS-Buffer	Miltenyl Biotec, Bergisch Gladbach, Germany
Beta mercaptoethanol	Roth, Karlsruhe, Germany
Sodium acetate	Merck, Darmstadt, Germany
Sodium chloride	Merck, Darmstadt, Germany
Sodium citrate	Merck, Darmstadt, Germany
Sodium dihydrogenphosphate	Merck, Darmstadt, Germany
Penicillin	Sigma, Deisenhofen, Germany
Roti-Aqua-Phenol	Carl Roth GmbH, Karlsruhe, Germany
Streptomycin	Sigma, Deisenhofen, Germany
Tissue Freezing Medium	Leica, Nussloch, Germany
Trypan Blue	Sigma, Deisenhofen, Germany
Oxygenated water	DAKO, Hamburg, Germany
Xylol	Merck, Darmstadt, Germany

Miscellaneous:

Cell death detection (TUNEL) kit	Roche, Mannheim, Germany
Microbeads	Miltenyl Biotech, Germany
Cell Titer 96 Proliferation Assay	Promega, Mannheim, Germany
LS+/VS+ Positive selection columns	Miltenyl Biotec, Bergish Gladbach, Germany
Preseparation Filters	Miltenyl Biotec, Bergish Gladbach, Germany
Super Frost® Plus microscope slides	Menzel-Gläser, Braunschweig, Germany
Needles	BD Drogheda, Ireland
Pipette's tip 1-1000µL	Eppendorf, Hamburg, Germany
Syringes	Becton Dickinson GmbH, Heidelberg, Germany
Plastic histocasettes	NeoLab, Heidelberg, Germany

Tissue culture dishes Ø 100x20mm   TPP, Trasadingen, Switzerland

Tissue culture dishes Ø 150x20mm   TPP, Trasadingen, Switzerland

Tissue culture dishes Ø 35x10mm   Becton Dickinson, Franklin Lakes, NJ, USA

Tissue culture flasks 150 cm2   TPP, Trasadingen, Switzerland

Tubes 15 and 50 mL   TPP, Trasadingen, Switzerland

Tubes 1.5 and 2 mL   TPP, Trasadingen, Switzerland

All other reagents were of analytical grade and are commercially available from Invitrogen, SIGMA or ROTH.

3.1 In-vitro methods

3.1.1 Isolation and cultured of human renal progenitors CD24+CD133+

Renal progenitor cells were characterized and isolated from human renal biopsies as described [206]. In brief, kidney biopsies were processed and sieved for isolating glomeruli (60, 80, and 150 mesh). During this process the glomeruli were separated from the tubules through graded mesh screening. To enrich the number of capsulated glomeruli non-enzymatic digestion was performed. The glomerular suspension was collected and plated on fibronectin-coated dishes (10 μg/ml; Sigma-Aldrich). After 4 to 5 days in culture, isolated glomeruli adhered to the plate, resulting in cellular outgrowth. Glomeruli were detached, and the cellular outgrowth was cultured as a bulk. The cells were cultured with EGM-MV 20% FBS (Hyclone, Logan, UT) media and they were checked for simultaneous expression of CD133 and CD24 by flow cytometer analysis. Generation of clones from CD24+CD133+ PECs was performed by limiting dilution in fibronectin-coated 96-well plates in EGM-MV 20% FBS. CD24$^+$CD133$^+$ PECs were also maintained in culture as a bulk, and routine cell passaging was performed. All the experiments were performed using cells at least at passage 3. Cells were grown at 37 ^{0}C supplied with 5 % CO_2. Trypsin and EDTA (1:1 vol/vol) was used for splitting the cells. Cells were counted using Neubauer's chamber and the desired number of cells were used for experiments.

3.1.2 In-vitro differentiation of human renal progenitors towards mature podocytes

To induce their differentiation towards podocytes, CD133+CD24+ PECs were seeded at 70% confluence and culture without FBS for a minimum of 4 h. The medium was replaced with a differentiation medium (VRADD) containing DMEM-F12 (Sigma, Munich, Germany) supplemented with 5% FBS (Hyclone, Thermo Scientific, UT, USA), vitamin D3 100 nM (Sigma, Munich, Germany), and all-trans retinoic acid 100 μM (Sigma, Munich, Germany); and dexamethasone 0,1 μM (Sigma, Munich, Germany) for 48h as described [105, 117] (Figure 8). After 48h the VRADD medium were removed and changes in changing of shape was observed and de novo expression

of podocytes marker was evaluated by real time PCR analysis. Human renal progenitors cultured with EGM-MV 20% FBS were use as control for morphological and molecular
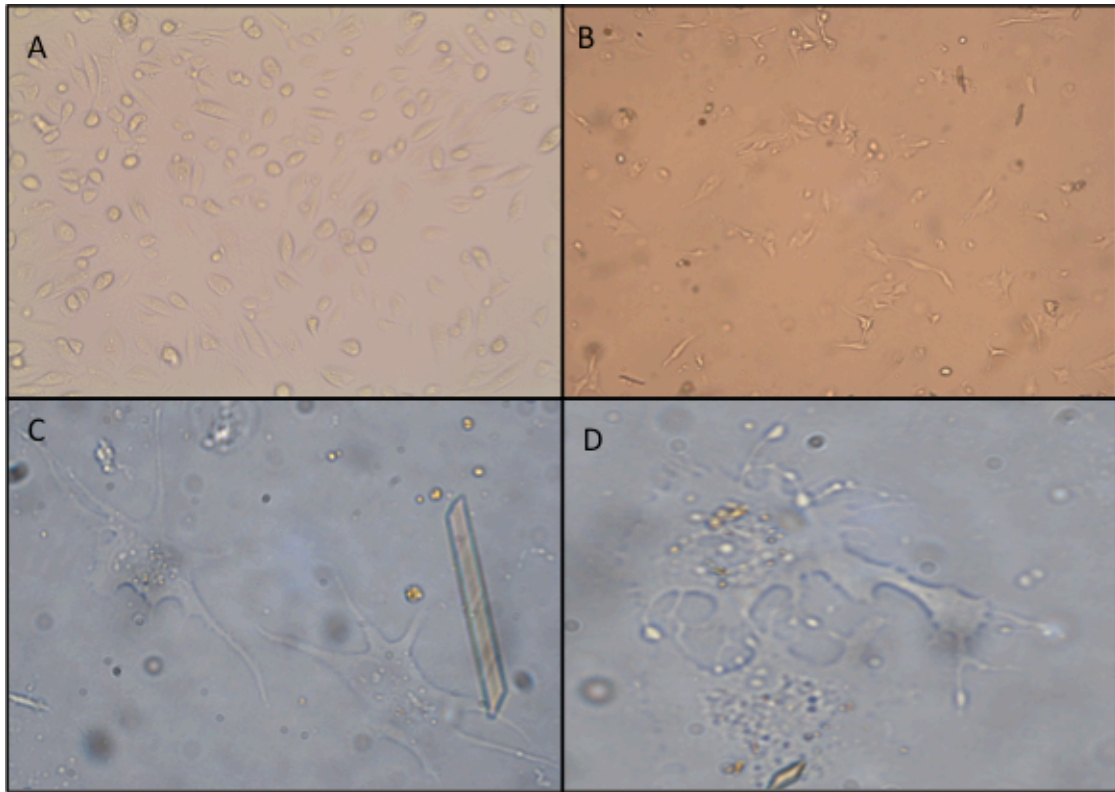
Figure 8. To induce their differentiation towards podocytes, CD133+CD24+ PECs were seeded at 70% confluence and culture without a differentiation medium (VRADD) containing DMEM-F12 supplemented with 5% FBS, vitamin D3 100 nM, and all-trans retinoic acid and dexamethasone for 48h. Human renal progenitors cultured with EGM-MV 20% FBS were use as control as described. After 48h the VRADD medium were removed and morphological changes were observed (C-D) compared to the controls (A-B).

analysis to verify the success of the in-vitro differentiation. To evaluate the complete differentiation, gene expression for podocyte marker nephrin was performed.

3.1.3 Culture of immortalized murine parietal epithelial cell and podocyte cell lines

Immortalized mouse parietal epithelial cells (mPECs) were isolated and characterized from preparations of mouse glomeruli as described [207]. mPECs were kept in culture at 33 °C on 10 cm plates (BD Biosciences, Heidelberg, Germany) coated with type I collagen, in RPMI1640 containing 5% FBS, 1mM Pyruvate (GIBCO/Invitrogen, Paisley, Scotland UK),10mM HEPES (GIBCO/Invitrogen, Paisley, Scotland UK), 0,0075% Sodium Bicarbonate (GIBCO/Invitrogen, Paisley, Scotland UK), and 50 U/ml IFN-γ (Roche, Munich, Germany) as described [207]. Under these conditions, the cells are able to grow due to the activation of the SV40 promoter, which is thermo sensitive (33°C) and regulated by the IFN-γ presence. Immortalized mouse podocytes (MPCs) were isolated and cultured at 33 °C on 10 cm plates (BD Biosciences, Heidelberg, Germany) coated with type I collagen, in RPMI1640 containing 50 U/ml IFN-γ as described.[208]. To induce their differentiation, mPECs and MPC were cultured under growth-restrictive conditions (at 37 °C, in absence of IFN-γ) for 14 days. Under growth restrictive conditions the SV40 promoter is switched off, allowing the cells to stop to replicate and to display a differentiated phenotype. After two weeks in culture under restrictive growth conditions, fully differentiated mouse parietal epithelial cells (mPECs) displayed a polygonal shape together with claudin marker expression; podocytes displayed an arborized shape expressing synaptodin. Cells exhibiting these features were used to perform all the experiments.

3.1.4 Cell freezing and thawing

At earlier passages large amounts of cells were grown under standard culture conditions and were frozen for future use. Cells to be frozen were detached from the culture plates and counted using Neubauer's chamber. One million (10^6) of cells were centrifuge under sterile conditions for 5 min at 1000 RPM. The cell pellet was maintained on ice and carefully re-suspended in cold freezing medium (90 % respective culture medium and 10 % DMSO) by pipetting the suspension repeatedly up and down. 1 ml aliquots were quickly dispensed into freezing vials. The cells were located in the freezing chamber at –80°C overnight. The next day, all aliquots were transferred to liquid nitrogen.In order to thaw cells a frozen vial was removed from liquid nitrogen and put in a water bath at 37 °C for 5 min. The cells were then re-suspended in 10 ml of

warm complete growth medium and transferred to new culture plates. After 12 h the cells were observed under the microscope and the medium was changes once more.

3.1.5 Proliferation assay

Human CD24+CD133 PECs where counted and seeded in 96 well plates (2500 cells/well). Full differentiated mPECs where seeded in a collagen I coated 96 well plates at a density of 5000 cells/well. Cells were cultured in absence of FBS for minimum 4 h to synchronize all the cells in the same cell cycle phase and then stimulated with medium or dsDNA complexes with lipofectamine or human IFN-α (5000 U/ml) or mouse IFN-β (5000 U/ml) respectively. Proliferation was determinate using microtetrazolium assay (MTT assay, Promega) according to the manufacturer instructions. The assay is based on the cellular conversion of a tetrazolium salt into a formazan product, according to the metabolic state of the cells. In Brief, 15 µl of dye solution (tetrazolium) was added in each well and the plate incubated for 4h at 37 °C in the dark. After 4 h the cells where observed under the microscope and intracellular dark crystals of formazan were detected. The reaction was stopped adding 100 µl of stop/ solubilization solution and the plate was incubated over night at room temperature. The next day the absorbance was recorded at 570 nm using a 96-well plate reader (TECAN-Genios Plus)

3.1.6 Migration assay

Human and murine PECs migration was determined using silicone inserts with a defined cell-free gap. (Ibidi, Munich, Germany). The inserts were placed on 12 wells and the cells were seeded at 100% confluence in both culture insert wells. After 24h the insert was removed and the cells were stimulated with medium, mouse IFNα/β (5000 U/ml) or human IFNα/β (5000 U/ml). To evaluate the cell migration rate, pictures of the wound were taken at 0h and every 3h on a digital phase contrast microscope. For each stimulation and time point, over 8 pictures of different spots were taken and then analyzed on our digital image analysis software (Photoshop Extended CS5 Software, Adobe Software, US). Two lab members independently performed digital image

analysis in order to minimize the possibility of cognitive bias. Change in wound sizes between two time points expressed the extent of healing in our experiment.

3.1.7 Flow cytometry

In order to study cell death, AnnexinV/PI assay was performed and analyzed using flow cytometry. Cells cultured with medium, human IFNα/β (5000 U/ml) or mouse IFNα/β (5000 U/ml), were detached and counted using Neubauer's chamber. Cell suspensions from the stimulation experiment together with supernatant, were prepared and washed two times with AnnexinV /PI buffer (140 mM NaCl, 4 mM KCl, 0.75 mM MgCl$_2$ and 10 mM HEPES in ddH$_2$0). After centrifugation, the pellet was re-suspended by pipetting the suspension repeatedly up and down in 100 μl of mix containing labeled annexin V (5μl) and PI(5μl) in Annexin V /PI buffer . The cells were incubated for 15 min in dark at room temperature. After the incubation, the cells were analyzed by flow cytometry using a FACScalibur machine.

3.1.8 Cell cycle analysis assay

In order to study cell cycle progression and cell death, PI staining was performed and analyzed using flow cytometry. Cells cultured with medium, human IFNα/β (5000 U/ml) or mouse IFNα/β (5000 U/ml), were detached and counted using Neubauer's chamber. 500000 cells from the stimulation experiment were collected and washed two times with PBS. After centrifugation, the pellet was re-suspended by pipetting the suspension repeatedly up and down in 100 μl solution, containing 50% FBS and 50% PBS. Then 300 μl of cold 70% ethanol was added (drop-wise) and the cellular suspensions were incubated for 24h at 4°C. After incubation, the pellets were washed two times with PBS and re-suspended with 100 μl of ma mix containing 50μg/ml PI and 100U/ml of RNAase. The cells were incubated for 30 min in dark at room temperature. After the incubation, the cells were analyzed by flow cytometry using a FACScalibur machine.

3.1.9 In-vitro assessment of podocyte detachment

Differentiated human and murine podocytes were cultured with medium or human IFNα/β (5000 U/ml) or mouse IFNα/β (5000 U/ml) respectively. After 24h of stimulation, the total number of attached and detached (in the supernatant) cells was evaluated by using Neubauer's chamber. In addition, detached podocytes in the supernatant were stained with PI 100 μl of mix containing PI (5μl) in annexin V /PI buffer and analyzed by flow cytometry. The amount of detached cells was determined as percentage of PI + cells found in the supernatant over the total number of cells (attached cells + detached cells).

3.1.10 Electric cell impedance sensing assay (ECIS)

IFNα/β induced changes in podocyte resistance and capacitance were analyzed using an ECIS device (Applied Biophysics, Troy, USA). The ECIS device is based on alternate current (AC) impedance measurements, using a weak and non-invasive AC signals [209, 210]. Detachment or spreading of cells on the electrode surface change the resistance in a way that morphological information can be inferred. The measurement system consists of an eight-well cell culture dish with electrodes deposited upon the bottom of each well, a lock-in amplifier with an internal oscillator, relays to switch between the different wells, and a personal computer that controls the measurement and stores the data [209]. During the experiment the current flow is approximately constant (1μM) and the voltages across the system are measured by the amplifier and converted to the components of the electrode impedance, which are presented formally as resistance and capacitance of a resistor-capacitor series circuit. The data are as a function of time in frequency scan mode, in which the impedance is measured at different frequencies between 10 and 100000 Hz [209]. Murine primary podocytes were isolated and cultured as described [211]. Cells were seeded on ECIS culture-ware (80BW10E+, Applied Biophysic) that was pre-incubated with podocyte cell medium overnight and connected to the ECIS device. Confluent podocytes were kept overnight at 37 °C and 5% CO_2 before medium was exchanged to HBSS +/- IFNα/β or solvent. Resistance (Ω) was analyzed for 30 min at 400 Hz or 40Hz, respectively.

3.2 Protein isolation and western blotting

3.2.1 Protein isolation

Proteins from cell culture were extracted using RIPA buffer (50 mM Tris HCl, pH 7.5; 150 mM NaCl; 100 μM sodium orthovanadate, 0.5 % sodium deoxycholat, 4 % NP-40, 2 % Triton-X-100; 5 mM EDTA; 300 mM sucrose), (Sigma, Germany) containing protease inhibitor tablets COMPLETE (Roche, Mannhein, Germany) In brief, cells were detached mechanically (in absence of trypsin) in Ripa Buffer containing protease inhibitor. All steps were performed at 4°C to avoid protein degradation. The lysates were collected and maintained at constant agitation for two h at 4^{0}C. The samples were then centrifuged for 20 min at 12000rpm at 4 ^{0}C to remove the cell membrane. The pellet was discarded and the supernatant collected in a fresh tube. Protein estimation was performed using Bradford′s assay (Biorad).

3.2.2 Western blotting

From each sample, 50μg of the protein was mixed with 5x SDS loading buffer (100 mM Tris-HCl, 4% SDS, 20% glycerol, and 0.2% bromo-phenol blue) and heated at 95°C for 5 min. Proteins were separated by SDS PAGE and subsequently transferred to an methanol-activated PVDV Immobilon-P membrane (Millipore, Eschborn, Germany) using the BioRad Semi-Dry Blotting System (BioRad, Munich, Germany). Electro transfer was performed for 1 h at 25V. After the transfer, the membrane was stained for 10 min in Ponceau solution (0.5 % Ponceau S in 1 % acetic acid) and de-stained with H2O to verify successful transfer of protein and note the position of the marker (peqGOLD protein marker; PeqLab, Erlangen, Germany. After blocking for 1hr at room temperature with 5% milk in Tris-buffered saline buffer (20 mM Tris-HCl, 150 mM NaCl, and 0.1% Tween 20), the membranes were then incubated overnight at 4°C with primary antibodies and kept in constant agitation to enhance binding. After washing, the membrane was incubated with respective secondary antibodies in Tris buffered saline buffer for one hour at room temperature. The signals were visualized by an enhanced chemiluminescence system (Amersham, Buckinghamshire, UK).

3.3 RNA analysis

3.3.1 RNA isolation from cells and tissue

At the end of the experiment, cells were harvested under sterile conditions for RNA isolation. Immediately after kidney isolation, a small piece of kidney from each mouse was preserved in RNA-later and stored at -20^0C until processed for RNA isolation. RNA isolation was performed using RNA isolation kit from Ambion (Ambion, CA, USA) according to the protocol provided. The harvested cells were washed two times with sterile PBS and centrifuged. The supernatant was discarded and the pellet was re-suspended in 350 μl lysis buffer containing 10μg/ml β-mercaptoethanol and frozen at -80 °C until RNA isolation. Tissues (30 mg) preserved in RNA-later were homogenized using blade homogenizer for 30 seconds at 4 °C in lysis buffer (600 μl) containing β-mercaptoethanol (10 μl/ml). During RNA isolation the samples thawed and 350 μl of 70 % ethanol made from 1% diethyl pyrocarbonate treated water (DEPC water) was added to the samples and mixed well. This mixture was then loaded onto RNeasy mini columns held in 2 ml collection tubes and centrifuged at 12000 xg for 15 seconds. The flow-through was discarded and the columns were loaded with 700μl of Wash buffer I and centrifuged at 12000 xg for 15 seconds. The collection tubes were discarded together with the flow-through and the columns were transferred to fresh 2 ml collection tubes.500 μl of Wash Buffer II was pipetted onto the column and centrifuged at 12000 x g for 15 seconds, and the flow-through was discarded. This step was repeated and the column was rendered dry by centrifugation and placed in a 1,5 ml fresh collection tube. Then, 40 μl of RNase free water was pipetted directly on the silica-gel membrane and was centrifuged to collect the RNA solution. Isolated RNA was measured, checked for purity and stored at -80^0C.

3.3.3 RNA quantification and purity check

The isolated RNA samples were quantified using Nano drop (PEQLAB Biotechnology GMBH, Erlangen, Germany). The ratio of optical densities at 260 nm and 280 nm is an indicator for RNA purity (indicative of protein contamination in the RNA samples). Only samples with a ratio of 1.8 or more were considered to be of acceptable quality.

3.3.4 cDNA synthesis and real-time PCR

The RNA samples, isolated according to procedures detailed above, were processed for cDNA conversion using reverse transcriptase II (Invitrogen, Karlsruhe, Germany). RNA samples were diluted in DEPC water to a concentration of 2 μg / 30 μl. A master mix was prepared with the following reagents: 9 μl of 5 x buffer (Invitrogen, Karlsruhe, Germany), 1μl of 25mM dNTP mixture (Amersham Pharmacia Biotech, Freiburg, Germany), 2 μl of 0.1 M DTT (Invitrogen, Karlsruhe, Germany), 1 μl of 40 U/μl RNasin (Promega, Mannheim, Germany), 0.5 μl of 15 μg/ml linear acrylamide (Ambion Ltd, 36 Cambridgeshire, UK), 0.5 μl of Hexanucleotide (Roche, Mannheim, Germany), 1 μl of Superscript (Invitrogen, Karlsruhe, Germany) or ddH2O as a control. The master mix was made to a volume of 13,2 μl and added to 1 μg / 20 μl RNA samples were taken in separate DEPC treated microcentrifuge tubes, which were mixed and placed at 42 °C on a thermal shaker incubator for 1 hour. After 1 hour the cDNA samples were collected and placed at -20 °C until use for RT-PCR analysis.

3.3.5 Real time PCR

The cDNA samples prepared as described above were diluted 1:10 for real-time polymerase-chain-reaction (RT-PCR). 2 μl of diluted cDNA samples was mixed with SYBR green master mix (10 μl), forward primer (0.6 μl) and, reverse primer (0.6 μl), both specific for the gene of interest, Taq polymerase (0.16 μl) and distilled water (6.64 μl). The RT-PCR was performed using Light Cycler480. Pre-incubation was carried out for 5 min at 95 ^{0}C so as to activate the polymerase and complete de-naturation of cDNA samples. Then the cDNA was amplified for 45 cycles, each comprising of 15 seconds incubation at 95 ^{0}C and 45 seconds incubation at 60 ^{0}C. The melting curve was set for initial 95 ^{0}C for 5 seconds followed by 65 ^{0}C for 1 min with continuous heating. The RT-PCR of the reference gene (18S rRNA) was carried out under similar conditions. The CT values were calculated using the Light Cycler480 and the results were normalized with respect to the reference gene expression. In all cases controls consisting of ddH2O were negative for target or reference genes. All designed SYBR green primers for all genes evaluated were obtained from Metabion (Metabion, Martinsried, Germany).

Table 5. Murine oligonucleotide primers used for SYBR-Green RT-PCR

Gene	Sequence	
18s	forward:	5' GCAATTATTCCCCATGAACG 3'
	reverse:	3' AGGGCCTCACTAAACCATCC 5'
mIFIT1	forward:	5'CAAGGCAGGTTTCTGAGGAG 3'
	reverse:	3' GACCTGGTCACCATCAGCAT 5'
mIFIT3	forward:	5' TTCCCAGCAGCACAGAAAC 3'
	reverse:	3' AAATTCCAGGTGAAATGGCA 5'
mMX1	forward:	5' TCTGAGGAGAGCCAGACGAT 3'
	reverse:	3' CTCAGGGTGTCGATGAGGTC 5'
mCXCL10	forward:	5' GGCTGGTCACCTTTCAGAAG 3'
	reverse:	3' ATGGATGGACAGCAGAGAGC 5'
mPUMA	forward:	5' CACCTAGTTGGGCTCCATTT 3'
	reverse:	3' ACCTCAACGCGCAGTACG 5'
mBAK	forward:	5' AGACCTCCTCTGTGTCCTGG 3'
	reverse:	3' AAAATGGCATCTGGACAAGG 5'
mBID	forward:	5' GTGTAGCTCCAAGCACTGCC 3'
	reverse:	3' GCAAACCTTTGCCTTAGCC 5'
mBAX	forward:	5' GATCAGCTCGGGCACTTTAG 3'
	reverse:	3' TTGCTGATGGCAACTTCAAC 5'
mTNFα	forward:	5' AGGGTCTGGGCCATAGAACT 3'
	reverse:	3' CCACCACGCTCTTCTGTCTAC 5'
mIL6	forward:	5' TGATGCACTTGCAGAAAACA 3'
	reverse:	3' ACCAGAGGAAATTTTCAATAGGC 5'
mCXCL9	forward:	5'CCTAGTGATAAGGAATGCACGATG 3'
	reverse:	3' CTAGGCAGGTTTGATCTCCGTTC 5'
mCXCL11	forward:	5' CCGAGTAACGGCTGCGACAAAG 3'
	reverse:	3' CCTGCATTATGAGGCGAGCTTG 5'
mIFNR1	forward:	5' CCAAGGCAAGAGCTATGTCCTG 3'
	reverse:	3' CAGTGCGTAGTCTGGACATTTGC 5'
mIFNR2	forward:	5' GAGCCTAGAGACTATCACACCG 3'
	reverse:	3' TACCAGAGGGTGTAGTTAGCGG 5'

Table 6. Human oligonucleotide primers used for SYBR-Green RT-PCR

Gene	Sequence	
18s	forward:	5' GCAATTATTCCCCATGAACG 3'
	reverse:	3' AGGGCCTCACTAAACCATCC 5'
hIFIT1	forward:	5' ATCCAGGCGATAGGCAGAGATC 3'
	reverse:	3' GCCTTGCTGAAGTGTGGAGGAA 5'
hIFIT3	forward:	5' CCTGGAATGCTTACGGCAAGCT 3'
	reverse:	3' GAGCATCTGAGAGTCTGCCCAA 5'
hMX1	forward:	5' GGCTGTTTACCAGACTCCGACA 3'
	reverse:	3' CACAAAGCCTGGCAGCTCTCTA 5'
hCXCL10	forward:	5' GGTGAGAAGAGATGTCTGAATCC 3'
	reverse:	3' GTCCATCCTTGGAAGCACTGCA 5'
hPUMA	forward:	5' ACGACCTCAACGCACAGTACGA 3'
	reverse:	3' CCTAATTGGGCTCCATCTCGGG 5'
hBAK	forward:	5' TTACCGCCATCAGCAGGAACAG 3'
	reverse:	3' GGAACTCTGAGTCATAGCGTCG 5'
hBID	forward:	5' TGGGACACTGTGAACCAGGAGT 3'
	reverse:	3' GAGGAAGCCAAACACCAGTAGG 5'
hBAX	forward:	5' TCAGGATGCGTCCACCAAGAAG 3'
	reverse:	3' TGTGTCCACGGCGGCAATCATC 5'
hIFNR1	forward:	5' CGCCTGTGATCCAGGATTATCC 3'
	reverse:	3' TGGTGTGTGCTCTGGCTTTCAC 5'
hIFNR2	forward:	5' ACCGTCCTAGAAGGATTCAGCG 3'
	reverse:	3' CCAACAATCTCAAACTCTGGTGG 5'

3.4 Experimental procedures

3.4.1 Animals

Combined Immunodeficient (BALB/cJHan™Hsd-*Prkdcscid*) mice obtained from Harlan, Udine, Italy. The experiments were performed in Italy according to the Italian animal care and were approved by local government authorities. Balb/c mice were obtained from Charles river, Germany. The experiments were performed in Germany according to the German animal care and were approved by the Regierung von Oberbayern. All mice were kept under sterile housing conditions under a 12h light and dark cycle. Water and standard chow (Ssniff, Soest, Germany) were available ad libitum for the complete duration of the study. Cages, bedding, nestles, food, and water were sterilized by autoclaving before use.

3.4.2 Adriamycin-induced nephropathy and type I IFN treatment

Adriamycin nephropathy was induced in 6-week old female mice by a single i.v injection of adriamycin on day 0. The dose of 6,5 mg/kg body weight in phosphate buffered saline PBS, Sigma) was used to induce nephropathy in SCID mice; dose of 11,5 mg/kg body weight in phosphate buffered saline PBS (Sigma) was used to induce nephropathy in Balb/c mice. Mice received daily subcutaneous injections of either saline (vehicle), IFN-α6 (1000 U) or IFN-β (1000 U). Group size was n=6 in each experiment, and each experiment was repeated three times. After 7 days plasma and urine samples were collected before sacrifice by cervical dislocation and afterwards kidney tissues were harvested. The harvested kidney tissues were divided into three parts each. One part was immediately flash frozen in liquid nitrogen and then further stored at -80^0C for protein isolation and cryo sections, the second part was collected in RNA later solution (Ambion, CA, USA) and stored at -20^0C for RNA isolation and the third part of the kidney was kept in formalin to fix the tissue before embedding in paraffin for histological analysis.

All experimental procedures were performed according to the German and the Italian animal care and ethics legislation and had been approved by the local government authorities.

3.4.3 Blood and urine sample collection

Urine sample were collected using metabolic cages. Animals were kept in metabolic cages in absence of food for 12 h to enhance sample collection. Collected urine was stored at -20^0C until used for further biochemical analysis. At the end of the study blood samples were collected by retro-orbital bleeding technique, under isoflurane anesthesia, in microcentrifuge tubes containing EDTA (10μl of 0.5 M solution per 200μl of blood). Samples were centrifuged at 8000 rpm for 5 min and plasma was separated and stored at -20^0C until used for analysis.

3.5 Urinary albumin to creatinine ratio

3.5.1 Urinary albumin

Urinary albumin levels were determined using Albuwell M kit from Exocell (Philadelphia, PA, USA) following manufacturer's instructions. Albuwell M is an indirect competitive ELISA designed to monitor urinary albumin. In the assay procedure, sample and rabbit anti-murine albumin antibody are added to albumin-coated wells. The antibody interacts and binds with the albumin immobilized to the stationary phase or with albumin in the fluid phase, hence the notion of competitive binding. Generally, albumin levels in urine samples from FSGS mice were quite high, so that urine samples were diluted 300 to 1500 times with EIA diluent (provided by the kit) before estimation. In short, diluted sample/standard and rabbit anti-murine albumin were added in the respective well of the pre-coated plate and incubated at room temperature for 30 min. After incubation, each well was washed 10 times with wash buffer (0.15 M NaCl, 0.01 M triethanolamine (pH 6.8), 0.05% Tween 20, and 0.05% Proclin 300). Anti-rabbit HRP conjugate detection antibody) was added and the plate was incubated in dark for further 30 min. After HRP-conjugate incubation, each well was washed 10 times with wash buffer and TMB reagent (freshly prepared by mixing equal volumes of two substrate reagents) was added and incubated in dark until

color reaction was completed followed by addition of stop solution (2 M H_2SO_4). The absorbance was read at 450 nm within 10 min of adding stop solution. The albumin content in each sample was determined using the equation of regression line generated by plotting absorbance of different standards against their known concentrations.

3.5.2 Urinary creatinine assay kit

Urinary creatinine and plasma creatinine levels were measured using Jaffe´s enzymatic reaction using a Creatinine FS kit (DiaSys Diagnostic system, GmBH, Holzheim, Germany). Urine samples were diluted 10 times with distilled water. Different dilutions of standard were prepared using the stock provided with the kit. Working mono reagent was prepared by mixing 4 parts of reagent 1 (R1) and 1 part of reagent 2 (R2) provided with the kit. Then, 10 µl of each diluted sample and standard was added to a 96 well plate with flat bottom (Nunc maxisorb plate). The mono reagent (200µl) was added to each well, and immediately after 1 minute of incubation, the absorbance of the reaction mixture was measured at 492nm using an ELISA plate reader. This was repeated at 1 and 2 min of additional incubation. The change in absorbance (Δ A) was calculated as Δ A = [(A2 − A1) sample or standard] − [(A2 − A1) blank]. And creatinine content of samples was calculated as:

Creatinine (mg/dl) = ΔA sample /ΔA standard * Concentration of standard (mg/dl)

Urinary albumin to creatinine ratio was calculated after converting values for albumin and creatinine to similar units (mg/dl). Albumin content for each sample calculated (mg/dl) was divided by creatinine content (mg/dl) for the same sample.

3.6 Periodic acid Schiff staining

For immunohistological studies one part of each kidney from each mouse was fixed in formalin (10 % in PBS or Saline) over night and processed using tissue processors (Leica) and paraffin blocks were prepared. Formalin-fixed

tissues were processed using tissue processors (Leica) and paraffin blocks were prepared. 2 μm thick paraffin-embedded sections were cut. De-paraffinization was carried out using xylene (3 * 5 min) followed by re-hydration by incubating the sections in 100% absolute ethanol (3 * 3 min), 95% ethanol (2 * 3 min) and 70% ethanol (1 * 3 min) followed by washing with distilled water (2 * 5 min). Re-hydrated sections were incubated with Periodic acid (2 % in distilled water) for 5 min followed by washing with distilled water (1* 5 min). Then sections were incubated with Schiff solution for 20 min at room temperature followed by washing with tap water (1* 7 min) and counter staining with Hematoxylin solution (1* 2 min). This was followed by washing with tap water (1* 5 min) and finally sections were dipped in alcohol 90% and dried and closed with cover slips.

Mac2 staining

Number of infiltrated macrophages in glomeruli was counted in sections stained with Mac2 (pan marker for macrophage) antibodies. Mac2 positive cells per glomerulus were counted manually in 25 glomeruli for each section and were presented as mean ± standard error of mean for respective groups

CD3 staining

Number of infiltrated lymphocytes in glomeruli was counted in sections stained with CD3 (pan marker for lymphocytes) antibodies. CD3 positive cells per glomerulus were counted manually in 25 glomeruli for each section and were presented as mean ± standard error of mean for respective groups

3.7 Immunostaining and Confocal imaging

All immunofluorescent studies were performed on five micrometer-thick frozen sections and analyzed with a LSM510 META laser confocal microscope (Carl Zeiss, Jena, Germany). Five μm thick frozen sections were cut and fixed in in cold formalin (4 % in PBS or Saline) for 20 min and washed for 5 min in PBS. Specific blocking buffer prepared in PBS+ 3% BSA+ diluted serum host of the secondary antibody, was added and sections were incubated for 30 min at room

temperature. The sections were incubated with diluted primary antibody for 15 min at 37°C followed by 1 h at 4 °C. After 5 min in PBS, 200μl of specific secondary antibody (diluted 1:1000) was added and the section incubated for 30 min in the dark at room temperature. At the end of the incubation with the secondary antibody the sections were washed for 5 min followed by the second staining performed as previously described. The nuclei staining were performed using TOPRO. The following primary antibodies were used: anti CD68 mAb (clone FA-11, Abcam, Cambridge, UK), anti-claudin-1 mAb (clone 2H10D10, Invitrogen, Carlsbad, CA), anti-nephrin (clone C17, Santa Cruz Biotechnologies, Santa Cruz, CA), anti-WT-1 (clone F-6, Santa Cruz Biotechnologies, Santa Cruz, CA); anti-H3-Ser10 (anti-phospho histone H3, Abcam, Cambridge, UK), anti-podocin (anti-NPHS2 Abcam). Double immunolabeling was performed using the following secondary antibody: Alexa Fluor 488 goat anti rat IgG (Invitrogen, Life Technologies GmbH, Darmstadt, Germany), Alexa Fluor 546 goat anti rabbit IgG (Invitrogen), Alexa flour 488 rabbit and goat IgG (Invitrogen), Alexa Fluor 546 goat anti mouse IgG1 (Invitrogen), Alexa Fluor 488 goat anti mouse IgG1 (Invitrogen). Double positive cells were quantified in 15 glomeruli of at least six sections for each mouse by two independent and blinded observed

3.8 Light and transmission electron microscopy

Light and transmission electron microscopy of 164 consecutive renal biopsies (2011-2012) from the Department of Pathology, Washington University, School of Medicine, St Louis, MO plus three selected cases of HIV+ collapsing FSGS (previously called HIV-associated nephropathy were performed. Renal biopsies were fixed in 10% formalin, 2% glutaraldehyde and frozen in liquid nitrogen for light-microscopy. Tissue for transmission electron microscopy was rinsed in phosphate buffer (0.1 M, pH 7.2), post-fixed in l% osmium tetroxide, dehydrated in graded alcohols and propylene oxide, and embedded in Polybed 812 (Polysciences). Ultrathin sections were stained with 2% aqueousmagnesium uranyl acetate for 30 min and then by lead citrate for 5 min. A JEOL JEM 100 CXanalytical TEMSCAN electron microscope was used at 60 kv. The sections

were retrospectively reviewed searching for abnormal mitoses and or multinucleated podocytes.

3.9 Statistical analysis

Statistical analysis was performed using GraphPad prism 5 Software (GraphPad Software, USA). Data are presented as mean ±SEM/SD. For multiple comparison of groups one-way ANOVA was used followed by post-hoc Bonferroni`s test. Paired Student`s t-test was used for the comparison between two groups. A value of $p < 0.05$ was considered as statistically significant.

4. Results

4.1 Glomerular epithelial cells express IFNR

The expression of both IFN I receptor chains (IFNAR1 and IFNAR2) was tested by RT-PCR, in podocytes as well as in PECs from human and murine origin. Glomerular podocytes and PECs were cultured for 12 h with IFNα/β . mRNA was isolated for real time PCR analysis. Epithelial glomerular cells from both species showed a basal expression of IFN I receptor. Upon type I IFN stimulation, PECs and podocytes from both species did not show increased expression of the IFNR1 and IFNR2 chains (Figure 9).
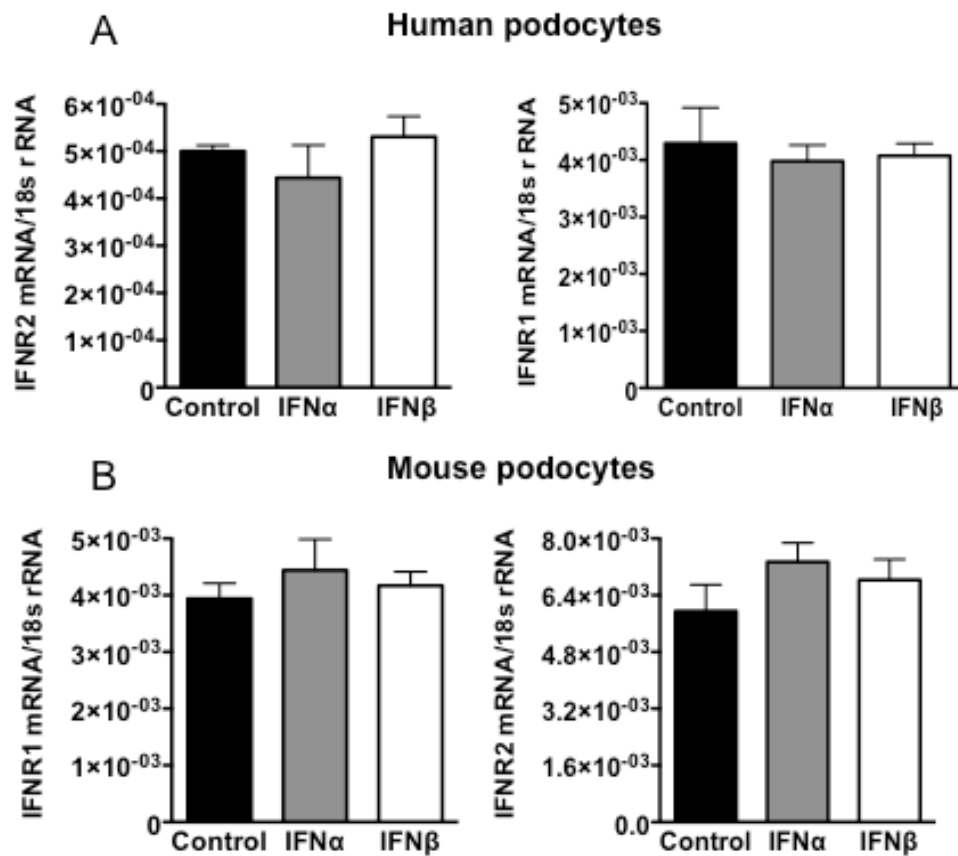
Figure 9. Glomerular parietal epithelial cell and podocyte express both IFN receptor chains. Glomerular podocyte and PECs mRNA from human (A, C) and mouse (B, D) was isolated after 12h of exposure to IFN-α and IFN-β. Real-time po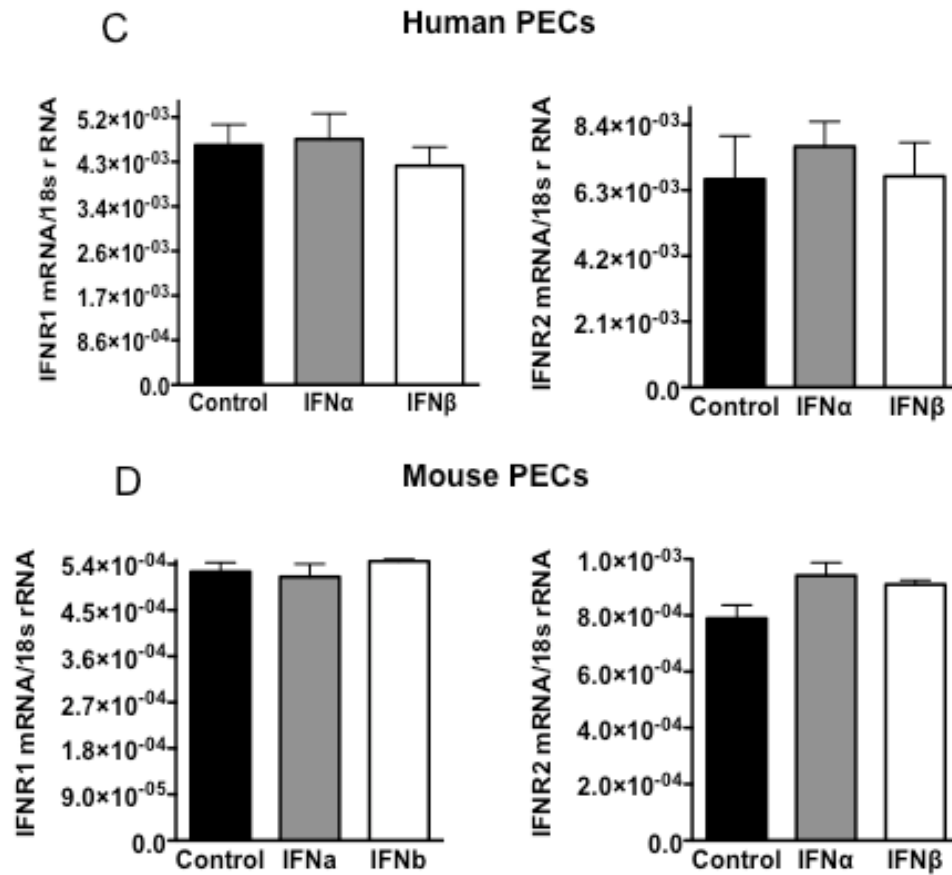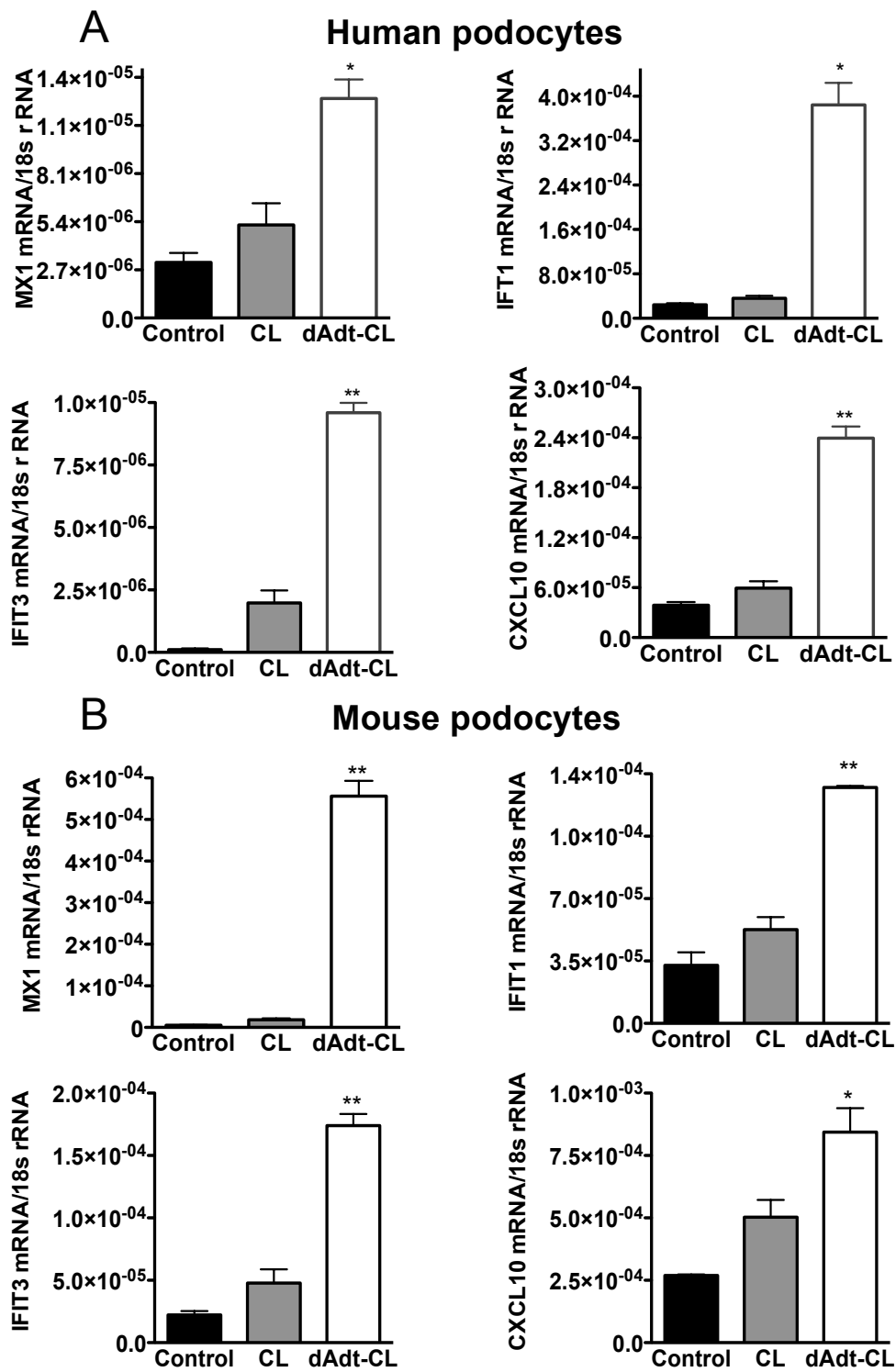lymerase chain reaction was performed for IFNR1 and IFNR2 as described in methods. Data are expressed relative to their respective 18s rRNA expression and are means ± SEM of three experiments.

4.2 dsDNA trigger IFN-stimulated genes (ISGs) in glomerular epithelial cells

During viral infection, cells secrete a large amount of IFNs that act in a paracrine and in an autocrine manner. Synthetic nucleic acids together with viral nucleic acids are the most potent inducers of type I IFNs. In order to study the potential of viral infections to activate the IFN induced antiviral state on glomerular epithelial cells, podocytes and PECs from human and mouse origin were stimulated with synthetic dsDNA (poly-dAdT) complexes with lipofectamine to mimic viral infection. After 12h the stimulation was stopped and cellular mRNA collected. RT-PCR analysis showed significant up-regulation of IFN stimulated genes (ISGs) in glomerular epithelial cells upon (poly-dAdT) stimulation compared to the controls for both species (Figure 10). The induction of ISGs is a mechanism through which type I IFNs establish the cellular antiviral state on target cells. MX proteins belong to the class of dynamin-like large guanosine triphosphateses (GTPases), and they have an antiviral activity against a wide range of RNA viruses. These proteins are major components of the antiviral state induced by IFN. [212]. IFT1 and IFIT3 genes belong to the ISG56 family genes. Under normal conditions these genes are silent and their transcription is strongly induced by type I IFNs stimulation and viral infection [212]. CXCL10, also known as IP-10, is an IFN induced chemokine involved in the recruitment of immune cells. [213]. Altogether, dsDNA stimulation significantly triggers expression of multiple ISGs in podocytes and PECs of both species.

A **Human podocytes**
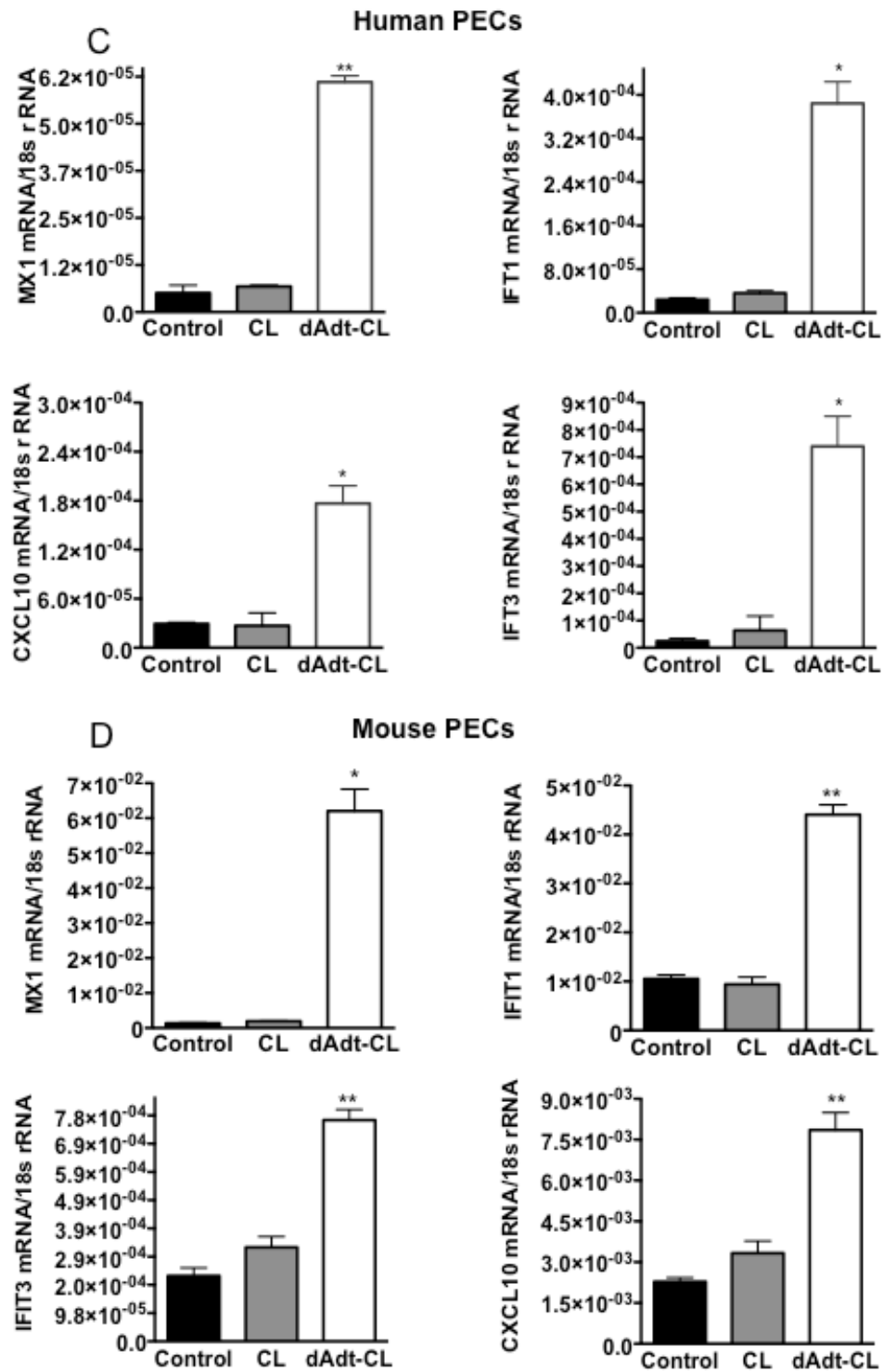
B **Mouse podocytes**

Figure 10. IFN type I signature in human and mouse parietal glomerular epithelial cells and podocytes. Human (A, C) and murine (B, D) glomerular epithelial cell mRNA was isolated after 12h of exposure to synthetic double strand DNA (poly-dAdT) complexes with lipofectamine. Real-time polymerase chain reaction was performed for the indicated ISG genes as described in results methods. Data are expressed relative to their respective 18s rRNA expression and are means ± SEM of three experiments and are means ± SEM of three independent experiments *$P < 0.05$ versus control; **$P < 0.01$ versus control.

4.3 dsDNA stimulation modulate CD133+/CD24+ PECs properties

In contrast to glomerular visceral epithelial cells, which do not proliferate in-vitro or in vivo, PECs have the ability to enter and successfully complete the cell cycle. Human CD133+/CD24+ renal progenitor cells within the PEC layer at the inner aspect of the Bowman`s capsule have been postulated to be involved in glomerular repair processes. Together with their ability to proliferate, they have been shown to have the capacity to differentiate towards podocytes in culture and to restore podocyte loss in-vivo [117, 206]. Many kidney diseases are directly or indirectly related to viral infections, but how and to which extend viral infections can affect glomerular regeneration is still unknown. In order to replace podocyte loss, human CD133+/CD24+ PECs need to increase their number to start the differentiation process. To address the question how viral infections can affect this process, human CD133+/CD24+ PECs were stimulated with dsDNA complexes and MTT proliferation assay was assessed. The cells were stimulated with three different concentrations of synthetic dsDNA complexes and the assay was carried out for three different time points. (Figure 11) Already after 24h of stimulation, dsDNA complexes down regulated human CD133+/CD24+PECs proliferation in dose dependent manner. The arrest of cell proliferation has been observed to be dose dependent.

Furthermore, the potential of renal progenitors to differentiate into podocytes was tested. This was achieved by exposing parietal epithelial renal progenitors to the appropriate differentiation medium (VRADD) in presence of dsDNA complexes or lipofectamine alone for 48h. At the end of the experiment, quantification of nephrin mRNA expression was used to evaluate the differentiation of renal progenitor towards podocytes. (Figure 11)   Renal progenitors were cultured in their normal medium for 48h as a control for nephrin expression. dsDNA complexes significantly reduced the capacity of podocyte progenitors to induce nephrin mRNA expression, indicating the negative role of viral infections and their mediators during the differentiation process. These data show two critical effects of IFNs and dsDNA on glomerular epithelial progenitor cells: dsDNA suppresses glomerular progenitor proliferation and inhibits their differentiation into mature podocytes.
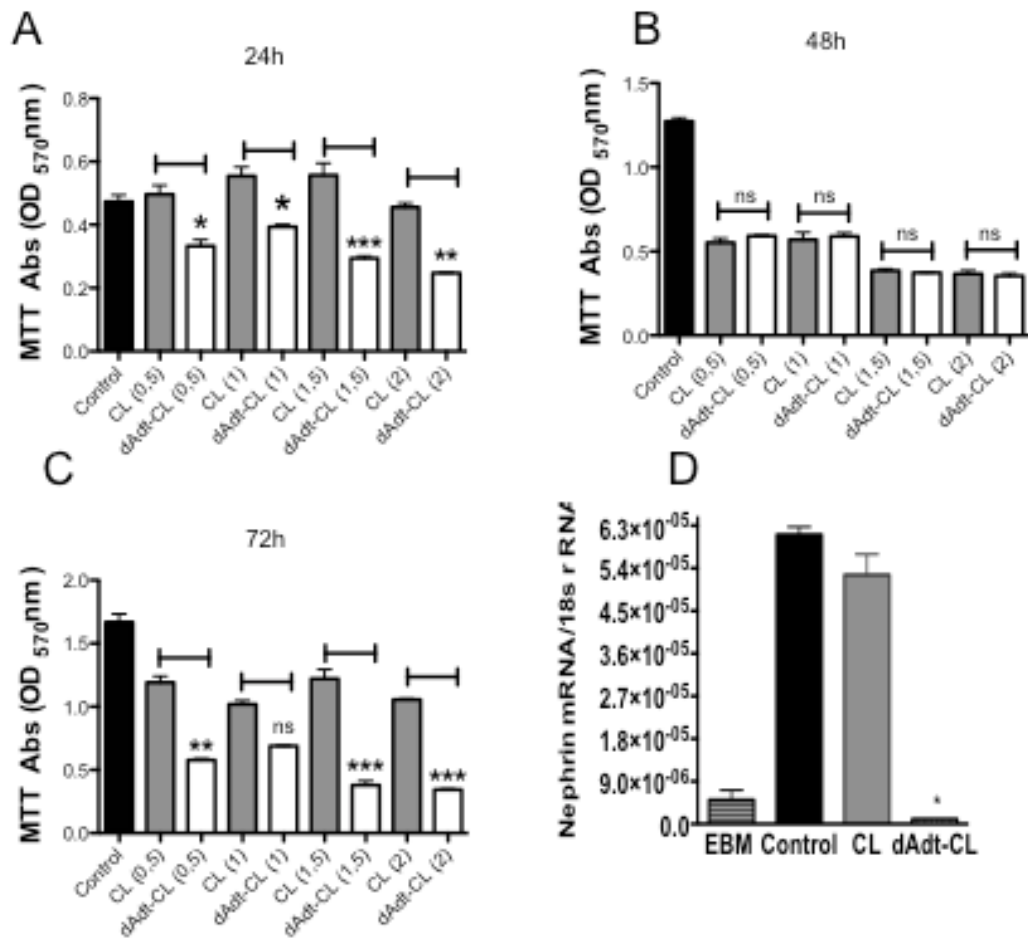
Figure 11. dsDNA modulate CD133/CD24+ PECs proliferation and differentation towards podocytes. (A-C) Human CD133/CD24+ PECs were cultured with synthetic ds DNA (poly-dAdT) complexes with lipofectamine (CL) for 24h (A), 48h (B) and 72h (C). Cells proliferation was evualated by MTT assay as described in the methods. Data are means ± SEM of three experiments, each analyzed in quadruplicate . *$P < 0.05$ versus CL; **$P < 0.01$ versus CL; ***$P < 0.001$ CL. (D) Human CD133/CD24+ PECs were cultured in the VRADD medium +/- ds DNA (poly-dAdT) complexes with lipofectamine (CL) at the concentration of 1,5μg/ml (v/v) for 48h and nephrin mRNA expression was quantified by Taq-Man RT-PCR as described in the methods. As control, renal progenitors were cultured for 48h in normal growth medium +/- ds DNA (poly-dAdT) complexes with lipofectamine (CL) at the concentration of 1,5μg/ml (v/v). Data are expressed relative to their respective 18s rRNA expression and are means ± SEM of three independent experiments *$P < 0.05$ versus CL; **$P < 0.01$ versus CL; ***$P < 0.001$ versus CL.

4.4 IFN-α and IFN-β trigger the expression of multiple ISGs in podocytes and PECs

To verify the potential of IFNs to activate the cellular antiviral state on glomerular epithelial cells, podocytes and PECs from human and mouse origin were exposed to IFN-α and IFN-β respectively. After 12h the stimulation was stopped and the cells collected. RT-PCR analysis showed significant up-regulation of ISGs in glomerular epithelial cells upon type I IFN stimulation compared to the controls. Therefore, it can be concluded that the induction of ISGs is the mechanism by which these cytokines establish the cellular antiviral state on the target cells. In podocytes from human and mouse origin, IFN beta stimulation resulted in a higher up-regulation of ISGs compared to IFN alpha, indicating a major susceptibility of podocytes to IFN beta stimulation. Altogether, both IFN-α and IFN-β induce significantly multiple ISGs in podocytes and PECs of both species (Figure 12). Thus, the antiviral cytokines IFN-α and IFN-β activate both podocytes and PECs.

A Human podocytes
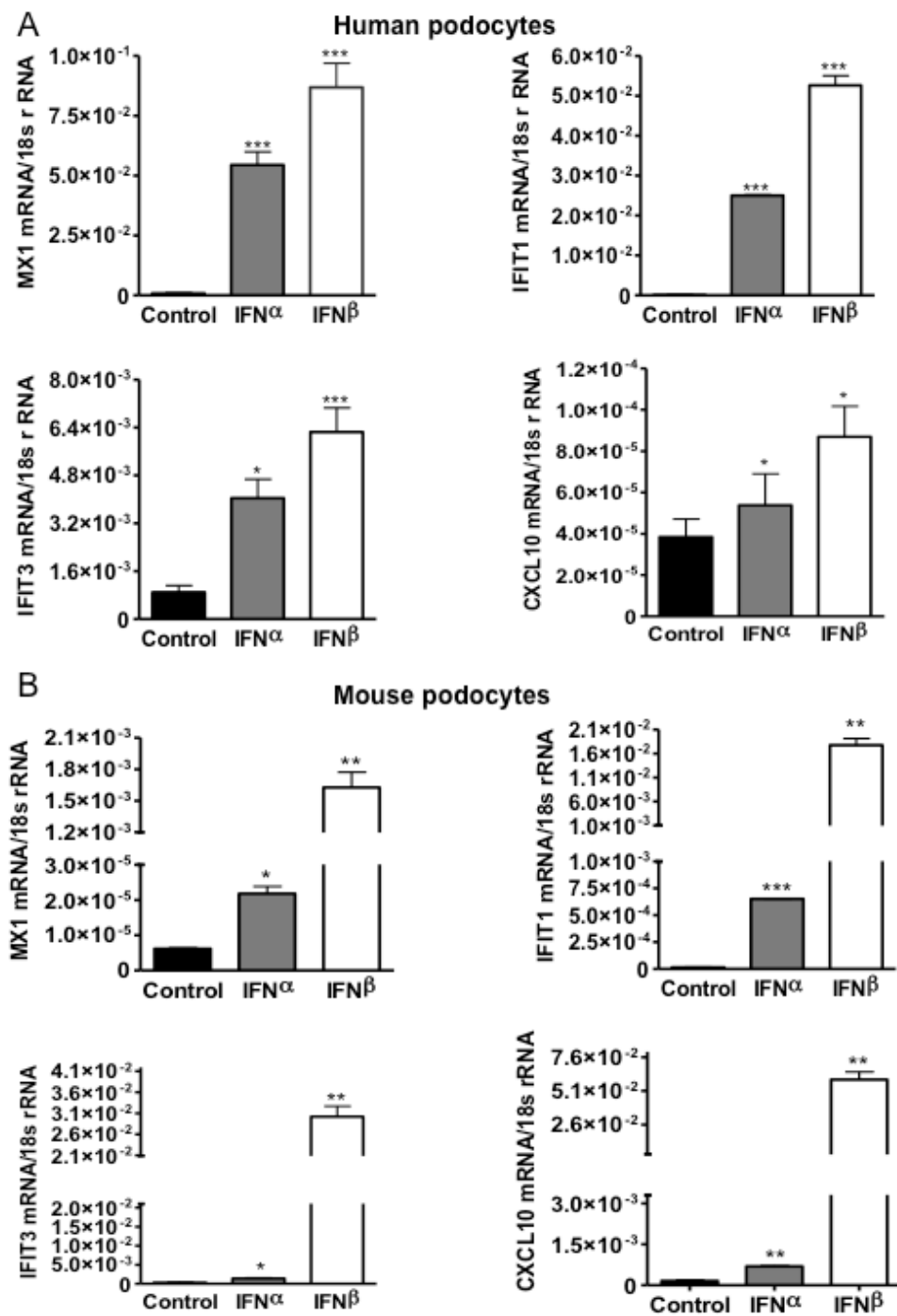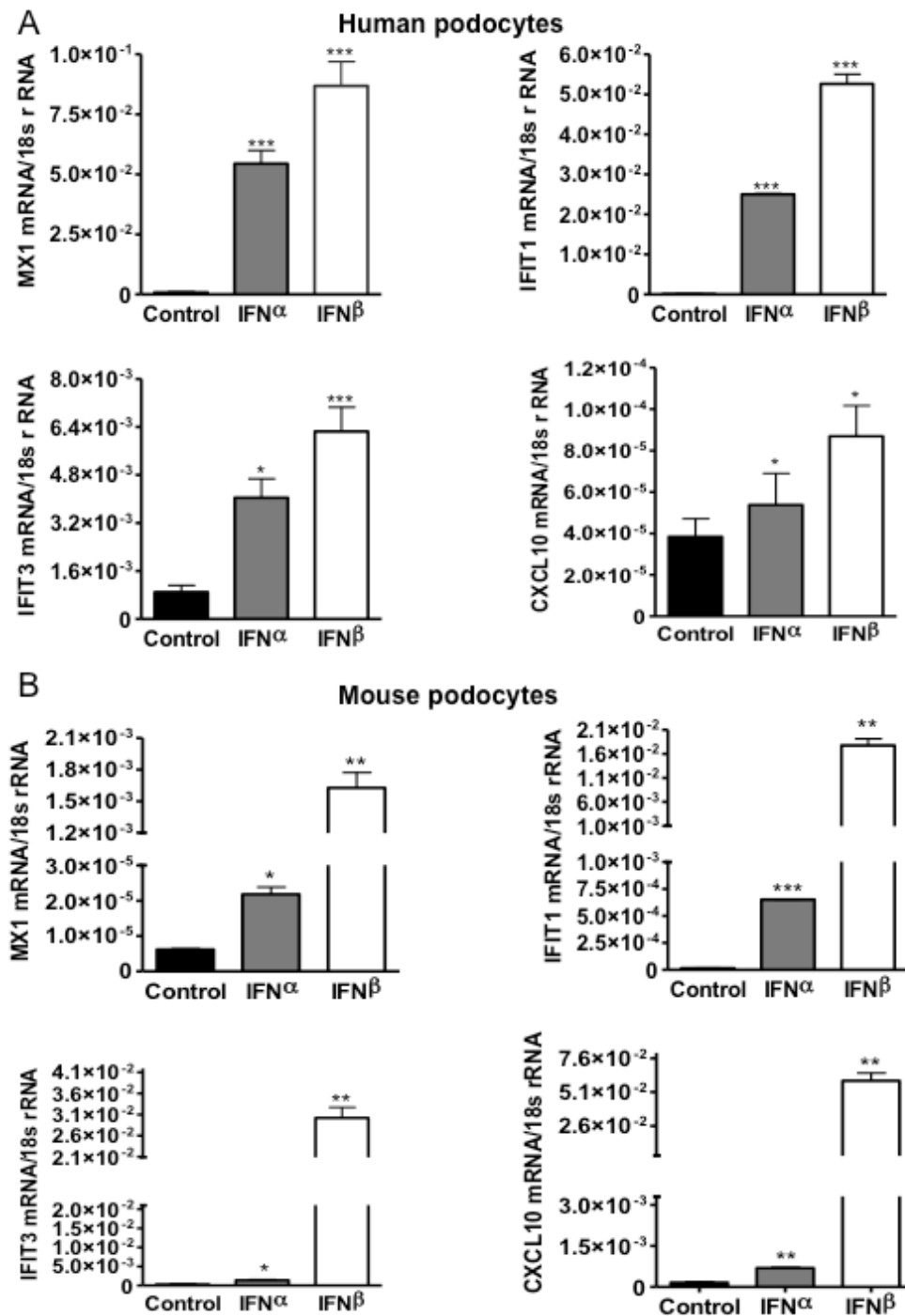
B Mouse podocytes

Figure 12. IFN type I signature in human and mouse PECs and podocytes. Human (A, C) and murine (B, D) glomerular epithelial cell mRNA was isolated after 12h of exposure to IFN α/β (1000U/ml). Real-time polymerase chain reaction was performed for the indicated ISG genes as described in results methods. Data are expressed relative to their respective 18s rRNA expression and are means ± SEM of three experiments and are means ± SEM of three independent experiments *P < 0.05 versus control **P < 0.01 versus control; ***P < 0.001 versus control

4.5 Only IFN-β increases monolayer permeability of podocyte

Based on the consistent activation of podocytes by both IFN-α and IFN-β, their effect on podocyte permeability, used as a biomarker of their glomerular filtration barrier function, was evaluated. Murine podocytes were used to perform electrical cell impedance assay (ECIS) to evaluate changes in podocyte resistance upon IFN stimulation and to quantify alterations in the barrier function of cell monolayers in-vitro [211, 214]. Cellular resistance was significantly decreased in response of IFN-β as early as 5 min of stimulation (Figure 10 B) in murine podocytes. In human podocytes IFN-β affected cellular resistance in a similar manner but not until 2h of stimulation (Figure 10 A). In contrast, IFN-α stimulation in both species did not affect podocyte monolayer resistance as compared to the control. Changes in podocyte activation can be transient or persistent and may eventually lead to podocyte detachment and/or death [95]. In order to address this question podocytes were exposed to IFN-β for 24h and cell death was analysed by flow cytometry. Flow cytometer analysis of podocyte culture supernatant showed an increased number of PI+ cells upon IFN-β stimulation as compared to control (31,6% vs. 16.4% of detached cells) (Figure 13). This suggests that IFN-β, but not IFN-α, modulates the glomerular filtration barrier by affecting stability of the podocyte monolayer architecture.
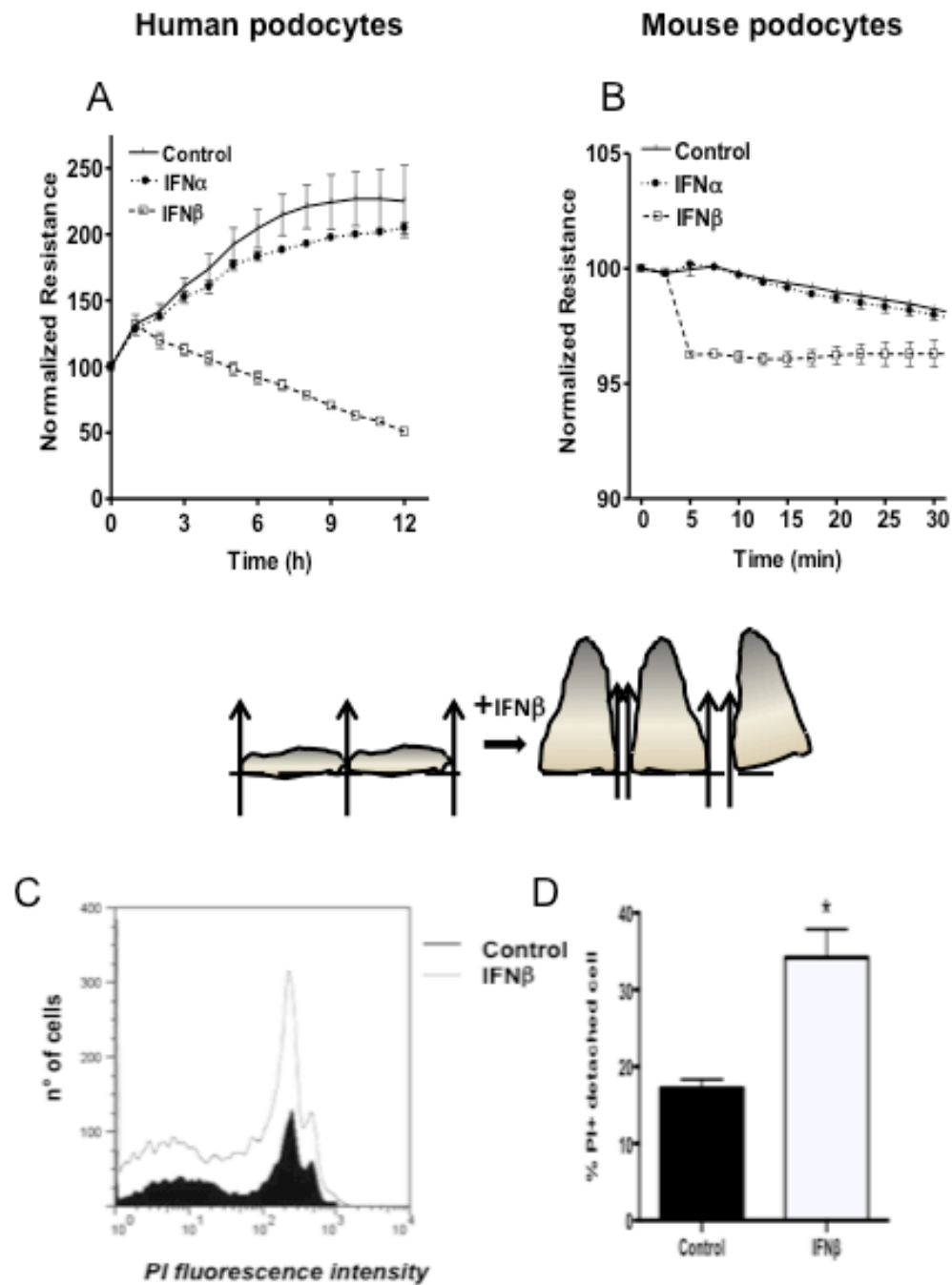
Figure 13. IFN-β increases podocyte monolayer permeability by causing podocyte detachment. (A) Human and (B) mouse podocytes were seeded into ECIS culture ware and grown to confluence. Monolayer resistance was analyzed for 30 min or 12 h, respectively. Data are expressed as normalized resistance ± SEM for three independent experiments. (C-D) An equal number of human podocytes were exposed to medium (black) or IFN-β (open/white). After 24 h propidium iodide (PI) flow cytometry of the cell culture supernatant of PI positive detached cells was performed. Data are means ± SEM of three experiments. *P < 0.05 *versus control*

4.6 IFN-β affects podocyte viability by promoting cell death

Increased podocyte permeability is associated with cytoskeleton modification and loss of podocyte architecture complexity [13]. Modification of the cellular shape can lead to cellular damage and death. Inflammatory cytokines have been reported to trigger in-vivo and in-vitro podocyte damage and progressive loss of kidney function. Yet, how the antiviral type I IFNs affect podocyte viability is still not clear [215, 216]. Based on the permeability data, only IFN-β modulated podocyte permeability by increasing the detachment. In order to understand if this increase of podocyte detachment was correlated with podocyte death, human and murine podocytes were exposed to IFN-β for 24h and analysed by flow cytometry. IFN-β exposure significantly increased the numbers of PI+ podocytes from both species while the effect on annexin V staining was stronger in mouse podocytes (Figure 14). Type I IFNs exert potent pro-apoptotic effects on several cell types, by inducing pro apoptotic molecules [217, 218]. To verify the effects of IFN-β on glomerular podocytes, pro-apoptotic gene expression analysis was performed. RT-PCR analysis showed a significantly increased expression of several pro-apoptotic genes, such as PUMA, BAK, BAX, and BID, compared to control (Figure 14).

Altogether, IFN-β modulates podocyte viability in-vitro by triggering detachment, leading to apoptosis and/or necrosis.
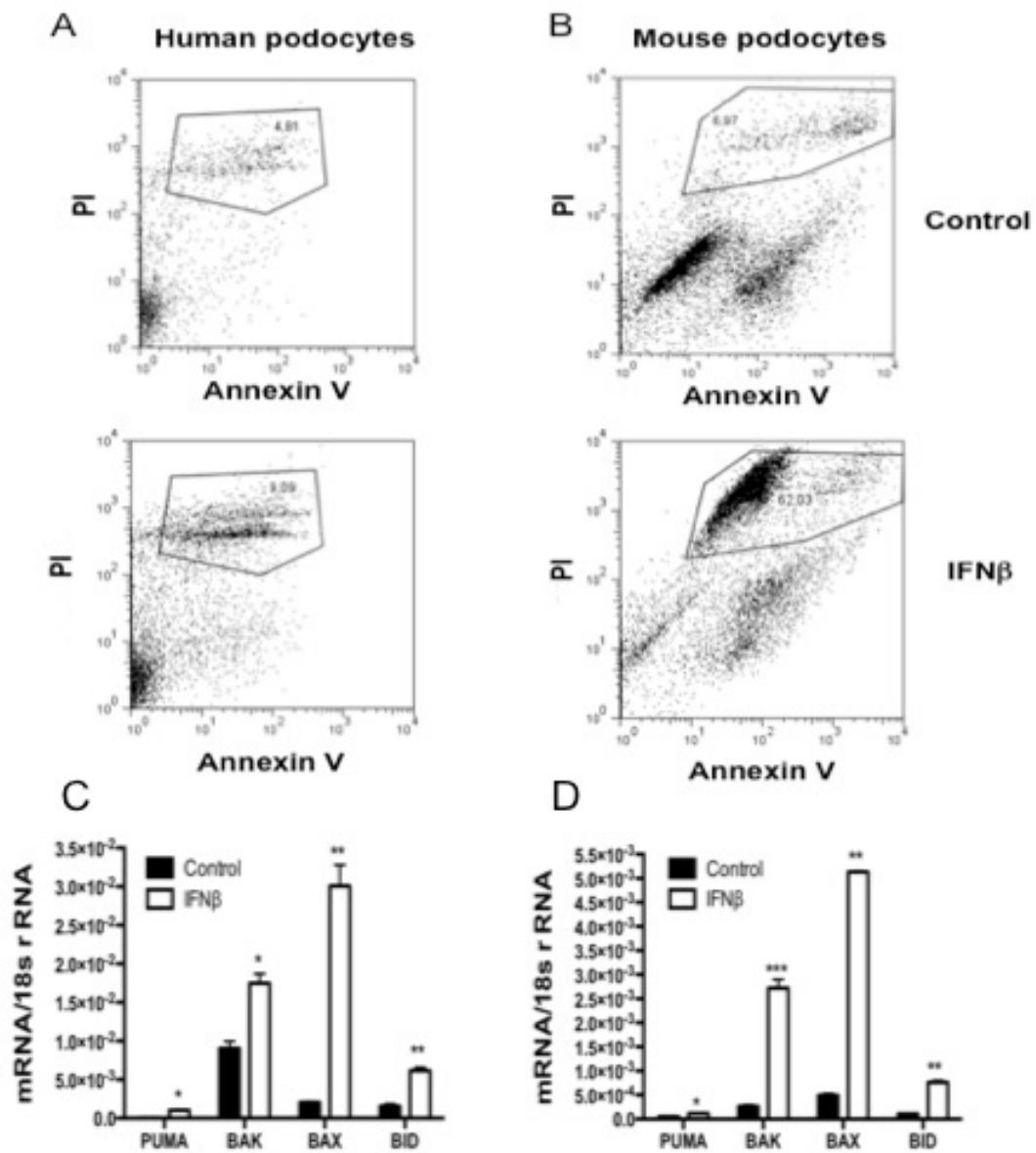
Figure 14. IFN-β modulate podocyte viability by promoting death. Human (A) and mouse (B) podocytes were cultured +/- IFN-β (5000U/ml) for 24h and propidium iodide (PI) and annexin V flow cytometry was assessed to quantifies their viability. Podocyte mRNA from both the species (C: human, D: mouse) was isolated after 12h of exposure to IFN-β (5000U/ml) and real-time polymerase chain reaction was performed for the indicated pro apoptotic genes as described in the Methods. Data are expressed relative to their respective 18s rRNA expression and are means ± SEM of three experiments. *$P < 0.05$ *versus control* ; **$P < 0.01$ *versus* control; ***$P < 0.001$ *versus control*

4.7 IFN-α but not IFN-β modulate parietal epithelial cell proliferation

In contrast to the highly differentiated podocytes, PECs easily proliferate in culture or in-vivo, for example when GBM rupture exposes them to serum. This drives PEC overgrowth in the Bowman`s space and ultimately leads to glomerular crescent formation [24]. During viral infection, local and systemic type I IFNs increased affecting homeostasis of target cells. PECs express both types of IFN receptor chains, but the pathogenic effects of these cytokines on PECs homeostasis is not known. To start out, how IFN-α and-β affected PECs proliferation, contributing or preventing aberrant parietal epithelial cells proliferation was investigated. To evaluate PEC viability and growth upon IFN-α and IFN-β stimulation, MTT assays were assessed. After 72h of stimulation, IFN-α but not IFN-β, significantly reduced the viability of both human and murine PECs (Figure 15). Reduced PEC viability correlated with IFN-α exposure and can be associated with induction of cellular death or cell cycle modulation. To evaluate if this decrease of proliferation was due to the ability of type I IFNs to trigger cell death, murine and human PECs were exposed to IFN-α and IFN-β for 24h, and PI/annexin V flow cytometry analysis was performed. Flow cytometry analysis revealed that the reduced viability of PECs upon IFN-α and IFN-β stimulation did not correlate with an increase in cellular death. (Figure 15) Altogether, this suggests that IFN-α, but not IFN-β, modulates PEC proliferation without triggering cell death.
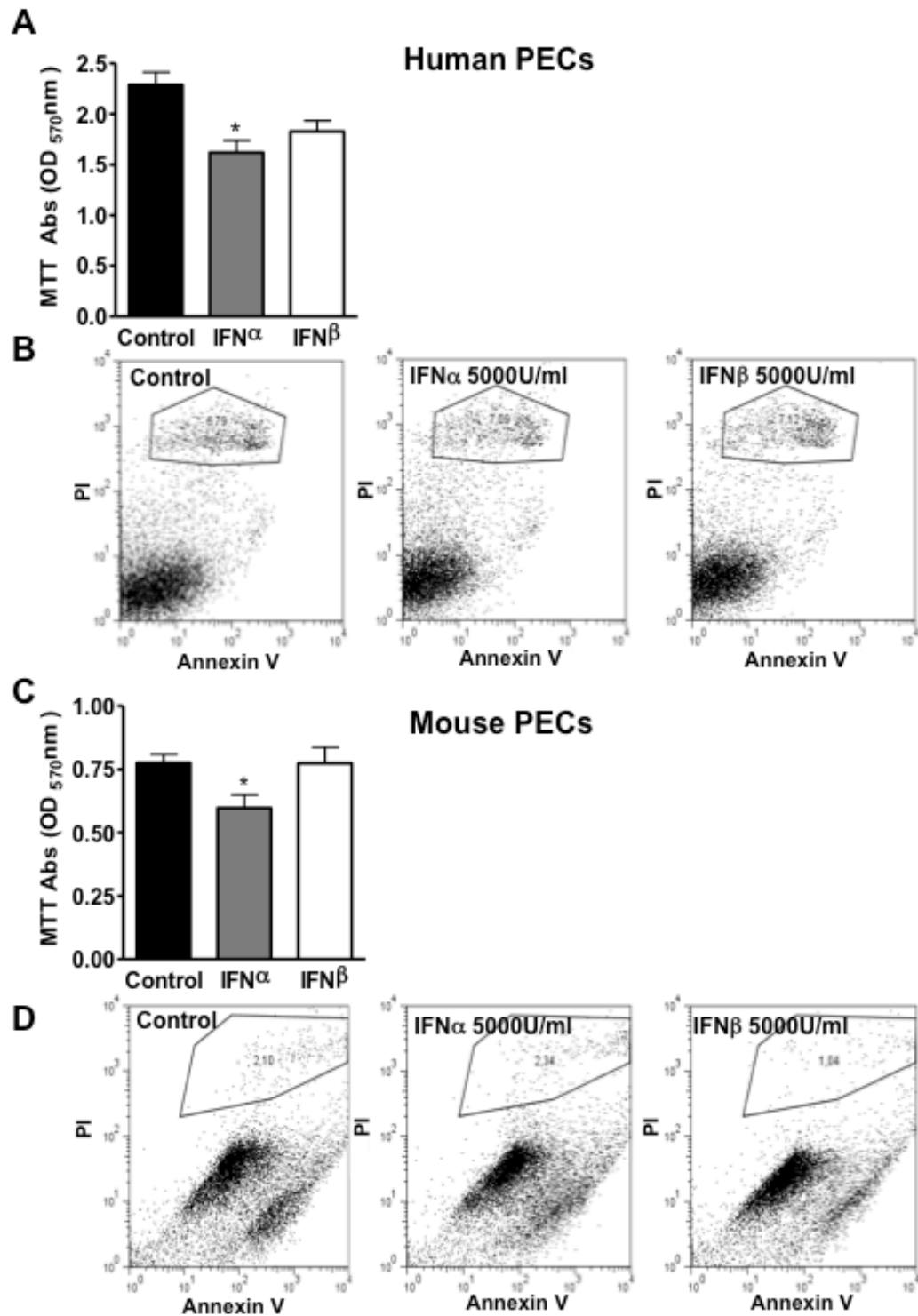
Figure 15. IFN-α affects PECs proliferation. Human and murine renal PEC were cultured with IFNα/β (5000U/ml) for 24h and cells proliferation was assessed (A, C). Data are means ± SEM of three experiments, each analysed in quadruplicate. *P < 0.05 versus. In similar experiment human and murine PEC stimulated for 24h with or without IFNα/β (5000U/ml) were stained with anti-annexin V and PI and analyzed by flow cytometry (B, D). The figure displays one representative of several experiments.

4.8 IFN-α modulate PECs cell cycle by p21 up-regulation

Cell cycle arrest has been reported to be part of the antiviral defense mechanism activated by the release of type I IFN cytokines to limit viral replication in the host [161, 219]. To investigate whether IFNα affects PECs viability by modulating cell cycle progression, human and mouse PECs were cultured +/- IFNα/β, and cell cycle analysis by PI staining was performed. Flow cytometry analysis showed a decrease of cell numbers in the S-phase (DNA replication phase) in the sample exposed to IFN-α compared to the control. This was not observed in samples exposed to IFN-β (Figure 16). The cell cycle is strictly regulated by expression of cyclins and cyclin-dependent Kinases (CKDs). Two distinct classes of these cell cycle regulators, inhibitors and activators orchestrate the entry or the arrest into the next cell cycle phase. To investigate through which mechanism IFN-α promotes cell cycle arrest in glomerular PECs, cells from humans and mice were cultured +/- IFNα/β for 24h, and cellular protein was harvested. Western-blot analysis for expression of the cyclin-dependent kinase inhibitor-1 p21, which is associated with arrest of the cell cycle in G1 phase, was performed (Figure 16). PECs exposed to IFNα, but not to IFN-β, showed an increased expression of p21 compared to the control. Thus, all together this shows that in parietal epithelial cells, IFN-α inhibit cell cycle progression from G1 phase to S phase, by p21 up-regulation.
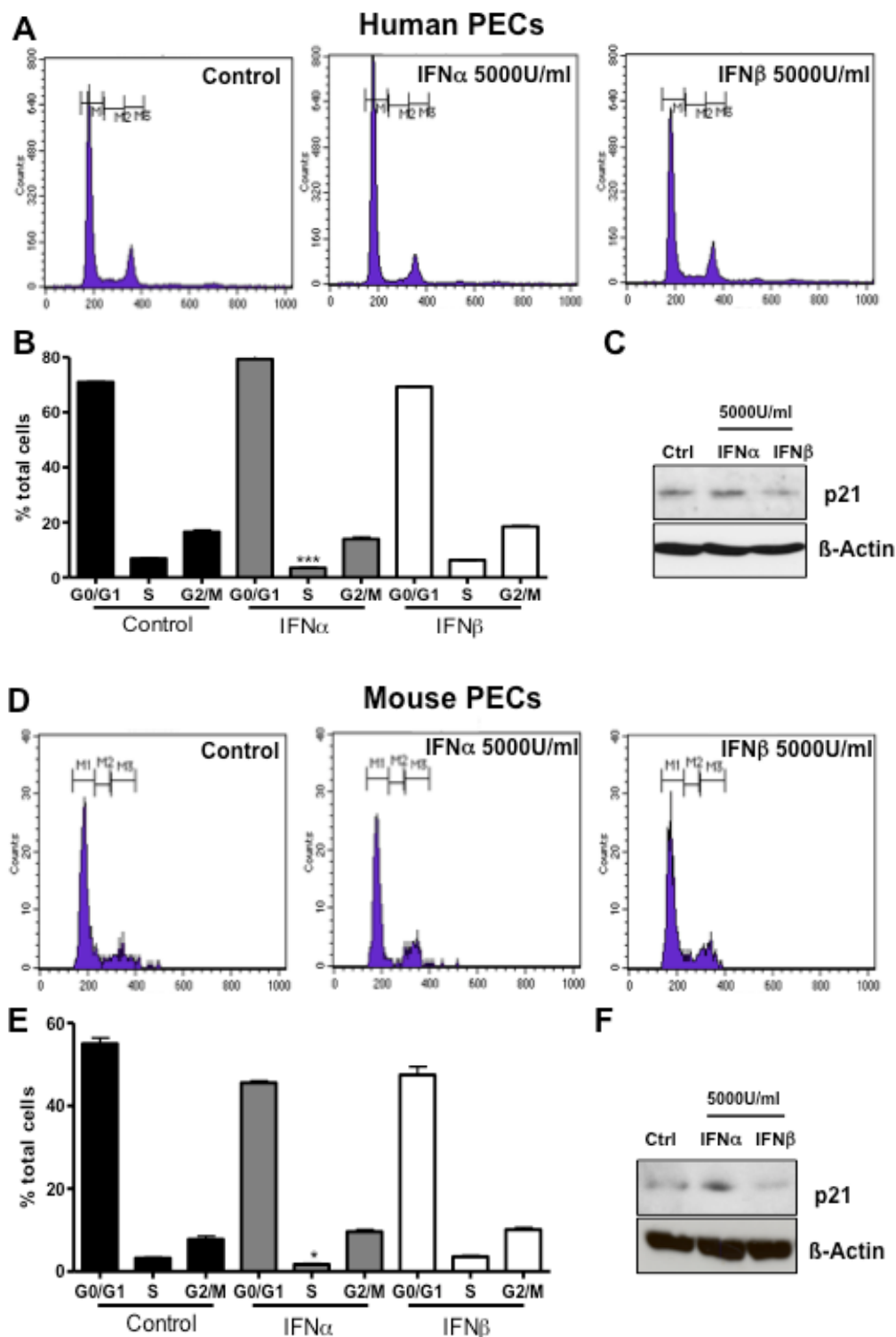
Figure 16. IFN-α arrest PEC growth affecting their cell cycle. Human (A-B) and mouse (D-E) were culture +/- IFNα/β 5000U/ml) for 24 h and cell cycle analysis by PI staining was performed as described in the methods. Data are means ± SEM of three experiments, each analyzed in duplicate.*P < 0.05 *versus control (S-phase)* ; **P < 0.01 *control (S-phase)* ; ***P < 0.001 *control (S-phase)*. (C,F) In similar experiment cellular lysates from human and murine PECs were analyzed by western blot for the expression of p21. β-Actin staining is shown as loading control. The figure displays one representative of several blots from three independent experiments

4.9 IFN-α modulate PEC migration but both IFN I suppress progenitor differentiation

Human CD133+/CD24+ renal progenitor cells within the PEC layer at the inner aspect of the Bowman`s capsule have the capacity to differentiate to podocytes in culture and may restore podocyte loss in-vivo [117, 206]. This concept of progenitor PEC-derived podocytes is supported by lineage tracing experiments in transgenic mice during renal development and growth [120]. Vice versa, persistent proteinuria and glomerular scaring may imply that the activation of quiescent PEC progenitors, their co-ordinated proliferation and migration to the glomerular tuft, and finally, their differentiation into mature podocytes is significantly impaired and podocyte loss rather results in focal scar formation [38]. In this scenario, intra and extra renal infections might interfere with glomerular regeneration by realising inflammatory antiviral cytokines, such as type I IFNs. To investigate if types I IFNs induce all necessary steps for podocyte regeneration from their PEC progenitors, the impact of IFN-α and IFN-β on renal human CD133+/CD24+PECs was evaluated. Wound healing assays on human renal progenitor monolayers and murine PECs was performed, which involve the activation and migration of surviving cells to close the wound, consistent with its negative regulation of migration. Exposure to IFN-α, but not to IFN-β, significantly reduced the migratory capacity of these cells to close the wound (Figure 17). Furthermore, the potential of renal progenitors to differentiate in-vitro towards podocytes was tested. This was achieved by exposing parietal epithelial renal progenitors to the appropriate differentiation medium (VRADD) in presence of type I IFNs for 48h. At the end of the experiment, quantification of nephrin mRNA expression was used to evaluate the differentiation of renal progenitors towards podocytes. IFN-α and IFN-β both significantly reduced the capacity of podocyte progenitors to induce nephrin mRNA expression, indicating the role of these inflammatory cytokines during the differentiation process (Figure 17). The effect was more pronounced for IFN-β, probably because IFN-β also killed mature podocytes as observed before. These data show two critical effects of the IFN subtypes on glomerular epithelial cells. First, IFN-α specifically suppresses PEC migration; second, both IFN-α and IFN-β inhibit

renal progenitor differentiation into mature podocytes, which then adds on to podocyte loss by IFN-β-induced podocyte death.
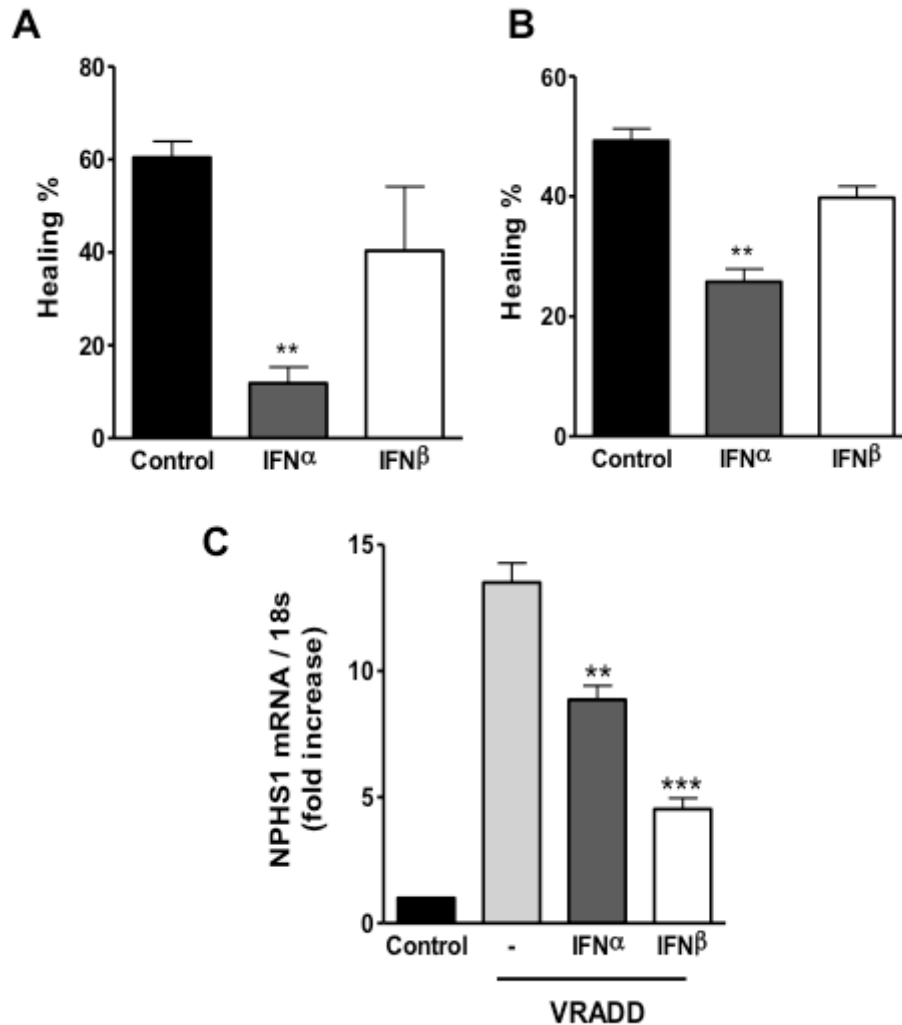
Figure 17. IFNα/β modulate PEC migration and podocyte progenitor differentiation
Cell migration assay +/- IFN-α/-β (5000U/ml) was performed with human (A) and murine (B) PECs using culture inserts as described in methods. Data shown represents mean wound size at the end of the experiment. (Data are expressed as means ± SEM of three independent experiments. **P < 0.01 versus control; ***P < 0.001 versus control. (C) Human renal progenitors were cultured in the VRADD medium +/- h IFNα/β (5000U/ml) for 48h and nephrin quantification by Taq-Man RT-PCR was performed as described in the Methods. As control, renal progenitors were cultured for 48h in normal growth medium as described in the Methods. Data are expressed relative to their respective 18s rRNA expression and are means ± SEM of three independent experiments *P < 0.05 versus control; **P < 0.01 versus control; ***P < 0.001 versus control.

4.10 IFN-α and IFN-β aggravate glomerulosclerosis in adriamicyn-induced nephropathy in SCID mice

Extra renal and intra renal infections can aggravate kidney damage by exposing glomerular cells to large amounts of type I IFNs. To test the functional significance of type I IFN in the pathogenesis of glomerular damage, recombinant IFN-α or IFN-β were injected into mice with adriamycin-induced FSGS [67]. To focus on the intrarenal effects of the IFNs, all experiments were performed in SCID mice lacking adaptive immunity. This allowed for exclusion of secondary effects due to immunomodulatory properties of type I IFNs. All animals received adriamycin at the dose of 6,5 mg/kg by retro-orbital injection and three groups were assessed. For seven days, the animals received injections of recombinant IFN-α or IFN-β or saline daily. At day 7 the animals were sacrificed and organs collected for retrospective analysis. Injections with either recombinant IFN-α or IFN-β significantly aggravated proteinuria and focal segmental tuft adhesions and sclerosis by day 7 of mice with adriamycin nephropathy (Figure18). However, the effect of IFN-β was much more prominent than that of IFN-α. Taken together, IFN-α and IFN-β both have the potential to aggravate proteinuria and glomerular pathology in SCID mice with FSGS.
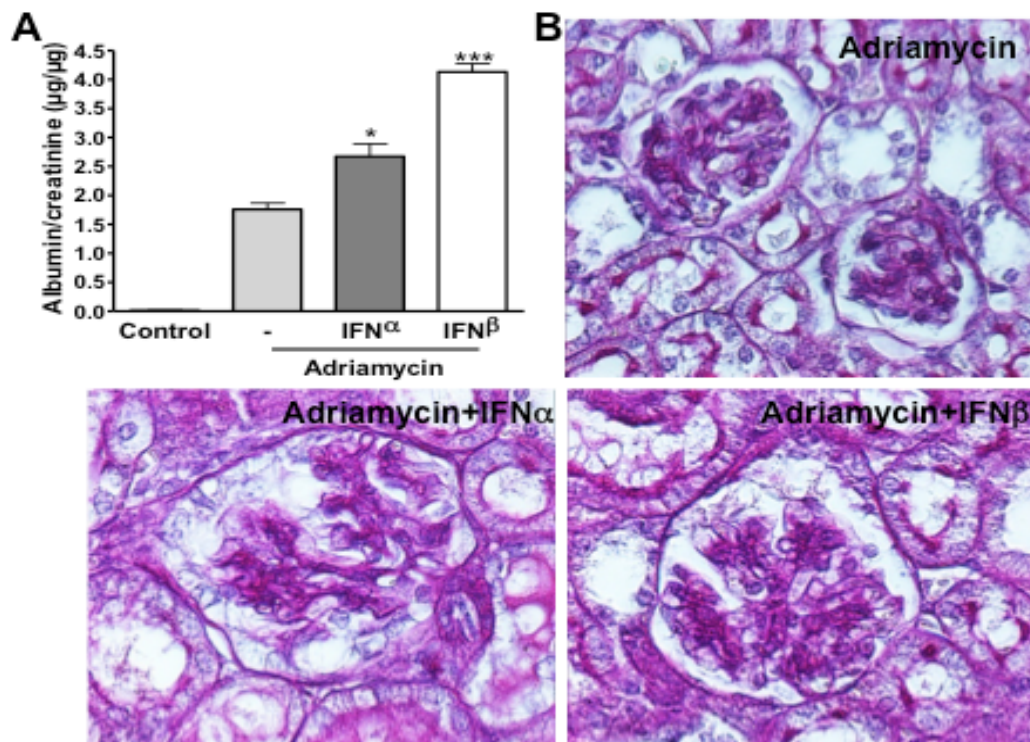
Figure 18. IFN-α and IFN-β aggravate adriamycin-induced nephropathy in SCID mice. (A) Albumin/creatinine ratios were measured in mice were measured in mice injected with adriamycin compared to adriamicyn+IFN-α (1000U) and adriamicyn+IFN-β (1000U) injected mice after 7 days. Data from one representative of three independent experiments in shown. Data are expressed as means ± SEM. (n=6 mice for each experiment and for each group of treatment). *$P < 0.05$ versus adriamycin; ***$P < 0.001$ versus adriamycin. (B) Representative images from periodic acid shiff stains of all groups are shown at original magnification of x 400

4.11 IFN-α and IFN-β trigger expression of multiple ISGs in-vivo

Consistent with the previous in-vitro data, IFN-α and IFN-β showed the ability to activate and induce the expression of ISGs in glomerular cells in-vitro. To extend this finding in-vivo, kidney samples from SCID mice with FSGS, were analyzed. Kidney mRNA from mice injected with both IFNs was extracted and RT-PCR analysis for ISG was performed. Both groups treated with IFN-α and IFN-β showed increased intrarenal mRNA expression of ISGs (MX1, IFIT1, IFIT3, and CXCL10), indicating the ability of IFNs to activate glomerular cells, both in-vitro and in-vivo (Figure 19).
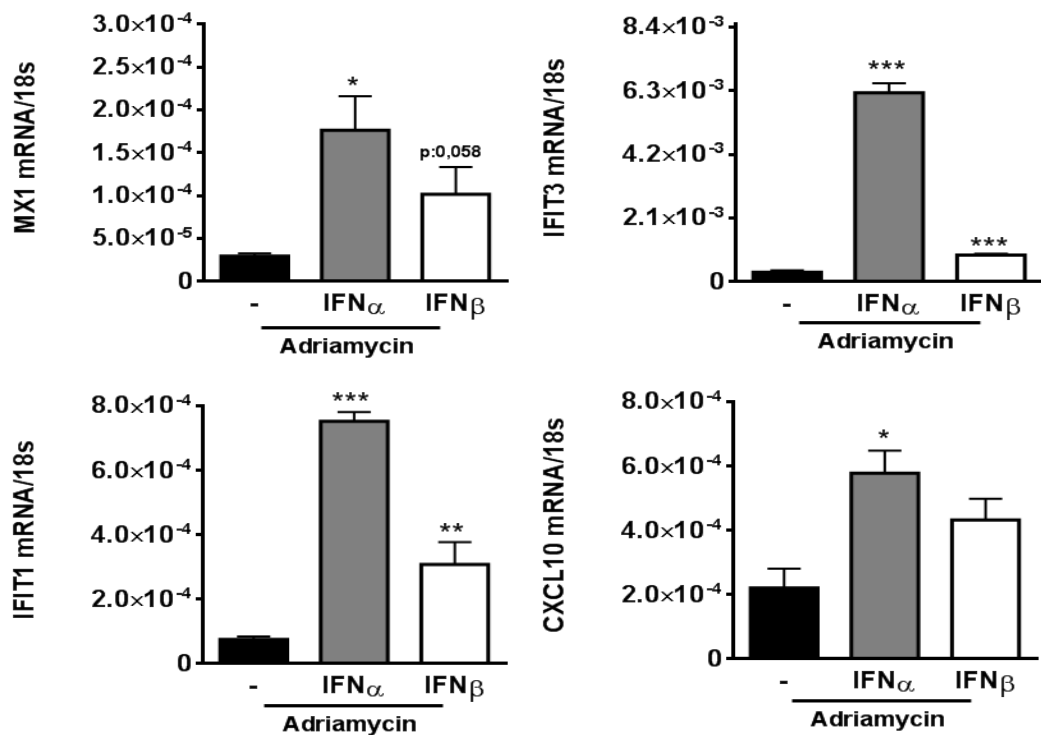
Figure 19. Both IFN-α and IFN-β induced intrarenal expression of ISGs and inflammatory markers. Total kidney mRNA was extracted from mice injected with adriamycin or with adriamycin +IFNα/β (1000U) after 7 days of treatment. Real-time polymerase chain reaction was performed for the targeted ISG genes as described in the Methods. Data are expressed relative to their respective 18S rRNA expression and are means ± SEM of three experiments (n=6 mice for each experiment and for each group of treatment) *P < 0.05 versus adriamycin; **P < 0.01 versus adriamycin; ***P < 0.001 versus adriamycin

4.12 IFN-α and IFN-β treatment increase glomerular inflammation

Classically, type I IFNs specifically target innate and adaptive immune responses. In vivo, they promote natural killer cell cytotoxicity, as well as they enhance macrophage maturation, and inducible nitric oxide synthase production. Both IFNs showed the ability to regulate the expression of multiple proinflammatory cytokines and chemokines, in immune cells and as well as in non-immune cells. SCID mice lack adaptive immune cells, but not innate immune cells like macrophages. To investigate to which extent IFN injections orchestrate the innate immune response in the pathogenesis of adriamycin-induced FSGS, glomerular macrophages were quantified by confocal microscopy. Kidney sections from the mice were stained for CD68, used as macrophage marker, and

Claudin I (CLDN1) to stain PECs lying of the Bowman's capsule. Increased numbers of glomerular CD68+ macrophages for both IFNs has been detected, confirming the role of IFNs in modulating innate immune cells (Figure 20) In accordance, mRNA gene expression analysis was performed to profile proinflammatory cytokines (IL-6, TNF-α) and chemokines (CXCL9, CXCL11) expression in the kidney. Samples from both groups treated with type I IFNs showed an increased level of proinflammatory cytokine expression compared with the vehicle group (Figure 20). Thus, IFN-α and IFN-β both have the potential to direct innate immunity and contribute to tissue inflammation by increasing glomerular macrophage numbers and triggering intrarenal proinflammatory secretion in-vivo. This type of immune response can aggravate glomerular damage in SCID mice with FSGS.
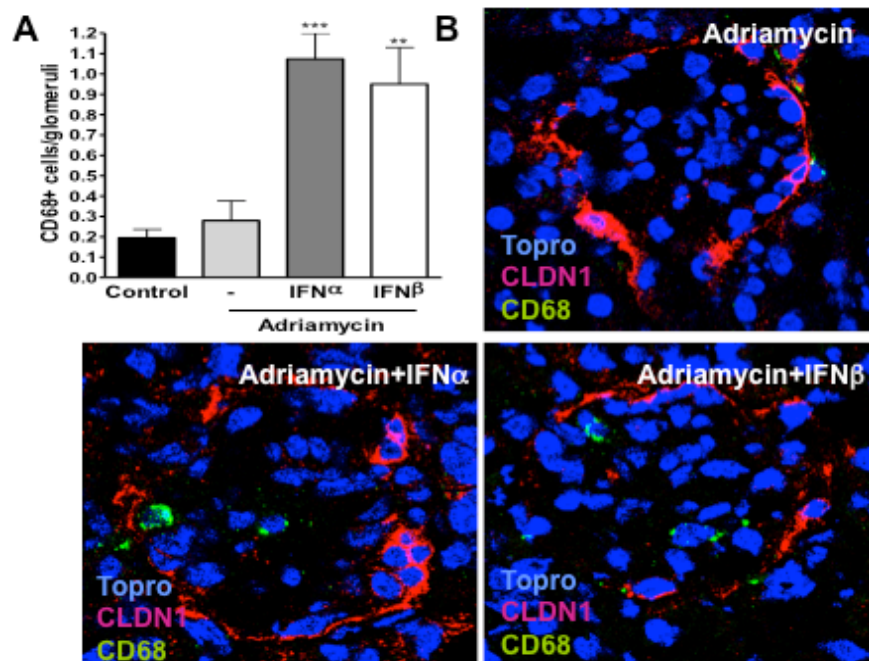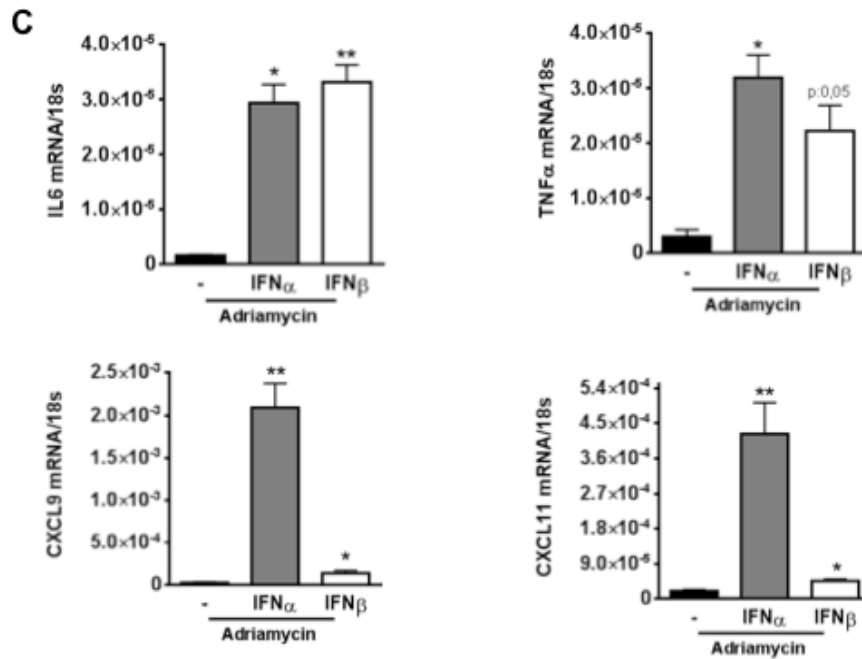
Figure 20. IFNs type I activate intrinsic renal cells and macrophages in vivo. (A) Quantification of CD68+ macrophages/glomerulus after 7 days of injury. Data are expressed as means ± SEM and are representative of three independent experiments (n=6 mice for each experiment and for each group of treatment). *$P < 0.05$ versus adriamycin; **$P < 0.01$ versus adriamycin; ***$P < 0.001$ versus adriamycin. (B) Representative picture of double-label immunofluorescence for Claudin-1 (CLDN1) (red) and CD68 macrophages (green). (C) Total kidney mRNA was extracted from mice injected with adriamycin or with adriamycin +IFNα/β (1000U) after 7 days of treatment. RT-PCR reaction was performed for the pro-inflammatory markers as described in the methods. Data are expressed relative to their respective 18S rRNA expression and are means ± SEM of three experiments *$P < 0.05$ versus adriamycin; **$P < 0.01$ versus adriamycin;

4.13 IFN-α and IFN-β have distinct effects on podocytes in-vivo

Since in-vitro studies showed that IFN-α and IFN-β elicit distinct and differential effects on podocytes in-vitro, we investigated this possibility in-vivo. Podocyte injury is the culprit in the pathogenesis of glomerular damage leading to development of proteinuria. According with the in-vitro data, IFN-β modulates the glomerular filtration barrier by triggering podocyte detachment/death in-vitro. To question the impact of IFN injection on glomerular podocyte numbers in adriamycin-induced FSGS, histological analysis of the kidney from all the groups was assessed. Kidney samples were stained for two different podocyte markers nephrin (NPHS1) and WT-1, and confocal analysis was performed. Consistent with our in-vitro data, IFN-β injections reduced the numbers of NPHS1+/WT-1+

podocytes in SCID mice with adriamycin nephropathy as compared to the vehicle control group (Figure 21). By contrast, impact of IFN-α injections on podocyte numbers was less dramatic compared to the group injected with IFN-β.

Prove of podocyte apoptosis are really poor in the literature, and a new concept regarding podocytes death is emerging How do podocytes die? It was believed that they die by apoptosis. But, there is a little experimental proof to this concept in the current literature. However, recently there are few reports which suggest catastrophic mitosis as a new mechanism of podocyte death *in-vivo*[104]. Podocyte are terminally differentiated epithelial cells, which have lost the capacity to divide. During inflammation, cytokines and other mediators might signal podocytes to re-entry the cell cycle to compensate the loss of neighbour cells. Frequently, this process leads to podocyte death by a mechanism called catastrophic mitosis. Podocytes can neither complete cytokinesis nor maintain their function as aneuploidy cells [105, 220, 221].

To characterize if IFN-β injection affects podocyte loss by inducing catastrophic mitosis, double immune-fluorescent for the podocyte marker podocin (NPHS2) and for histone H3 phosphorylated at serine 10 (P-H3) was performed in the kidney sections (Figure 21C, 21D). P-H3 marks the prophase of nuclear division in cells that are about to complete mitosis. Podocyte P-H3 staining was absent in healthy mouse kidneys. Control SCID mice with adriamycin nephropathy showed a small number of P-H3 positive podocytes, however, the number of P-H3 positive podocytes per glomerulus was increased in mice that had received IFN-β injections. Mice treated with IFN-α did not show any change in the number of P-H3 positive podocytes, while mice treated with IFN-β showed significantly less P-H3 positive podocytes compared to the control. This suggests that IFN-β affect podocyte viability in-vivo by triggering podocyte through catastrophic mitosis.
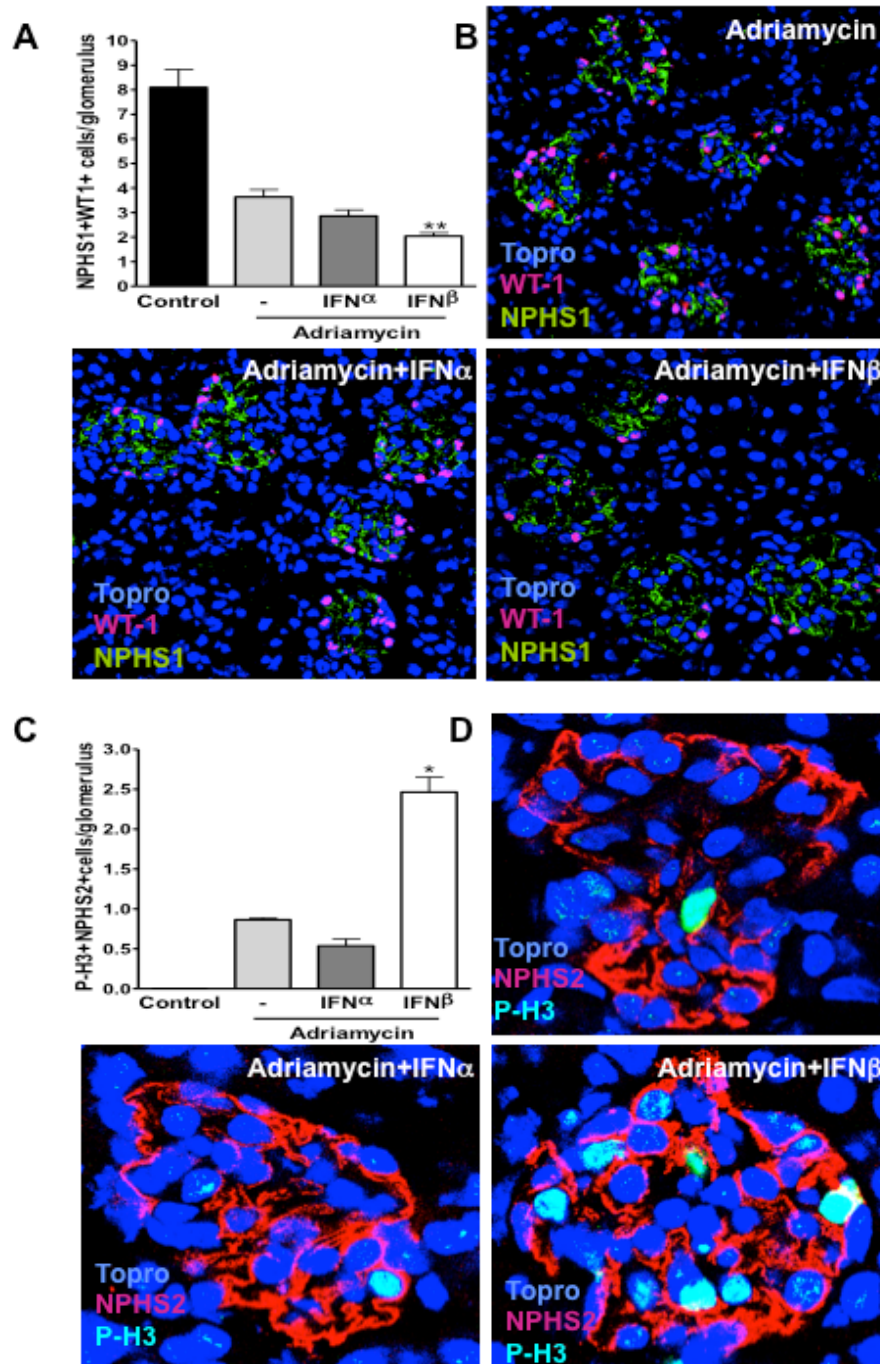
Figure 21. IFN-β aggravates podocyte loss in FSGS. (A) Quantification of number of podocyte (NPHS1+WT-1+)/glomerulus after 7 days of treatment. Data are expressed as means ± SEM and they are representative of three independent experiment. (n=6 mice for each experiment and for each group of treatment).; **$P < 0.01$ versus adriamycin;. (B) Representative pictures of double-label immunofluorescence for WT-1 (red) and NPHS1 (green). (C) Quantification of number of mitotic podocyte (NPHS2+P-H3+)/glomerulus after 7 days of treatment. Data are expressed as means ± SEM and they are representative of three independent experiment. (n=6 mice for each experiment and for each group of treatment).; *$P < 0.05$ versus adriamycin;. (D) Representative picture of double-label immunofluorescence for NPHS2 (red) and P-H3 (green).

4.14 IFN-α and IFN-β have distinct effects on PEC mitosis in-vivo

The in-vitro results imply that predominantly IFN-α, not IFN-β, affects PECs, for example by inducing PEC senescence. To study the impact of IFN injection on proliferating PECs in adriamycin-induced FSGS, histological analysis of the kidney from all the groups was assessed. Kidney sections were stained for the PEC marker CLDN1 and for P-H3, used as marker for mitotic cells (Figure 22). CLDN1/P-H3 positive PECs were absent in healthy mouse kidneys; by contrast, SCID mice with adriamycin nephropathy displayed P-H3 positive PECs, in accordance with their role in glomerular regeneration. However, their numbers were significantly decreased upon IFN-α injections while IFN-β injections had no such effect (Figure 22). Thus, although IFN-α and IFN-β both aggravate adriamycin-induced proteinuria and FSGS, both have differential effects on glomerular epithelial cells, podocytes and PECs, which are consistent with the in-vitro results.
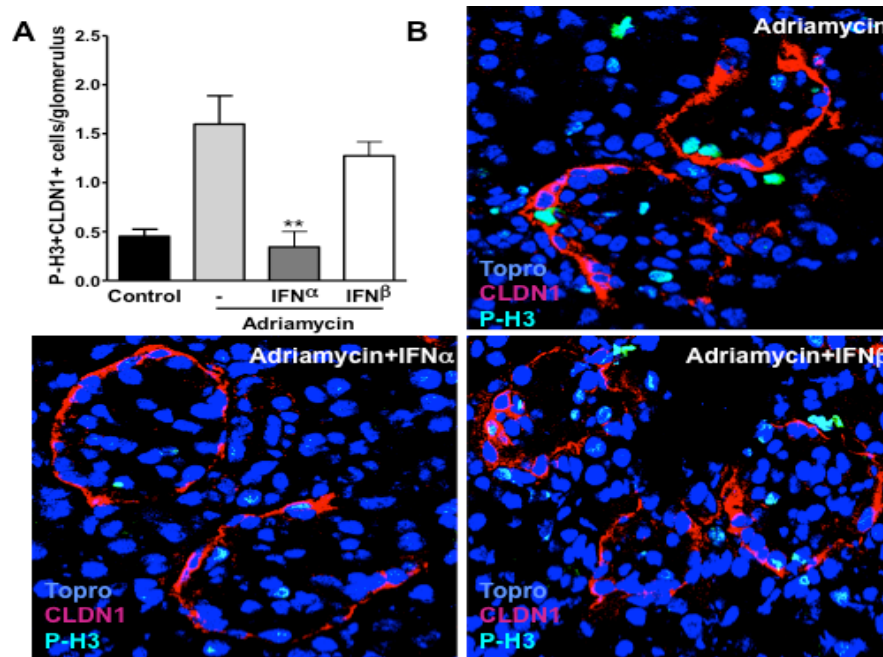
Figure 22. IFN-α affect PEC proliferation in-vivo. (A) Quantification of number of proliferating PEC (P-H3+CLDN1+)/glomerulus after 7 days of treatment. Data are expressed as means ± SEM and they are representative of three independent experiment. (n=6 mice for each experiment and for each group of treatment).; **$P < 0.01$ versus adriamycin;. (B) Representative pictures of double-label immunofluorescence for CLDN1 (red) and P-H3 (green).

4.15 IFN-α and IFN-β aggravate proteinuria and podocyte damage in adriamycin-induced nephropathy in Balb/c mice

Adriamycin-induced nephropathy is a model that, to a certain extent, induces a significant component of extra renal adaptive immunity. In order to test the functional significance of Type I IFN in the pathogenesis of FSGS, injection of either recombinant IFN-α or IFN-β into immunocompetent Balb/c treated with adriamycin was performed. All animals received adriamycin at the dose of 11,5 mg/kg by retro-orbital injection. Study mice were divided into three groups: animals received injections of either recombinant IFN-α or IFN-β or saline daily for seven days. After day seven the animals were sacrificed and organs collected for retrospective analysis. Injections with either recombinant IFN-α or IFN-β aggravated proteinuria by day 7, compared with the control (Figure 23). To investigate how IFN injection affects glomerular podocyte homeostasis, confocal analysis of podocytes was performed. Kidney sections from all groups were stained for the podocyte markers NPHS1 and WT-1 (Figure 23). Samples from both groups treated with type I IFNs showed a slightly decreased number of NPHS1+/WT-1+ podocytes compared with the vehicle group. No significant difference has been observed between the two groups, as it was observed in SCID mice. These data indicate that both IFNs have the ability to aggravate glomerular injury in immunocompetent model, with a different extent when compared to non-immunocompetent model
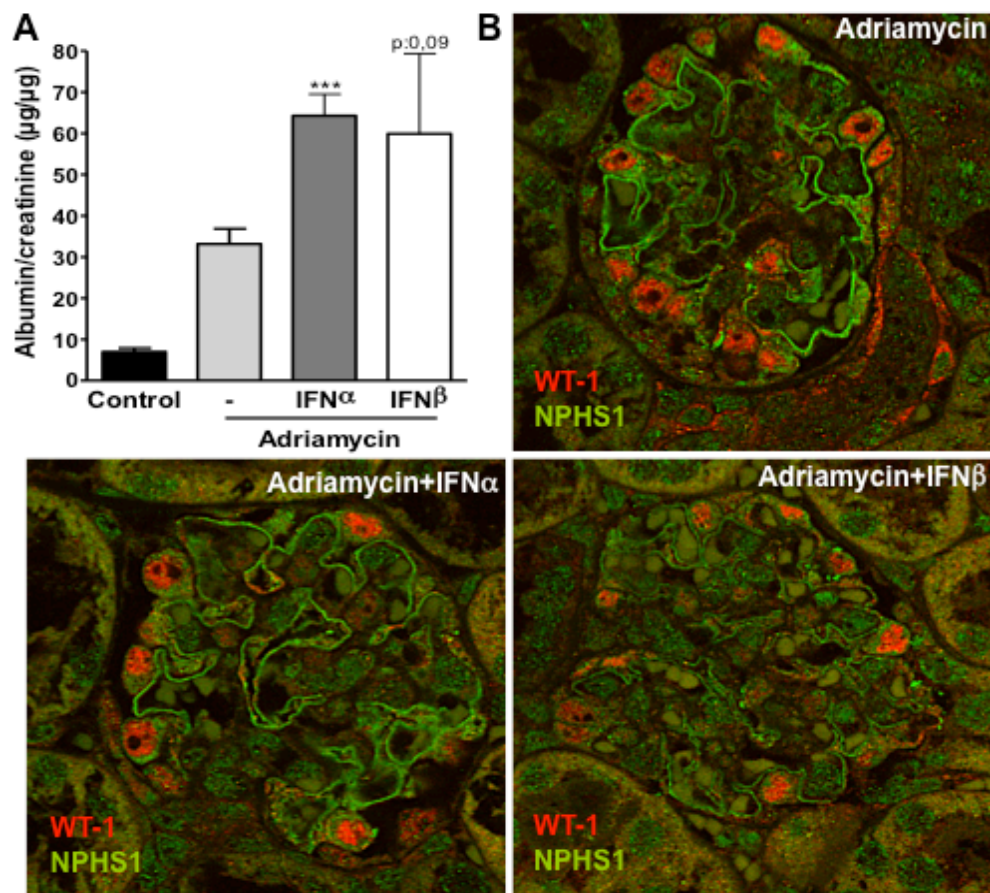
Figure 23. IFN-α and IFN-β aggravate adriamycin-induced nephropathy in Balb/c mice. (A) Albumin/creatinine ratios were measured in mice were measured in mice injected with adriamycin compared to adriamicyn+IFN-α (1000U) and adriamicyn+IFN-β (1000U) injected mice after 7 days. Data from one representative of three independent experiments in shown. Data are expressed as means ± SEM. (n=6 mice for each experiment and for each group of treatment). ***$P < 0.001$ versus adriamycin. (B) Representative pictures of double-label immunofluorescence for WT-1 (red) and NPHS1(green).

4.16 IFN-α and IFN-β injection modulate glomerular infiltrated immune cells

Podocyte damage and loss is the culprit in the pathogenesis of FSGS. However, this model involves intra and extra renal adaptive immune responses that might be modulated, by systemic IFN-α/β injections. Classically, type I IFNs specifically target innate and adaptive immune responses in vivo, activating immune cells and promoting their maturation. This mechanism could potentially aggravate renal disease. To investigate to which extent IFN injections orchestrate intra renal innate and adaptive immune response in adriamycin-induced FSGS, immunohistochemical analysis of immune cells was performed. Kidney sections

from animals sacrificed after 7 days of treatment were stained for CD3, a lymphocyte marker and for Mac2, a macrophage marker. It was observed that the glomerular CD3 lymphocytes remain unchanged (Figure 24) while the numbers of glomerular mac-2 positive macrophages were increased after the treatment of both IFN-α and-β, compared to the control (Figure 25). In summary, these data showed that both IFNs increased glomerular macrophage infiltrate, a mechanism that contributes to aggravate glomerular damage in adriamycin-induced FSGS in Balb/c mice.
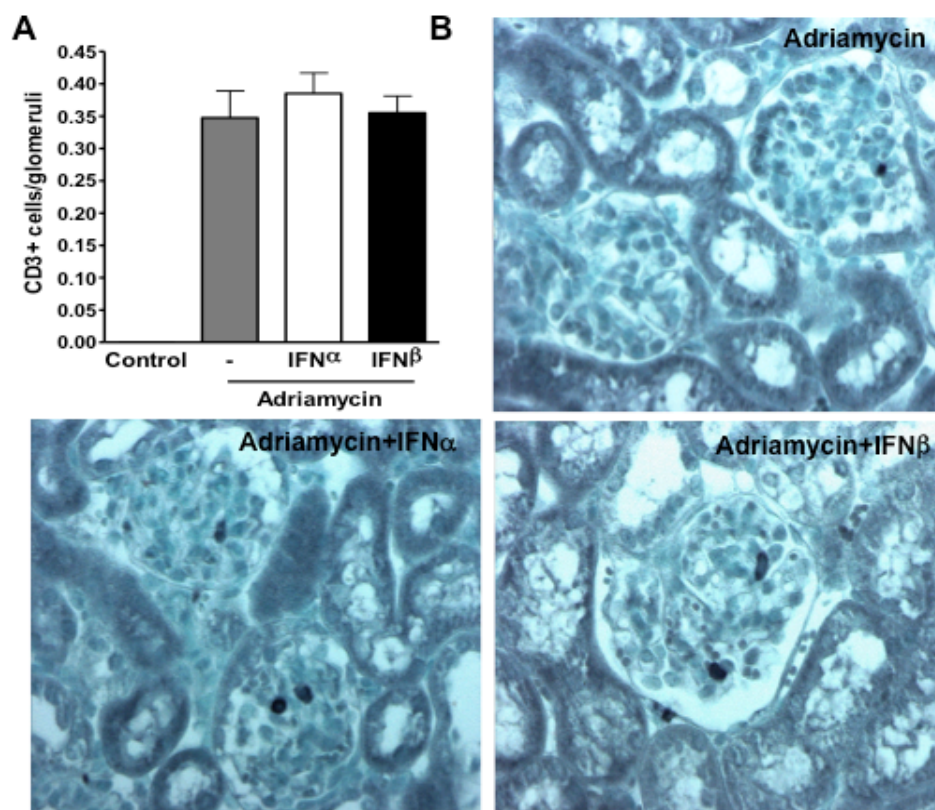
Figure 24. IFN-α and IFN-β do not increase intra glomerular lymphocyte infiltrate. (A) Quantification of number of lymphocyte (CD3+)/glomerulus after 7 days of IFNα/β treatment. Data are expressed as means ± SEM and they are representative of three independent experiment. (n=6 mice for each experiment and for each group of treatment). (B) Representative pictures of CD3 immune staining (black).
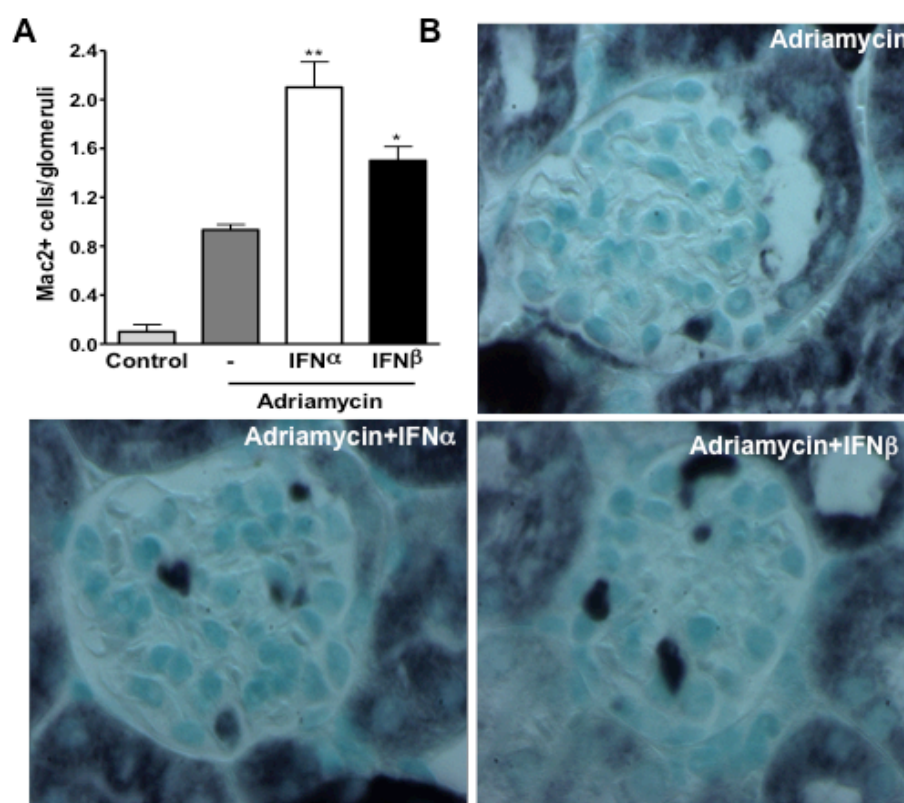
Figure 25. IFN-α and IFN-β modulates glomerular macrophages. (A) Quantification of number of macrophages (Mac2+)/glomerulus after 7 days of IFNα/β treatment. Data are expressed as means ± SEM and they are representative of three independent experiment. (n=6 mice for each experiment and for each group of treatment).; *$P < 0.05$ versus adriamycin;**$P < 0.01$ versus adriamycin;. (B) Representative pictures of Mac2 immune staining (black).

5. Discussion

We have hypothesized that during viral glomerulonephritis, e.g HIVAN, viral replication inside podocytes and PECs would trigger IFN type I-dependent antiviral responses, process that contributes to glomerular damage. IFN-α and IFN-β coordinate antiviral immunity, which involves the activation of innate and adaptive immunity in addition to numerous other biological effects that support antiviral host defense [204, 222]. Even though viral nephropathies represent an important entity in clinical nephropathy little is known about the biological effects of these enigmatic cytokines inside the kidney. During viral infection, viral nucleic acid enters into the cells and is recognized by innate immune pathways [223, 224]. Intracellular nucleic acid recognition mediated by TLRs or RIG-I helicases, leads to activation of interferon regulatory factors (IRFs), resulting in type I IFNs secretion. These cytokines mediate induction of "cellular antiviral state" that restricts further viral spread [180]. Activation of "cellular antiviral state" is characterized by the up-regulation of ISGs, normally silent, that are involved in the inhibition of both viral replication and cellular proliferation. These genes, like IFIT family genes or MX1, are strictly regulated by type I IFNs [222, 225]. It has been reported that glomerular epithelial cells can be infected by certain viruses in-vivo, for example HIV and parvovirus B19, leading to viral nephropathy [132, 226-229]. Podocytes, even though they lack the classical HIV receptors, are susceptible to infection by this virus, resulting in the development of collapsing FSGS. HIV-1 is a single-stranded positive- sense enveloped RNA virus, which has a strong tropism for lymphoid tissue. However, it has been reported to infect many different cell types. PECs are not susceptible to HIV infection during HIV mediated collapsing FSGS, however, they have been shown to be infected by PVB19, leading to nephropathy.

In this thesis it has been shown that podocytes and PECs from mouse and human origin can be infected and activated by synthetic nucleic acid. Infection with synthetic nucleic acid leads to activation of "the type I IFN dependent antiviral state" in both cell types, a mechanism which is induced by the up-regulation of ISGs. It is likely to assume that up-regulation of ISGs upon viral infection is a mechanism of glomerular epithelial cells to protect themselves from

infection and virus propagation. The ISGs found up-regulated in both cell types after synthetic nucleic acid infection correspond to the typical gene expression profile regulated by type I IFNs, also known as " type I IFN signature".

To further investigate how the activation of "cellular antiviral state", regulated by type I IFNs, might modulate glomerular epithelial cell homeostasis and turnover, the impact of nucleic acid infection on human CD133+/CD24+ PECs was studied. This particular subpopulation of PEC layer has shown to be involved in glomerular regeneration by restoring podocyte loss through differentiation processes similar to that of adult stem cell progenitors [16, 25, 38, 84, 117]. In accordance with the activation of the cellular antiviral state upon synthetic nucleic acid activation, the present study demonstrates that viral infections modulate CD133+/CD24+PECs homeostasis by arresting cell proliferation.

In order to replace podocyte loss, human CD133/CD24+ PECs need to increase their number to start the differentiation process. Furthermore, the present work has demonstrated that infection with synthetic nucleic acid inhibits CD133+/CD24+PECs differentiation towards mature podocytes. These effects, modulated by dsDNA induced IFNs, might contribute to the development of glomerular lesion during viral nephropathy. In order to confirm the hypothesis that all these results can be derived from induction of type I IFNs upon viral infection, the direct effects of IFN-α and IFN-β on PECs and podocytes from human and mouse origin were tested. The data obtained demonstrate the ability of both IFNs to activated the cellular antiviral state by up-regulation of ISGs, with a prominent effect of IFN-β on podocytes from both the species, indicating a major susceptibility of these cells by IFN-β.

Despite the fact that IFNAR deficiency has been reported to protect mice from glomerulonephritis [199, 204, 205], Satchell et al. reported anti-proteinuric effects of IFN-β in glomerular diseases of immunocompetent rodents and Schwarting et al. reported protective effects of IFN-β on lupus nephritis of MRLlpr mice [201] [200]. In order to interpret these discrepant results, the underlying mechanisms of type I IFNs affecting podocyte and PEC homeostasis was studied in-vitro. Based on the observation that human and mouse podocytes exposed to IFN-b and IFN-a strongly up-regulate ISGs, the effects of both IFNs

on podocyte permeability were studied. Hence, ISG levels were used as a biomarker for glomerular filtration barrier function.

In contrast to previous reports in literature, this work demonstrates that IFN-β, but not IFN-α affects the glomerular filtration barrier in-vitro. Within few min of IFN-β exposure cultured podocytes changed their shape, possibly by retracting cytoplasmic extensions. This altered ECIS bio impedance measurements, a functional parameter of podocyte monolayer permeability and cellular shape [211]. Satchell et al. had used the same bio impedance device and reported opposite results upon IFN-β stimulation [201] . Their studies were performed with immature and proliferating glomerular epithelial cells of human origin, which does not allow predictions on the filtration barrier created by terminally differentiated podocytes that we studied. In this thesis, decrease in podocyte permeability driven by IFN-β, was observed in podocytes from murine origin after few min. In contrast, the same effect on human podocytes was observed after 6 h. Murine and human podocytes show the same response but at different time points, probably due to intrinsic differences between the two species analyzed. Decreased cellular permeability was not detected in podocytes from human and murine origin exposed to IFN-α, indicating distinct effects of type I IFNs on glomerular podocytes.

What are the consequences of the dramatically decreased podocyte permeability, driven by IFN-β? The bio-impedance data gathered during this thesis has shown that treatment with IFN-β engenders podocyte detachment, leading to cellular death as assessed by annexin V/PI flow cytometry. Similarly, gene expression profiles confirm this new finding by showing a prominent up-regulation of apoptotic genes in podocytes upon IFN-β exposure. How does IFN-β kill podocytes in-vivo?

The in-vivo results support in-vitro findings, since IFN-β-treated SCID mice suffered from higher podocyte loss and proteinuria during adriamycin nephropathy compared to the IFN-α or vehicle treatment. Increased podocyte mitotic activity was detected in IFN-β-treated SCID mice. This corresponds to typical features of viral glomerulonephritis that displays multinucleated podocytes in association with podocyte loss and glomerulosclerosis [40, 230]. This is in line

with previous reports on how podocytes enter the cell cycle to undergo hypertrophy while the M phase of nuclear division is inhibited by cyclin kinase inhibitors at the restriction point during the G2/M phase [13, 221]. This is because podocytes are terminally differentiated cells with a complex and sophisticated cytoskeletal structure, which links them to neighboring cells via the slit membrane [13]. Therefore, stimuli that force podocytes to pass the M-phase of nuclear division trigger podocyte death within or shortly after mitosis [13, 231]. This variant of cell death was named "mitotic catastrophe" and can involve apoptosis, necrosis or both [220, 232].

IFN-β and IFN-α aggravates adriamycin nephropathy in SCID mice that lack adaptive immunity. This finding implies that the type I IFNs have complex immune-regulatory effects on innate and adaptive immunity and distinct direct effects on glomerular epithelial cells. Injections of either recombinant IFN-α/β both increased the intrarenal expression of ISGs including the chemokine CXCL10. CXCL10 attracts proinflammatory macrophages (and cytotoxic T cells) via the chemokine receptor CXCR3, explaining the increased numbers of intrarenal CD68+ macrophages of SCID mice with both IFNs [233]. This per se might be sufficient to explain the associated increase in proteinuria but IFN-β also affected the glomerular filtration barrier also via direct effects on podocytes [234]. It has been reported that IFN-β ameliorates glomerular injury and proteinuria in immunocompetent rodents [200, 201] but this effect was not observed in the present study. Balb/c mice injected with adriamycin and treated daily with IFN-α and IFN-β showed an aggravated phenotype with increased proteinuria. Balb/c mice injected with adriamycin and treated daily with IFN-α and IFN-β showed an aggravated phenotype with increased proteinuria. In contrast with what has been observed in the SCID mice study, in Balb/c the effect of IFN-α treatment on proteinuria was more prominent than observed with IFN-β. Yet, no protection due the IFN-β treatment was apparent in the present work. The mild effect on proteinuria in Balb/c mice injected with IFN-β might be due to immunosuppressive action of IFN-β in an immunocompetent system, together with the variability within the group of study.

IFN-α and IFN-β had similar effects on proteinuria, glomerular

inflammation, and scaring, which should relate to their consistent induction of ISGs and chemokines. IFN-α and IFN-β also shared the inhibitory effect on renal progenitor differentiation towards podocytes, which favors glomerular scaring instead of regeneration[38]. However, IFN-α did not cause immediate changes in cell shape that affect the resistance and capacitance of podocyte monolayers and did not affect podocyte viability within 24 h. IFN-α was shown to induce cell cycle arrest in PECs in-vitro and in-vivo and thus further impair podocyte repair. This anti-mitotic effect of IFN-α relates to the induction of p21, a cell cycle inhibitor that protects podocytes from cell cycle progression [235, 236].

How can IFN-α and IFN-β elicit unique biological effects when they both ligate the same IFN-receptor? The IFNAR consists of two transmembranous receptor chains with different binding affinities for the sixteen type I IFN variants including IFN-α and IFN-β setting off different signaling events which can explain their shared and their distinct biological activities [237].

What are the clinical implications of these findings? Type I IFNs are important mediators of viral infection thus their local effects on podocytes and PECs may contribute to podocyte loss, FSGS, and collapsing glomerulopathy, for example in viral nephropathies [238, 239]. HIV and parvovirus B19 replicates in podocytes and PECs, and viral nucleic acids induce IFN production and ISG expression in glomerular cells [175, 176]. Type I IFN also contributes to other forms of glomerulonephritis as evidenced by reduced disease activity in IFNAR-deficient mice [199, 205]. Type I IFNs are also essential mediators of systemic lupus and lupus nephritis including local effects on podocytes as shown by the IFN-α/β-specific reticular inclusions in podocytes [154, 240]. Finally, recombinant types I IFNs are frequently used for the treatment of a number of autoimmune diseases and chronic viral hepatitis [225, 241]. The aggravation of proteinuria has been reported as a side effect that may relate to the pathomechanisms described in this thesis [155, 242].
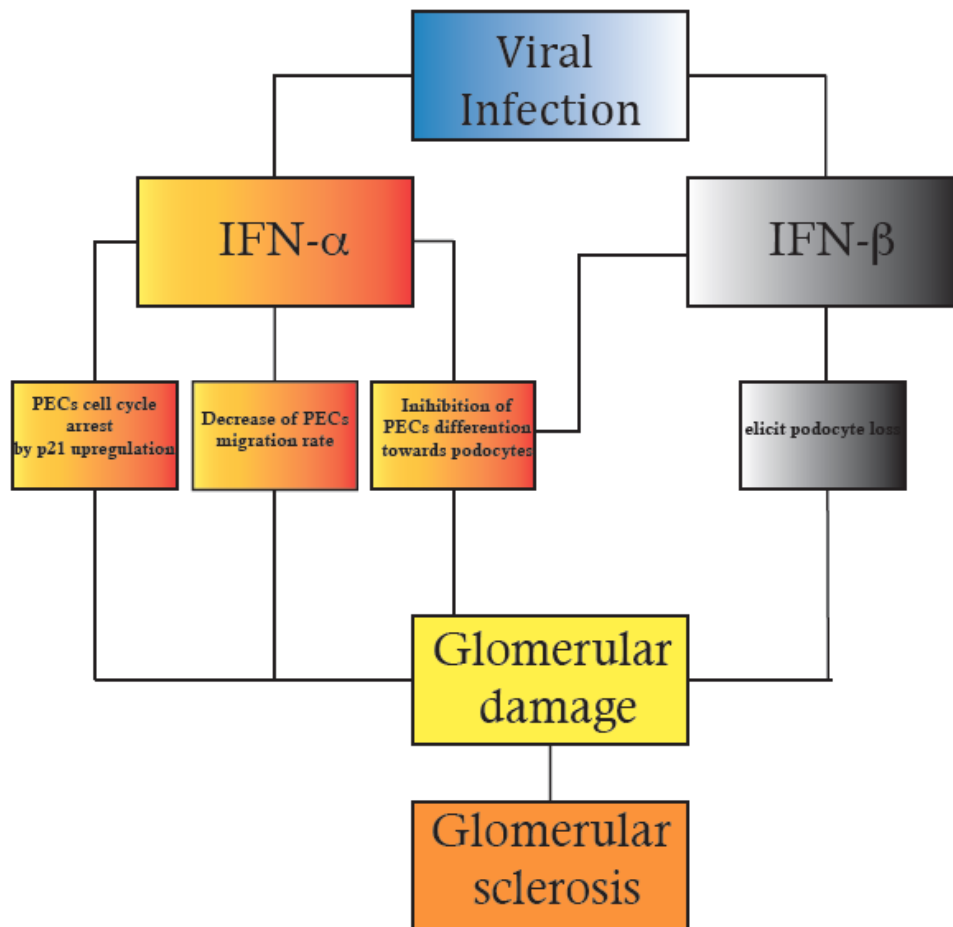
Figure 26. Schematics of the effects of IFN-α and IFN-β on glomerular epithelial cells..

In summary, IFN-α and IFN-β both enhance adriamycin nephropathy in SCID mice by intensifying intrarenal inflammation. IFN-β specifically promotes podocyte loss by enforcing mitotic catastrophe on podocytes, whereas IFN-α affects the proliferation and migration of PECs. Nevertheless, both IFNs impair the differentiation of renal progenitors into mature podocytes, which might favor focal scaring over glomerular repair. Altogether, these data provide a mechanistic model for how the antiviral responses triggered by IFN-α/β drive podocyte loss, proteinuria, and glomerulosclerosis (Figure 26).

6. Summary

Even though nucleic acid recognition and IFN-α and IFN-β play an important role during viral infections, little is known about their role in viral glomerulonephritis e.g. in HIV nephropathy. Viral infections activate systemic antiviral immune response, mainly via IFN-α and IFN-β production. These inflammatory cytokines have been shown to exert a pleiotropic immunomodulatory effect on renal mesangial cells, which directly contribute to glomerular disease. But, it is not known whether the viral nucleic acids and type I IFN have an effect on glomerular epithelial cells (i.e. podocytes and PECs). Therefore, to investigate the effect of nucleic acids on podocytes and PECs, we stimulated these cells with synthetic dsDNA (poly-dAdT) complexes with lipofectamine to mimic a viral infection. We found that dsDNA consistently induced numerous IFN-stimulated genes in podocytes and PECs. Furthermore, we found that dsDNA decreased PECs proliferation and inhibited CD24+/CD133+PECs differentiation towards mature podocytes. To confirm the hypothesis that this was due to the secretion of IFN-α and IFN-β triggered by nucleic acids, we investigated the effect of these antiviral cytokines on PECs and podocytes homeostasis. We found that both IFNs consistently induced podocytes and PECs to express numerous IFN-stimulated genes. However, only IFN-β significantly induced podocyte death and increased the permeability of podocyte monolayers. In contrast, only IFN-α caused cell cycle arrest by up-regulation of p21 CKD inhibitor and inhibited migration in PECs. Both IFNs suppressed CD24+/CD133+PECs differentiation into mature podocytes. In adriamycin-induced nephropathy in SCID mice, injections with either IFN-α or IFN-β aggravated proteinuria, macrophage influx, and glomerulosclerosis. However, only IFN–β induced mitotic podocyte death (mitotic catastrophe) leading to reduced podocyte number. We observed that IFN-α induces cell cycle arrest in PECs in-vivo, which contributes to glomerular damage. Balb/c mice injected with adriamycin and treated daily with IFN-α and IFN-β showed an aggravated phenotype with increased proteinuria. In contrast to what has been observed in the SCID mice study, in Balb/c the effect of IFN-α treatment on proteinuria was more prominent compared to IFN-β. Thus, the type

I IFNs have distinct effects on podocytes and parietal epithelial cells, and together they promote glomerulosclerosis by enhancing podocyte loss as well as suppressing their regeneration from local progenitors.

7. Zusammenfassung

Obwohl die immunstimulatorischen Effekte viraler Nukleinsäursen, wie auch IFN -α und IFN-β, während Virusinfektionen eine wichtige Rolle spielen, ist wenig über ihre Funktion bei viraler Glomerulonephritis, wie beispielsweise HIV Nephropathie, bekannt. Virusinfektionen aktivieren, vor allem mittels IFN-α und IFN-β Produktion eine systemische antivirale Immunantwort. Es wurde gezeigt, dass diese inflammatorischen Zytokine einen pleiotropen immunmodulatorischen Effekt auf renale Mesangialzellen ausüben, was direkt zu glomerulären Krankheiten führt. Aber es ist bisher nicht bekannt, ob die viralen Nukleinsäuren und Typ I IFN einen Effekt auf die glomerulären Epithelzellen haben. (z.B. Podozyten und PECs). Um den Effekt von Nukleinsäuren auf Podozyten und PECs zu erforschen, stimulierten wir diese Zellen mit synthetischen dsDNA-(poly-dAdT) Komplexen mit lipofectamine, um eine virale Infektion zu imitieren. Wir haben herausgefunden, dass dsDNA stetig viele IFN-stimulierte Gene in Podozyten und PECs induziert. Desweitern haben wir herausgefunden, dass dsDNA die PECs Proliferation mindert und die CD24+/CD133+PECs Differenzierung zu ausgereiften Podozyten inhibiert. Um unsere Hypothese, dass deis aufgrund von der Sekretion von IFN-α und IFN-β passiert ist, zu bestätigen, haben wir den Effekt von diesen anitviralen Zytokinen auf PECs- und Podozyten-Homöostase etabliert. Wir haben herausgefunden, dass beide IFNs stetig Podozyten und PECs dazu anregen, stetig mehrere IFN-stimulierte Gene zu exprimieren. Trotzdem hat nur IFN-β das Podozytensterben induziert und die Permeabilität der Podozyten-Monolayer erhöht.

In der Adriamycin-induzierter Nephropathie bei SCID Mäusen haben Injektionen mit IFN-α oder IFN-β die Proteinurie, den Makrophagen Influx und die Glomerulosklerose verstärkt. Trotzdem induziert nur IFN-β das mitotische Podozytensterben (katastrophale Mitose), welches zu einer reduzierten Podozytenanzahl führt. Wir haben führt, dass IFN-α einen Zellzyklusarrest in-vivo bei PECs induziert, der zur glomerulären Schädigung führt. Balb/c Mäuse, die Adriamycin gespritzt bekommen haben und täglich mit IFN-α und IFN-β behandelt wurden zeigten einen aggravierten Phänotyp mit vermehrter Proteinurie. Im Gegensatz zu dem, was an Studien in SCID Mausen gezeigt

wurde, war der Effekt auf die Proteinurie nach IFN-α Behandlung prominenter bei Balb/c Mäusen, verglichen mit IFN-β. Deshalb haben Typ I IFNs einen deutlichen Effekt auf Podozyten und Parietalzellen. Zusammen fördern die Typ I IFNs die Glomerulosklerose durch verstärkten Untergang der Podozyten sowie durch Unterdrückung ihrer Regeneration aus Vorläuferzellen.

8. Reference

1.   Heron, M., *Deaths: leading causes for 2007.* Natl Vital Stat Rep, 2011. **59**(8): p. 1-95.

2.   Ju, W., S. Smith, and M. Kretzler, *Genomic biomarkers for chronic kidney disease.* Transl Res, 2012. **159**(4): p. 290-302.

3.   Levey, A.S., et al., *Definition and classification of chronic kidney disease: a position statement from Kidney Disease: Improving Global Outcomes (KDIGO).* Kidney Int, 2005. **67**(6): p. 2089-100.

4.   Levey, A.S., et al., *Proteinuria as a surrogate outcome in CKD: report of a scientific workshop sponsored by the National Kidney Foundation and the US Food and Drug Administration.* Am J Kidney Dis, 2009. **54**(2): p. 205-26.

5.   Stevens, L.A. and A.S. Levey, *Measurement of kidney function.* Med Clin North Am, 2005. **89**(3): p. 457-73.

6.   *Chronic kidney disease: New KDIGO CKD Clinical Practice Guideline published.* Nat Rev Nephrol, 2013. **9**(3): p. 126.

7.   Abrahamson, D.R., *Structure and development of the glomerular capillary wall and basement membrane.* Am J Physiol, 1987. **253**(5 Pt 2): p. F783-94.

8.   Mundel, P. and W. Kriz, *Structure and function of podocytes: an update.* Anat Embryol (Berl), 1995. **192**(5): p. 385-97.

9.   LeHir, M. and W. Kriz, *New insights into structural patterns encountered in glomerulosclerosis.* Curr Opin Nephrol Hypertens, 2007. **16**(3): p. 184-91.

10.   Steffes, M.W., et al., *Glomerular cell number in normal subjects and in type 1 diabetic patients.* Kidney Int, 2001. **59**(6): p. 2104-13.

11.   Steffes, M.W., *Affecting the decline of renal function in diabetes mellitus.* Kidney Int, 2001. **60**(1): p. 378-9.

12.   Kriz, W., et al., *A frequent pathway to glomerulosclerosis: deterioration of tuft architecture-podocyte damage-segmental sclerosis.* Kidney Blood Press Res, 1996. **19**(5): p. 245-53.

13.   Shankland, S.J., *The podocyte's response to injury: role in proteinuria and glomerulosclerosis.* Kidney Int, 2006. **69**(12): p. 2131-47.

14.   Nagata, M., et al., *Cell cycle regulation and differentiation in the human podocyte lineage.* Am J Pathol, 1998. **153**(5): p. 1511-20.

15.   Little, M.H., *Regrow or repair: potential regenerative therapies for the kidney.* J Am Soc Nephrol, 2006. **17**(9): p. 2390-401.

16.   Romagnani, P. and R. Kalluri, *Possible mechanisms of kidney repair.* Fibrogenesis Tissue Repair, 2009. **2**(1): p. 3.

17.   Zoja, C., et al., *Mesenchymal stem cell therapy promotes renal repair by limiting glomerular podocyte and progenitor cell dysfunction in adriamycin-induced nephropathy.* Am J Physiol Renal Physiol, 2012. **303**(9): p. F1370-81.

18.   Kriz, W., *Podocyte is the major culprit accounting for the progression of chronic renal disease.* Microsc Res Tech, 2002. **57**(4): p. 189-95.

19.   Wiggins, R.C., *The spectrum of podocytopathies: a unifying view of glomerular diseases.* Kidney Int, 2007. **71**(12): p. 1205-14.

20.   Kriz, W., *Progressive renal failure--inability of podocytes to replicate and the consequences for development of glomerulosclerosis.* Nephrol Dial Transplant, 1996. **11**(9): p. 1738-42.

21.   Kriz, W., N. Gretz, and K.V. Lemley, *Progression of glomerular diseases: is the podocyte the culprit?* Kidney Int, 1998. **54**(3): p. 687-97.

22.   Kriz, W. and K.V. Lemley, *The role of the podocyte in glomerulosclerosis.* Curr Opin Nephrol Hypertens, 1999. **8**(4): p. 489-97.

23.   Ophascharoensuk, V., et al., *Role of intrinsic renal cells versus infiltrating cells in glomerular crescent formation.* Kidney Int, 1998. **54**(2): p. 416-25.

24.   Ryu, M., et al., *Plasma leakage through glomerular basement membrane ruptures triggers the proliferation of parietal epithelial cells and crescent formation in non-inflammatory glomerular injury.* J Pathol, 2012.

25.   Smeets, B., et al., *Tracing the origin of glomerular extracapillary lesions from parietal epithelial cells.* J Am Soc Nephrol, 2009. **20**(12): p. 2604-15.

26.   Alpers, C.E., et al., *Human renal cortical interstitial cells with some features of smooth muscle cells participate in tubulointerstitial and crescentic glomerular injury.* J Am Soc Nephrol, 1994. **5**(2): p. 201-9.

27.   Smeets, B., et al., *Lessons from studies on focal segmental glomerulosclerosis: an important role for parietal epithelial cells?* J Pathol, 2006. **210**(3): p. 263-72.

28.   Cockwell, P., et al., *Interleukin-8: A pathogenetic role in antineutrophil cytoplasmic autoantibody-associated glomerulonephritis.* Kidney Int, 1999. **55**(3): p. 852-63.

29.   Cockwell, P., et al., *In situ analysis of C-C chemokine mRNA in human glomerulonephritis.* Kidney Int, 1998. **54**(3): p. 827-36.

30.   Kanemoto, K., et al., *Connective tissue growth factor participates in scar formation of crescentic glomerulonephritis.* Lab Invest, 2003. **83**(11): p. 1615-25.

31.   Barnes, J.L., et al., *Expression of alternatively spliced fibronectin variants during remodeling in proliferative glomerulonephritis.* Am J Pathol, 1995. **147**(5): p. 1361-71.

32.   Eitner, F., et al., *PDGF-C expression in the developing and normal adult human kidney and in glomerular diseases.* J Am Soc Nephrol, 2003. **14**(5): p. 1145-53.

33.   Smeets, B., et al., *Renal progenitor cells contribute to hyperplastic lesions of podocytopathies and crescentic glomerulonephritis.* J Am Soc Nephrol, 2009. **20**(12): p. 2593-603.

34.   Asano, T., et al., *Permanent genetic tagging of podocytes: fate of injured podocytes in a mouse model of glomerular sclerosis.* J Am Soc Nephrol, 2005. **16**(8): p. 2257-62.

35.   Matsusaka, T., et al., *Genetic engineering of glomerular sclerosis in the mouse via control of onset and severity of podocyte-specific injury.* J Am Soc Nephrol, 2005. **16**(4): p. 1013-23.

36.   Wharram, B.L., et al., *Podocyte depletion causes glomerulosclerosis: diphtheria toxin-induced podocyte depletion in rats expressing human diphtheria toxin receptor transgene.* J Am Soc Nephrol, 2005. **16**(10): p. 2941-52.

37.   Romagnani, P., L. Lasagni, and G. Remuzzi, *Renal progenitors: an evolutionary conserved strategy for kidney regeneration.* Nat Rev Nephrol, 2013. **9**(3): p. 137-46.

38.   Lasagni, L. and P. Romagnani, *Glomerular epithelial stem cells: the good, the bad, and the ugly.* J Am Soc Nephrol, 2010. **21**(10): p. 1612-9.

39.   Sharif, K., et al., *Podocyte phenotypes as defined by expression and distribution of GLEPP1 in the developing glomerulus and in nephrotic glomeruli from MCD, CNF, and FSGS. A dedifferentiation hypothesis for the nephrotic syndrome.* Exp Nephrol, 1998. **6**(3): p. 234-44.

40.   Barisoni, L., et al., *The dysregulated podocyte phenotype: a novel concept in the pathogenesis of collapsing idiopathic focal segmental glomerulosclerosis and HIV-associated nephropathy.* J Am Soc Nephrol, 1999. **10**(1): p. 51-61.

41.   D'Agati, V.D., F.J. Kaskel, and R.J. Falk, *Focal segmental glomerulosclerosis.* N Engl J Med, 2011. **365**(25): p. 2398-411.

42.   Wei, C., et al., *Circulating urokinase receptor as a cause of focal segmental glomerulosclerosis.* Nat Med, 2011. **17**(8): p. 952-60.

43.   Hinkes, B.G., et al., *Nephrotic syndrome in the first year of life: two thirds of cases are caused by mutations in 4 genes (NPHS1, NPHS2, WT1, and LAMB2).* Pediatrics, 2007. **119**(4): p. e907-19.

44.   Santin, S., et al., *Nephrin mutations cause childhood- and adult-onset focal segmental glomerulosclerosis.* Kidney Int, 2009. **76**(12): p. 1268-76.

45.   Kim, J.M., et al., *CD2-associated protein haploinsufficiency is linked to glomerular disease susceptibility.* Science, 2003. **300**(5623): p. 1298-300.

46.   Boute, N., et al., *NPHS2, encoding the glomerular protein podocin, is mutated in autosomal recessive steroid-resistant nephrotic syndrome.* Nat Genet, 2000. **24**(4): p. 349-54.

47.   Kambham, N., et al., *Congenital focal segmental glomerulosclerosis associated with beta4 integrin mutation and epidermolysis bullosa.* Am J Kidney Dis, 2000. **36**(1): p. 190-6.

48.   Winn, M.P., et al., *A mutation in the TRPC6 cation channel causes familial focal segmental glomerulosclerosis.* Science, 2005. **308**(5729): p. 1801-4.

49.   Zenker, M., et al., *Human laminin beta2 deficiency causes congenital nephrosis with mesangial sclerosis and distinct eye abnormalities.* Hum Mol Genet, 2004. **13**(21): p. 2625-32.

50.	Hinkes, B., et al., *Positional cloning uncovers mutations in PLCE1 responsible for a nephrotic syndrome variant that may be reversible.* Nat Genet, 2006. **38**(12): p. 1397-405.

51.	Boyer, O., et al., *Mutations in INF2 are a major cause of autosomal dominant focal segmental glomerulosclerosis.* J Am Soc Nephrol, 2011. **22**(2): p. 239-45.

52.	Ghiggeri, G.M., et al., *Genetics, clinical and pathological features of glomerulonephritis associated with mutations of nonmuscle myosin IIA (Fechtner syndrome).* Am J Kidney Dis, 2003. **41**(1): p. 95-104.

53.	Choi, H.J., et al., *Familial focal segmental glomerulosclerosis associated with an ACTN4 mutation and paternal germline mosaicism.* Am J Kidney Dis, 2008. **51**(5): p. 834-8.

54.	Ingelfinger, J.R., *MYO1E, focal segmental glomerulosclerosis, and the cytoskeleton.* N Engl J Med, 2011. **365**(4): p. 368-9.

55.	Iijima, K., et al., *Focal segmental glomerulosclerosis in patients with complete deletion of one WT1 allele.* Pediatrics, 2012. **129**(6): p. e1621-5.

56.	Benetti, E., et al., *A novel WT1 gene mutation in a three-generation family with progressive isolated focal segmental glomerulosclerosis.* Clin J Am Soc Nephrol, 2010. **5**(4): p. 698-702.

57.	Heeringa, S.F., et al., *COQ6 mutations in human patients produce nephrotic syndrome with sensorineural deafness.* J Clin Invest, 2011. **121**(5): p. 2013-24.

58.	Moudgil, A., et al., *Association of parvovirus B19 infection with idiopathic collapsing glomerulopathy.* Kidney Int, 2001. **59**(6): p. 2126-33.

59.	Detwiler, R.K., et al., *Cytomegalovirus-induced necrotizing and crescentic glomerulonephritis in a renal transplant patient.* Am J Kidney Dis, 1998. **32**(5): p. 820-4.

60.	Tomlinson, L., et al., *Acute cytomegalovirus infection complicated by collapsing glomerulopathy.* Nephrol Dial Transplant, 2003. **18**(1): p. 187-9.

61.	Wyatt, C.M., K. Meliambro, and P.E. Klotman, *Recent progress in HIV-associated nephropathy.* Annu Rev Med, 2012. **63**: p. 147-59.

62.	Markowitz, G.S., et al., *Collapsing focal segmental glomerulosclerosis following treatment with high-dose pamidronate.* J Am Soc Nephrol, 2001. **12**(6): p. 1164-72.

63.	Markowitz, G.S., et al., *Treatment with IFN-{alpha}, -{beta}, or -{gamma} is associated with collapsing focal segmental glomerulosclerosis.* Clin J Am Soc Nephrol, 2010. **5**(4): p. 607-15.

64.	Jaffe, J.A. and P.L. Kimmel, *Chronic nephropathies of cocaine and heroin abuse: a critical review.* Clin J Am Soc Nephrol, 2006. **1**(4): p. 655-67.

65.	Wang, Y., et al., *Progressive adriamycin nephropathy in mice: sequence of histologic and immunohistochemical events.* Kidney Int, 2000. **58**(4): p. 1797-804.

66.	Gewirtz, D.A., *A critical evaluation of the mechanisms of action proposed for the antitumor effects of the anthracycline antibiotics adriamycin and daunorubicin.* Biochem Pharmacol, 1999. **57**(7): p. 727-41.

67. Lee, V.W. and D.C. Harris, *Adriamycin nephropathy: a model of focal segmental glomerulosclerosis.* Nephrology (Carlton), 2011. **16**(1): p. 30-8.

68. Zheng, Z., et al., *A Mendelian locus on chromosome 16 determines susceptibility to doxorubicin nephropathy in the mouse.* Proc Natl Acad Sci U S A, 2005. **102**(7): p. 2502-7.

69. Barbey, M.M., et al., *Adriamycin affects glomerular renal function: evidence for the involvement of oxygen radicals.* Free Radic Res Commun, 1989. **7**(3-6): p. 195-203.

70. Otaki, Y., et al., *Dissociation of NEPH1 from nephrin is involved in development of a rat model of focal segmental glomerulosclerosis.* Am J Physiol Renal Physiol, 2008. **295**(5): p. F1376-87.

71. Lee, V.W., et al., *Adriamycin nephropathy in severe combined immunodeficient (SCID) mice.* Nephrol Dial Transplant, 2006. **21**(11): p. 3293-8.

72. Jefferson, J.A., C.E. Alpers, and S.J. Shankland, *Podocyte biology for the bedside.* Am J Kidney Dis, 2011. **58**(5): p. 835-45.

73. Greka, A. and P. Mundel, *Cell biology and pathology of podocytes.* Annu Rev Physiol, 2012. **74**: p. 299-323.

74. Saxen, L. and H. Sariola, *Early organogenesis of the kidney.* Pediatr Nephrol, 1987. **1**(3): p. 385-92.

75. Schnabel, E., et al., *Biogenesis of podocalyxin--the major glomerular sialoglycoprotein--in the newborn rat kidney.* Eur J Cell Biol, 1989. **48**(2): p. 313-26.

76. Schnabel, E., J.M. Anderson, and M.G. Farquhar, *The tight junction protein ZO-1 is concentrated along slit diaphragms of the glomerular epithelium.* J Cell Biol, 1990. **111**(3): p. 1255-63.

77. Mundlos, S., et al., *Nuclear localization of the protein encoded by the Wilms' tumor gene WT1 in embryonic and adult tissues.* Development, 1993. **119**(4): p. 1329-41.

78. Cui, S., L. Schwartz, and S.E. Quaggin, *Pod1 is required in stromal cells for glomerulogenesis.* Dev Dyn, 2003. **226**(3): p. 512-22.

79. Reeves, W., J.P. Caulfield, and M.G. Farquhar, *Differentiation of epithelial foot processes and filtration slits: sequential appearance of occluding junctions, epithelial polyanion, and slit membranes in developing glomeruli.* Lab Invest, 1978. **39**(2): p. 90-100.

80. Mundel, P., P. Gilbert, and W. Kriz, *Podocytes in glomerulus of rat kidney express a characteristic 44 KD protein.* J Histochem Cytochem, 1991. **39**(8): p. 1047-56.

81. Holthofer, H., et al., *Expression of vimentin and cytokeratin types of intermediate filament proteins in developing and adult human kidneys.* Lab Invest, 1984. **50**(5): p. 552-9.

82. Reiser, J. and S. Sever, *Podocyte biology and pathogenesis of kidney disease.* Annu Rev Med, 2013. **64**: p. 357-66.

83. Schmieder, S., et al., *Podocalyxin activates RhoA and induces actin reorganization through NHERF1 and Ezrin in MDCK cells.* J Am Soc Nephrol, 2004. **15**(9): p. 2289-98.

84. Romagnani, P., *Toward the identification of a "renopoietic system"?* Stem Cells, 2009. **27**(9): p. 2247-53.

85. Miner, J.H., *The glomerular basement membrane.* Exp Cell Res, 2012. **318**(9): p. 973-8.

86. Menon, M.C., P.Y. Chuang, and C.J. He, *The glomerular filtration barrier: components and crosstalk.* Int J Nephrol, 2012. **2012**: p. 749010.

87. Pavenstadt, H., W. Kriz, and M. Kretzler, *Cell biology of the glomerular podocyte.* Physiol Rev, 2003. **83**(1): p. 253-307.

88. Jefferson, J.A., et al., *Podocyte disorders: Core Curriculum 2011.* Am J Kidney Dis, 2011. **58**(4): p. 666-77.

89. Patrie, K.M., et al., *Interaction of two actin-binding proteins, synaptopodin and alpha-actinin-4, with the tight junction protein MAGI-1.* J Biol Chem, 2002. **277**(33): p. 30183-90.

90. Leeuwis, J.W., et al., *Targeting podocyte-associated diseases.* Adv Drug Deliv Rev, 2010. **62**(14): p. 1325-36.

91. Combs, H.L., et al., *Expression of the cyclin kinase inhibitor, p27kip1, in developing and mature human kidney.* Kidney Int, 1998. **53**(4): p. 892-6.

92. Marshall, C.B. and S.J. Shankland, *Cell cycle and glomerular disease: a minireview.* Nephron Exp Nephrol, 2006. **102**(2): p. e39-48.

93. Shankland, S.J., et al., *Differential expression of cyclin-dependent kinase inhibitors in human glomerular disease: role in podocyte proliferation and maturation.* Kidney Int, 2000. **58**(2): p. 674-83.

94. Marshall, C.B. and S.J. Shankland, *Cell cycle regulatory proteins in podocyte health and disease.* Nephron Exp Nephrol, 2007. **106**(2): p. e51-9.

95. Lasagni, L., et al., *Podocyte mitosis - a catastrophe.* Curr Mol Med, 2012.

96. Tharaux, P.L. and T.B. Huber, *How many ways can a podocyte die?* Semin Nephrol, 2012. **32**(4): p. 394-404.

97. Susztak, K., et al., *Glucose-induced reactive oxygen species cause apoptosis of podocytes and podocyte depletion at the onset of diabetic nephropathy.* Diabetes, 2006. **55**(1): p. 225-33.

98. Susztak, K. and E.P. Bottinger, *Diabetic nephropathy: a frontier for personalized medicine.* J Am Soc Nephrol, 2006. **17**(2): p. 361-7.

99. Schiffer, M., et al., *Apoptosis in podocytes induced by TGF-beta and Smad7.* J Clin Invest, 2001. **108**(6): p. 807-16.

100. Ryu, M., et al., *Tumour necrosis factor-alpha drives Alport glomerulosclerosis in mice by promoting podocyte apoptosis.* J Pathol, 2012. **226**(1): p. 120-31.

101. Srivastava, T., et al., *Cell-cycle regulatory proteins in podocyte cell in idiopathic nephrotic syndrome of childhood.* Kidney Int, 2003. **63**(4): p. 1374-81.

102.   Hoshi, S., et al., *Podocyte injury promotes progressive nephropathy in zucker diabetic fatty rats.* Lab Invest, 2002. **82**(1): p. 25-35.

103.   Nitta, K., et al., *Glomerular expression of cell-cycle-regulatory proteins in human crescentic glomerulonephritis.* Virchows Arch, 1999. **435**(4): p. 422-7.

104.   Lasagni, L., et al., *Podocyte mitosis - a catastrophe.* Curr Mol Med, 2013. **13**(1): p. 13-23.

105.   Lasagni, L., et al., *Notch activation differentially regulates renal progenitors proliferation and differentiation toward the podocyte lineage in glomerular disorders.* Stem Cells, 2010. **28**(9): p. 1674-85.

106.   Neef, R., et al., *Cooperation between mitotic kinesins controls the late stages of cytokinesis.* Curr Biol, 2006. **16**(3): p. 301-7.

107.   Shkreli, M., et al., *Reversible cell-cycle entry in adult kidney podocytes through regulated control of telomerase and Wnt signaling.* Nat Med, 2012. **18**(1): p. 111-9.

108.   Horster, M.F., G.S. Braun, and S.M. Huber, *Embryonic renal epithelia: induction, nephrogenesis, and cell differentiation.* Physiol Rev, 1999. **79**(4): p. 1157-91.

109.   Dressler, G.R., *The cellular basis of kidney development.* Annu Rev Cell Dev Biol, 2006. **22**: p. 509-29.

110.   Romagnani, P., *Parietal epithelial cells: their role in health and disease.* Contrib Nephrol, 2011. **169**: p. 23-36.

111.   Kreidberg, J.A., *Podocyte differentiation and glomerulogenesis.* J Am Soc Nephrol, 2003. **14**(3): p. 806-14.

112.   Ryan, G., et al., *Repression of Pax-2 by WT1 during normal kidney development.* Development, 1995. **121**(3): p. 867-75.

113.   Ohse, T., et al., *A new function for parietal epithelial cells: a second glomerular barrier.* Am J Physiol Renal Physiol, 2009. **297**(6): p. F1566-74.

114.   Ohse, T., et al., *The enigmatic parietal epithelial cell is finally getting noticed: a review.* Kidney Int, 2009. **76**(12): p. 1225-38.

115.   Webber, W.A. and J. Blackbourn, *The permeability of the parietal layer of Bowman's capsule.* Lab Invest, 1971. **25**(5): p. 367-73.

116.   Arakawa, M. and J. Tokunaga, *A scanning electron microscope study of the human Bowman's epithelium.* Contrib Nephrol, 1977. **6**: p. 73-8.

117.   Ronconi, E., et al., *Regeneration of glomerular podocytes by human renal progenitors.* J Am Soc Nephrol, 2009. **20**(2): p. 322-32.

118.   Macconi, D., et al., *Podocyte repopulation contributes to regression of glomerular injury induced by ACE inhibition.* Am J Pathol, 2009. **174**(3): p. 797-807.

119.   Remuzzi, G., A. Benigni, and A. Remuzzi, *Mechanisms of progression and regression of renal lesions of chronic nephropathies and diabetes.* J Clin Invest, 2006. **116**(2): p. 288-96.

120.   Appel, D., et al., *Recruitment of podocytes from glomerular parietal epithelial cells.* J Am Soc Nephrol, 2009. **20**(2): p. 333-43.

121.   Duffield, J.S. and B.D. Humphreys, *Origin of new cells in the adult kidney: results from genetic labeling techniques.* Kidney Int, 2011. **79**(5): p. 494-501.

122.   Humphreys, B.D., et al., *Repair of injured proximal tubule does not involve specialized progenitors.* Proc Natl Acad Sci U S A, 2011. **108**(22): p. 9226-31.

123.   Sagrinati, C., et al., *Stem-cell approaches for kidney repair: choosing the right cells.* Trends Mol Med, 2008. **14**(7): p. 277-85.

124.   Lazzeri, E., et al., *Regenerative potential of embryonic renal multipotent progenitors in acute renal failure.* J Am Soc Nephrol, 2007. **18**(12): p. 3128-38.

125.   Angelotti, M.L., et al., *Characterization of renal progenitors committed toward tubular lineage and their regenerative potential in renal tubular injury.* Stem Cells, 2012. **30**(8): p. 1714-25.

126.   Fogo, A.B., *Mechanisms of progression of chronic kidney disease.* Pediatr Nephrol, 2007. **22**(12): p. 2011-22.

127.   Chambers, S.M., et al., *Aging hematopoietic stem cells decline in function and exhibit epigenetic dysregulation.* PLoS Biol, 2007. **5**(8): p. e201.

128.   Conboy, I.M., et al., *Rejuvenation of aged progenitor cells by exposure to a young systemic environment.* Nature, 2005. **433**(7027): p. 760-4.

129.   Lai, A.S. and K.N. Lai, *Viral nephropathy.* Nat Clin Pract Nephrol, 2006. **2**(5): p. 254-62.

130.   Cheema, S.R., et al., *IgA-dominant glomerulonephritis associated with hepatitis A.* Clin Nephrol, 2004. **62**(2): p. 138-43.

131.   Tsai, J.D., et al., *Epstein-Barr virus-associated acute renal failure: diagnosis, treatment, and follow-up.* Pediatr Nephrol, 2003. **18**(7): p. 667-74.

132.   Nakazawa, T., et al., *Acute glomerulonephritis after human parvovirus B19 infection.* Am J Kidney Dis, 2000. **35**(6): p. E31.

133.   Couser, W.G., *Mechanisms of glomerular injury in immune-complex disease.* Kidney Int, 1985. **28**(3): p. 569-83.

134.   Golbus, S.M. and C.B. Wilson, *Experimental glomerulonephritis induced by in situ formation of immune complexes in glomerular capillary wall.* Kidney Int, 1979. **16**(2): p. 148-57.

135.   Conaldi, P.G., et al., *HIV-1 kills renal tubular epithelial cells in vitro by triggering an apoptotic pathway involving caspase activation and Fas upregulation.* J Clin Invest, 1998. **102**(12): p. 2041-9.

136.   Meyers, C.M., et al., *Hepatitis C and renal disease: an update.* Am J Kidney Dis, 2003. **42**(4): p. 631-57.

137.   Perico, N., et al., *Hepatitis C infection and chronic renal diseases.* Clin J Am Soc Nephrol, 2009. **4**(1): p. 207-20.

138. Lin, C.Y., *Clinical features and natural course of HBV-related glomerulopathy in children.* Kidney Int Suppl, 1991. **35**: p. S46-53.

139. Lai, F.M., et al., *Primary glomerulonephritis with detectable glomerular hepatitis B virus antigens.* Am J Surg Pathol, 1994. **18**(2): p. 175-86.

140. Kimmel, P.L., et al., *HIV-associated immune-mediated renal disease.* Kidney Int, 1993. **44**(6): p. 1327-40.

141. Marras, D., et al., *Replication and compartmentalization of HIV-1 in kidney epithelium of patients with HIV-associated nephropathy.* Nat Med, 2002. **8**(5): p. 522-6.

142. Eitner, F., et al., *Chemokine receptor CCR5 and CXCR4 expression in HIV-associated kidney disease.* J Am Soc Nephrol, 2000. **11**(5): p. 856-67.

143. Winston, J.A. and P.E. Klotman, *Are we missing an epidemic of HIV-associated nephropathy?* J Am Soc Nephrol, 1996. **7**(1): p. 1-7.

144. Khan, S., L. Haragsim, and Z.G. Laszik, *HIV-associated nephropathy.* Adv Chronic Kidney Dis, 2006. **13**(3): p. 307-13.

145. Kopp, J.B., et al., *MYH9 is a major-effect risk gene for focal segmental glomerulosclerosis.* Nat Genet, 2008. **40**(10): p. 1175-84.

146. Freedman, B.I., et al., *The apolipoprotein L1 (APOL1) gene and nondiabetic nephropathy in African Americans.* J Am Soc Nephrol, 2010. **21**(9): p. 1422-6.

147. Genovese, G., et al., *Association of trypanolytic ApoL1 variants with kidney disease in African Americans.* Science, 2010. **329**(5993): p. 841-5.

148. Rosenstiel, P., et al., *Transgenic and infectious animal models of HIV-associated nephropathy.* J Am Soc Nephrol, 2009. **20**(11): p. 2296-304.

149. Husain, M., et al., *HIV-1 Nef induces proliferation and anchorage-independent growth in podocytes.* J Am Soc Nephrol, 2002. **13**(7): p. 1806-15.

150. Zhong, J., et al., *Expression of HIV-1 genes in podocytes alone can lead to the full spectrum of HIV-1-associated nephropathy.* Kidney Int, 2005. **68**(3): p. 1048-60.

151. Mikulak, J. and P.C. Singhal, *HIV-1 and kidney cells: better understanding of viral interaction.* Nephron Exp Nephrol, 2010. **115**(2): p. e15-21.

152. Mikulak, J., et al., *DC-specific ICAM-3-grabbing nonintegrin mediates internalization of HIV-1 into human podocytes.* Am J Physiol Renal Physiol, 2010. **299**(3): p. F664-73.

153. Swiecki, M. and M. Colonna, *Type I interferons: diversity of sources, production pathways and effects on immune responses.* Curr Opin Virol, 2011. **1**(6): p. 463-75.

154. Migliorini, A. and H.J. Anders, *A novel pathogenetic concept-antiviral immunity in lupus nephritis.* Nat Rev Nephrol, 2012. **8**(3): p. 183-9.

155. Nakao, K., et al., *Minimal change nephrotic syndrome developing during postoperative interferon-beta therapy for malignant melanoma.* Nephron, 2002. **90**(4): p. 498-500.

156. Dizer, U., et al., *Minimal change disease in a patient receiving IFN-alpha therapy for chronic hepatitis C virus infection.* J Interferon Cytokine Res, 2003. **23**(1): p. 51-4.

157.   Kumasaka, R., et al., *Nephrotic syndrome associated with interferon-beta-1b therapy for multiple sclerosis.* Clin Exp Nephrol, 2006. **10**(3): p. 222-5.

158.   Shah, M., et al., *Interferon-alpha-associated focal segmental glomerulosclerosis with massive proteinuria in patients with chronic myeloid leukemia following high dose chemotherapy.* Cancer, 1998. **83**(9): p. 1938-46.

159.   Dressler, D., et al., *Another case of focal segmental glomerulosclerosis in an acutely uraemic patient following interferon therapy.* Nephrol Dial Transplant, 1999. **14**(8): p. 2049-50.

160.   Willson, R.A., *Nephrotoxicity of interferon alfa-ribavirin therapy for chronic hepatitis C.* J Clin Gastroenterol, 2002. **35**(1): p. 89-92.

161.   Stetson, D.B. and R. Medzhitov, *Type I interferons in host defense.* Immunity, 2006. **25**(3): p. 373-81.

162.   Liu, H., et al., *Anti-macrophage-derived chemokine antibody relieves murine lupus nephritis.* Rheumatol Int, 2011. **31**(11): p. 1459-64.

163.   Sato, S., et al., *Toll/IL-1 receptor domain-containing adaptor inducing IFN-beta (TRIF) associates with TNF receptor-associated factor 6 and TANK-binding kinase 1, and activates two distinct transcription factors, NF-kappa B and IFN-regulatory factor-3, in the Toll-like receptor signaling.* J Immunol, 2003. **171**(8): p. 4304-10.

164.   Goncalves, G.M., et al., *New roles for innate immune response in acute and chronic kidney injuries.* Scand J Immunol, 2011. **73**(5): p. 428-35.

165.   Medzhitov, R. and C.A. Janeway, Jr., *Decoding the patterns of self and nonself by the innate immune system.* Science, 2002. **296**(5566): p. 298-300.

166.   Medzhitov, R. and C. Janeway, Jr., *The Toll receptor family and microbial recognition.* Trends Microbiol, 2000. **8**(10): p. 452-6.

167.   Tsan, M.F. and B. Gao, *Endogenous ligands of Toll-like receptors.* J Leukoc Biol, 2004. **76**(3): p. 514-9.

168.   Kawai, T. and S. Akira, *TLR signaling.* Cell Death Differ, 2006. **13**(5): p. 816-25.

169.   Hoffmann, J.A., *The immune response of Drosophila.* Nature, 2003. **426**(6962): p. 33-8.

170.   Medzhitov, R., *Recognition of microorganisms and activation of the immune response.* Nature, 2007. **449**(7164): p. 819-26.

171.   Medzhitov, R., *Toll-like receptors and innate immunity.* Nat Rev Immunol, 2001. **1**(2): p. 135-45.

172.   Kumar, H., T. Kawai, and S. Akira, *Toll-like receptors and innate immunity.* Biochem Biophys Res Commun, 2009. **388**(4): p. 621-5.

173.   Palm, N.W. and R. Medzhitov, *Pattern recognition receptors and control of adaptive immunity.* Immunol Rev, 2009. **227**(1): p. 221-33.

174.   Takeda, K. and S. Akira, *TLR signaling pathways.* Semin Immunol, 2004. **16**(1): p. 3-9.

175.   Yamashita, M., et al., *Antiviral Innate Immunity Disturbs Podocyte Cell Function.* J Innate Immun, 2012.

176. Allam, R., et al., *Viral RNA and DNA trigger common antiviral responses in mesangial cells.* J Am Soc Nephrol, 2009. **20**(9): p. 1986-96.

177. Tsuboi, N., et al., *Roles of toll-like receptors in C-C chemokine production by renal tubular epithelial cells.* J Immunol, 2002. **169**(4): p. 2026-33.

178. Brown, H.J., S.H. Sacks, and M.G. Robson, *Toll-like receptor 2 agonists exacerbate accelerated nephrotoxic nephritis.* J Am Soc Nephrol, 2006. **17**(7): p. 1931-9.

179. Patole, P.S., et al., *Expression and regulation of Toll-like receptors in lupus-like immune complex glomerulonephritis of MRL-Fas(lpr) mice.* Nephrol Dial Transplant, 2006. **21**(11): p. 3062-73.

180. Flur, K., et al., *Viral RNA induces type I interferon-dependent cytokine release and cell death in mesangial cells via melanoma-differentiation-associated gene-5: Implications for viral infection-associated glomerulonephritis.* Am J Pathol, 2009. **175**(5): p. 2014-22.

181. Anders, H.J., J. Lichtnekert, and R. Allam, *Interferon-alpha and -beta in kidney inflammation.* Kidney Int, 2010. **77**(10): p. 848-54.

182. Imaizumi, T., et al., *Retinoic acid-inducible gene-I (RIG-I) is induced by IFN-{gamma} in human mesangial cells in culture: possible involvement of RIG-I in the inflammation in lupus nephritis.* Lupus, 2010. **19**(7): p. 830-6.

183. Suzuki, K., et al., *Expression of retinoic acid-inducible gene-I in lupus nephritis.* Nephrol Dial Transplant, 2007. **22**(8): p. 2407-9.

184. Girardin, S.E., et al., *Nod2 is a general sensor of peptidoglycan through muramyl dipeptide (MDP) detection.* J Biol Chem, 2003. **278**(11): p. 8869-72.

185. Inohara, N., et al., *An induced proximity model for NF-kappa B activation in the Nod1/RICK and RIP signaling pathways.* J Biol Chem, 2000. **275**(36): p. 27823-31.

186. Shigeoka, A.A., et al., *Nod1 and nod2 are expressed in human and murine renal tubular epithelial cells and participate in renal ischemia reperfusion injury.* J Immunol, 2010. **184**(5): p. 2297-304.

187. Anders, H.J. and D.A. Muruve, *The inflammasomes in kidney disease.* J Am Soc Nephrol, 2011. **22**(6): p. 1007-18.

188. Jaks, E., et al., *Differential receptor subunit affinities of type I interferons govern differential signal activation.* J Mol Biol, 2007. **366**(2): p. 525-39.

189. Pulverer, J.E., et al., *Temporal and spatial resolution of type I and III interferon responses in vivo.* J Virol, 2010. **84**(17): p. 8626-38.

190. Stark, G.R., *How cells respond to interferons revisited: from early history to current complexity.* Cytokine Growth Factor Rev, 2007. **18**(5-6): p. 419-23.

191. Stark, G.R., et al., *How cells respond to interferons.* Annu Rev Biochem, 1998. **67**: p. 227-64.

192. van Boxel-Dezaire, A.H., M.R. Rani, and G.R. Stark, *Complex modulation of cell type-specific signaling in response to type I interferons.* Immunity, 2006. **25**(3): p. 361-72.

193. Le Bon, A., et al., *Cross-priming of CD8+ T cells stimulated by virus-induced type I interferon.* Nat Immunol, 2003. **4**(10): p. 1009-15.

194. Lee, C.K., et al., *Distinct requirements for IFNs and STAT1 in NK cell function.* J Immunol, 2000. **165**(7): p. 3571-7.

195. Nguyen, K.B., et al., *Coordinated and distinct roles for IFN-alpha beta, IL-12, and IL-15 regulation of NK cell responses to viral infection.* J Immunol, 2002. **169**(8): p. 4279-87.

196. Ronnblom, L., G.V. Alm, and M.L. Eloranta, *Type I interferon and lupus.* Curr Opin Rheumatol, 2009. **21**(5): p. 471-7.

197. Fairhurst, A.M., et al., *Type I interferons produced by resident renal cells may promote end-organ disease in autoantibody-mediated glomerulonephritis.* J Immunol, 2009. **183**(10): p. 6831-8.

198. Braun, D., P. Geraldes, and J. Demengeot, *Type I Interferon controls the onset and severity of autoimmune manifestations in lpr mice.* J Autoimmun, 2003. **20**(1): p. 15-25.

199. Nacionales, D.C., et al., *Deficiency of the type I interferon receptor protects mice from experimental lupus.* Arthritis Rheum, 2007. **56**(11): p. 3770-83.

200. Schwarting, A., et al., *Interferon-beta: a therapeutic for autoimmune lupus in MRL-Faslpr mice.* J Am Soc Nephrol, 2005. **16**(11): p. 3264-72.

201. Satchell, S.C., et al., *Interferon-beta reduces proteinuria in experimental glomerulonephritis.* J Am Soc Nephrol, 2007. **18**(11): p. 2875-84.

202. Schreiner, B., et al., *Interferon-beta enhances monocyte and dendritic cell expression of B7-H1 (PD-L1), a strong inhibitor of autologous T-cell activation: relevance for the immune modulatory effect in multiple sclerosis.* J Neuroimmunol, 2004. **155**(1-2): p. 172-82.

203. Rees, A.J. and R. Kain, *Interferon-beta: a novel way to treat nephrotic syndrome?* J Am Soc Nephrol, 2007. **18**(11): p. 2797-8.

204. Theofilopoulos, A.N., et al., *Type I interferons (alpha/beta) in immunity and autoimmunity.* Annu Rev Immunol, 2005. **23**: p. 307-36.

205. Santiago-Raber, M.L., et al., *Type-I interferon receptor deficiency reduces lupus-like disease in NZB mice.* J Exp Med, 2003. **197**(6): p. 777-88.

206. Sagrinati, C., et al., *Isolation and characterization of multipotent progenitor cells from the Bowman's capsule of adult human kidneys.* J Am Soc Nephrol, 2006. **17**(9): p. 2443-56.

207. Ohse, T., et al., *Establishment of conditionally immortalized mouse glomerular parietal epithelial cells in culture.* J Am Soc Nephrol, 2008. **19**(10): p. 1879-90.

208. Mundel, P., et al., *Rearrangements of the cytoskeleton and cell contacts induce process formation during differentiation of conditionally immortalized mouse podocyte cell lines.* Exp Cell Res, 1997. **236**(1): p. 248-58.

209. Wegener, J., C.R. Keese, and I. Giaever, *Electric cell-substrate impedance sensing (ECIS) as a noninvasive means to monitor the kinetics of cell spreading to artificial surfaces.* Exp Cell Res, 2000. **259**(1): p. 158-66.

210. Lo, C.M., C.R. Keese, and I. Giaever, *Impedance analysis of MDCK cells measured by electric cell-substrate impedance sensing.* Biophys J, 1995. **69**(6): p. 2800-7.

211. Giaever, I. and C.R. Keese, *A morphological biosensor for mammalian cells.* Nature, 1993. **366**(6455): p. 591-2.

212. Fensterl, V. and G.C. Sen, *The ISG56/IFIT1 gene family.* J Interferon Cytokine Res, 2011. **31**(1): p. 71-8.

213. Lande, R., et al., *IFN-alpha beta released by Mycobacterium tuberculosis-infected human dendritic cells induces the expression of CXCL10: selective recruitment of NK and activated T cells.* J Immunol, 2003. **170**(3): p. 1174-82.

214. Henao, D.E., et al., *Preeclamptic sera directly induce slit-diaphragm protein redistribution and alter podocyte barrier-forming capacity.* Nephron Exp Nephrol, 2008. **110**(3): p. e73-81.

215. Lai, K.N., et al., *Podocyte injury induced by mesangial-derived cytokines in IgA nephropathy.* Nephrol Dial Transplant, 2009. **24**(1): p. 62-72.

216. Han, G.D., et al., *IFN-inducible protein-10 plays a pivotal role in maintaining slit-diaphragm function by regulating podocyte cell-cycle balance.* J Am Soc Nephrol, 2006. **17**(2): p. 442-53.

217. Fuertes Marraco, S.A., et al., *Type I interferon drives dendritic cell apoptosis via multiple BH3-only proteins following activation by PolyIC in vivo.* PLoS One, 2011. **6**(6): p. e20189.

218. Chen, Q., et al., *Apo2L/TRAIL and Bcl-2-related proteins regulate type I interferon-induced apoptosis in multiple myeloma.* Blood, 2001. **98**(7): p. 2183-92.

219. Ziske, C., et al., *Retroviral IFN-alpha gene transfer combined with gemcitabine acts synergistically via cell cycle alteration in human pancreatic carcinoma cells implanted orthotopically in nude mice.* J Interferon Cytokine Res, 2004. **24**(8): p. 490-6.

220. Galluzzi, L., et al., *Molecular definitions of cell death subroutines: recommendations of the Nomenclature Committee on Cell Death 2012.* Cell Death Differ, 2012. **19**(1): p. 107-20.

221. Petermann, A.T., et al., *Mitotic cell cycle proteins increase in podocytes despite lack of proliferation.* Kidney Int, 2003. **63**(1): p. 113-22.

222. Sadler, A.J. and B.R. Williams, *Interferon-inducible antiviral effectors.* Nat Rev Immunol, 2008. **8**(7): p. 559-68.

223. Hagele, H., et al., *Double-stranded RNA activates type I interferon secretion in glomerular endothelial cells via retinoic acid-inducible gene (RIG)-1.* Nephrol Dial Transplant, 2009. **24**(11): p. 3312-8.

224. Hagele, H., et al., *Double-stranded DNA activates glomerular endothelial cells and enhances albumin permeability via a toll-like receptor-independent cytosolic DNA recognition pathway.* Am J Pathol, 2009. **175**(5): p. 1896-904.

225. Gonzalez-Navajas, J.M., et al., *Immunomodulatory functions of type I interferons.* Nat Rev Immunol, 2012. **12**(2): p. 125-35.

226. Flandre, P., et al., *Risk factors of chronic kidney disease in HIV-infected patients.* Clin J Am Soc Nephrol, 2011. **6**(7): p. 1700-7.

227. Genderini, A., et al., *HIV-associated nephropathy: a new entity. A study of 12 cases.* Nephrol Dial Transplant, 1990. **5 Suppl 1**: p. 84-7.

228. Gupta, R., et al., *Collapsing glomerulopathy occurring in HIV-negative patients with systemic lupus erythematosus: report of three cases and brief review of the literature.* Lupus, 2011. **20**(8): p. 866-70.

229. Obeid, K.M., A.R. Effendi, and R. Khatib, *Association of parvovirus B19 infection with glomerulonephritis in an immunocompetent host: a case report.* Scand J Infect Dis, 2009. **41**(11-12): p. 890-2.

230. Strauss, J., et al., *Renal disease in children with the acquired immunodeficiency syndrome.* N Engl J Med, 1989. **321**(10): p. 625-30.

231. Niranjan, T., et al., *The Notch pathway in podocytes plays a role in the development of glomerular disease.* Nat Med, 2008. **14**(3): p. 290-8.

232. Vakifahmetoglu, H., M. Olsson, and B. Zhivotovsky, *Death through a tragedy: mitotic catastrophe.* Cell Death Differ, 2008. **15**(7): p. 1153-62.

233. Lee, P.Y., et al., *Type I interferon modulates monocyte recruitment and maturation in chronic inflammation.* Am J Pathol, 2009. **175**(5): p. 2023-33.

234. Wang, Y., et al., *Ex vivo programmed macrophages ameliorate experimental chronic inflammatory renal disease.* Kidney Int, 2007. **72**(3): p. 290-9.

235. Marshall, C.B., et al., *CDK inhibitor p21 is prosurvival in adriamycin-induced podocyte injury, in vitro and in vivo.* Am J Physiol Renal Physiol, 2010. **298**(5): p. F1140-51.

236. Ohse, T., et al., *De novo expression of podocyte proteins in parietal epithelial cells during experimental glomerular disease.* Am J Physiol Renal Physiol, 2010. **298**(3): p. F702-11.

237. Thomas, C., et al., *Structural linkage between ligand discrimination and receptor activation by type I interferons.* Cell, 2011. **146**(4): p. 621-32.

238. Bruggeman, L.A., et al., *Renal epithelium is a previously unrecognized site of HIV-1 infection.* J Am Soc Nephrol, 2000. **11**(11): p. 2079-87.

239. Khatua, A.K., et al., *Non-productive HIV-1 infection of human glomerular and urinary podocytes.* Virology, 2010. **408**(1): p. 119-27.

240. Rich, S.A., *Human lupus inclusions and interferon.* Science, 1981. **213**(4509): p. 772-5.

241. *Intramuscular interferon beta-1a therapy initiated during a first demyelinating event in multiple sclerosis. Jacobs LD,*(1) Beck RW, Simon JH, Kinkel RP, Brownscheidle CM,*

Murray TJ, Simonian NA, Slasor PJ, Sandrock AW, and the CHAMPS Study Group. N Engl J Med 2000;343:898-904. Am J Ophthalmol, 2001. **131**(1): p. 154-155.

242.   Ohta, S., et al., *Exacerbation of glomerulonephritis in subjects with chronic hepatitis C virus infection after interferon therapy.* Am J Kidney Dis, 1999. **33**(6): p. 1040-8.

9. List of Abbreviations

AER: albumin excretion rate

ACR: albumin to creatinine ratio

AIDS: acquired immunodeficiency syndrome

AP-1:   activator protein 1

CKD: chronic kidney disease

CLDN1:   claudin 1

FSGS: focal segmental glomerulosclerosis

GBM: glomerular basement membrane

GFB: glomerular filtration barrier

GFR: glomerular filtration rate

HBV: hepatitis B virus

HCV: hepatitis C virus

HIV: human immunodeficiency virus (),

HIVAN: HIV-associated nephropathy

IFN: interferon

KDIGO: Kidney Disease Improving Global Outcomes

NKF-K/DOQI: National Kidney Foundation Kidney Disease Quality
                    Outcome Initiative

MPGN: Membranoproliferative glomerulonephritis

NPHS1:   nephrin

NPHS2:   podocin

NFKB: nuclear factor kappa-light-chain-enhancer of activated B
                    cells)

NLRs: nucleotide-binding oligomerization domains containing
                    (NOD)-like receptors

NOD: nucleotide-binding oligomerization domain

NOS: not-otherwise -specified variant

PAMP: pathogen-associated molecular patterns

PEC: parietal epithelial cells

PRR: pattern recognition receptors

PVB19:	parvovirus B19
RLRs:	retinoic acid-inducible gene (RIG)-I-like receptors
SCID:	severe combined immunodeficient
SLE:	Systemic lupus erythematosus
TIR:	toll-interleukine 1 receptor
TLRs:	toll-like receptors
TRIF:	TIR domain containing adapter inducing IFN-β
TUNEL:	terminal deoxynucleotidyl transferase mediated dUTP Nick End Labeling
WT-1:	Williams tumor protein-1
ZO-1:	zonula occludens-1

10. Appendix

Composition of buffers used

Annexin V/PI Buffer :

10mM Hepes ;140mM NaCl;2,5CaCl$_2$

Hepes	2,40 g	
NaCl	8,26g (0.1 %)	
CaCl$_2$	222 mg	

Ripa Buffer:

50 mM Tris-HCl (pH 8);150 mM NaCl, 1% NP-40; 0,05%sodium deoxycholate, 0,1% SDS

For 1000 ml:

Tris-HCL	6,057 g
NaCl	8,772 g
NP-40	10 ml
Sodium deoxycholate	0,5 ml
SDS	1 ml

10X HBSS (Hank's Balanced Saline Solution) with Ca, Mg:

For 1000 ml

KCl	4 g
KH$_2$PO$_4$	0,6 g
NaCl	80 g
Na$_2$HPO$_4$.2H$_2$O	0,621 g
NaHCO$_3$	3.5 g
CaCl$_2$	1,4 g (or CaCl$_2$.2H$_2$O 1,854 g)
MgCl$_2$.6H$_2$O	1 g
MgSO$_4$.7H$_2$O	1 g
D-Glucose	10 g

Dissolve in 900 ml of distilled water and adjust to pH 7.4 with 1N HCl or 1N NaOH. Make up the volume with distilled water to 1000 ml.

10X HBSS (Hank's Balanced Saline Solution) without Ca, Mg:

      For 1000 ml

KCl	4 g
KH_2PO_4	0,6 g
NaCl	80 g
$Na_2HPO_4.2H_2O$	0,621 g

      Dissolve in 1000 ml and autoclave.

50 % Glycerol in 20 mM Tris-HCl (pH 7.5);1 mM $MgCl_2$:

      a. 0,48 g of Tris-HCl in 100 ml of distilled water, adjust pH to 7,4 (= 40 mM)

      b. 50 ml of Glycerol 100 % + 50 ml of 40 mM Tris-HCl (20 mM)

      c. Add 100 µl of 1M $MgCl_2$ solution.

EDTA 2 mM:

      EDTA 7,44 mg in 10 ml HBSS (without Ca, Mg)

      To be preheated in 37 °C water bath before use.

MACS Buffer:

      PBS pH 7.2

      0,5% bovine serum albumin

      2 mM EDTA

Citrate buffer 10X:

      110 mM Sodiumcitrate in ddH2O

      with 2N NaOH to pH 6

PBS:

      2,74 M NaCl

      54 mM KCl

      30 mM KH2PO4

130 mM Na2HPO4

in ddH2O

Adjust pH to 7,5 with HCl

Gel Running Buffer (10x):

Tris   30g

Glycine   144g

SDS   5g

Make up volume to 1000ml (pH 8.3)

Transfer Buffer (1x):

Tris   1,5g

Glycine   7,2g

Make up volume to 500ml

TBS (10x):

Tris   24,23g

NaCl   80,06g

Conc. HCL   around 17,5ml

Make up volume to 1000ml (pH 7,6)

TBS-T (1x):

TBS (1x)   1000ml

Tween 20   1ml

Sample buffer:

Milipore water   3,8 ml

0,5 M Tris HCl, pH 6,8   1 ml

Glycerol   0,8 ml

10% SDS   1,6 ml

2- mercaptoehanol   0,4 ml

1% (w/v) bromophenol blue 0,4 ml

Total: 8 ml

Separating Buffer (1x):

       Tris (1.5mM)   18,2g

       SDS   400mg

   Make up volume to 100ml (pH 8.8)

Stacking Buffer (1x):

       Tris (0.5mM)   6,05g

       SDS   400mg

   Make up volume to 100ml (pH 6.8)

Staining solution:

       Methanol   500ml

       Acetic acid   100ml

       Water   400ml

   Coomasie Brilliant blue R : 2.5 g (0.25%)

Destaining solution:

       Methanol   150ml

       Acetic acid   100ml

       Water   750ml

11. Acknowledgments

Firstly I would like to thanks and to express my deepest sense of gratitude to my mentor and supervisor Prof. Hans-Joachim Anders. He provided me guidance, inspiration and advice during my research work. I appreciated his trust in my scientific skills, his constant support and I am grateful for the numerous scientific discussions we had together, which contribute to my progress as a scientist.

It is my pleasure to thank Prof. Dr. Stefan Endres, Leader of GRAKO1202, LMU, for allowing me to become a member of graduate students network during my Ph.D. tenure, and Deutsche Forschungsgemeinschaft (DFG) for the grant that supported me during the course of my research term (2010-2013).

I would like to acknowledge Prof. Paola Romagnani (University of Florence, Italy) and all her scientific staff, for giving me the opportunity to perform part of my work on their laboratory and providing me excellent suggestions and outstanding experimental supports for my research work.

I would like to thanks Prof. Alexander Dietrich (Walther-Straub-Institute for Pharmacology and Toxicology, LMU, Munich) and Jana Demleitner for providing me excellent experimental support for the ECIS experiments during my research work.

My sincere thanks goes to Dr. Peter Nelson, Dr. Bruno Luckow, Dr. Volker Vielhauer, and their respective research teams for their support and constant encouragement for my research work throughout my stay at Klinische Biochemie.

I wish to express my profound gratitude to Ewa Radomska, Dan Draganovici, and Jana Mandelbaum for providing skillful technical assistance to carry out the research work successfully.

Many thanks to all the lab colleagues and friends, from Munich and Florence; Anna, Costanza, Eliana, Elena, Laura, Lara, Marialucia, Dana, Khader, Kirstin, Henny, Maciej, Mi, Murthy, Onkar, Regina, Santhosh, Shrikant, Simone and all medical students for all your help and for the delightful time we had together. Especially to Maciej and Henny to have helped me and have been my friend since the beginning of my Munich stay, to Shrikant for sharing your knowledge and for listening me and every time, and to Simone, for all your precious help and support, as friend and as colleague. I also owe special gratitude to all my friends all over the word, who always gave me warm encouragement.

There are not enough words to express my love and gratitude to my mother, my father, my sister and to all my relatives, for their constant faithfulness, love and encouragement through my life.
I am grateful to everybody who has been part of my life and helped in some way or other, but if I failed to mention their names, THANK YOU ALL!!

I cannot end without thanking Damiano, for all your love and trust; without you I could not have reached this far in my career.